UNIVERSITÀ DEGLI STUDI DI PADOVA

Facoltà di Ingegneria

Corso di laurea magistrale in Ingegneria Elettrica

Tesi di laurea

Steady state and dynamic performance analysis of KIRSCH micro CHP L 4.12 generator.

Relatore UNIPD: Prof.-Ing. Michele De Carli

Relatore TUD: Dr.-Ing. habil. Joachim Seifert

Correlatore TUD: Dipl.-Ing. Paul Seidel

Candidato: Edoardo Alfonsi

Numero di matricola UNIPD: 1058620

Anno accademico: 2013/2014

Acknowledgements

At the end of these months in Dresden, I would like to say thanks to the people who gave me the possibility to develop this thesis.

First of all, my supervisors at TU Dresden, Dr.-Ing. habil. Joachim Seifert, and at the home university in Padova, Prof.-Ing. Michele De Carli.

I want to express my gratitude especially to Dipl.-Ing. Paul Seidel, who answered to all my recurring questions, taught me how to use the laboratory and the software, and had in general a lot of patience with me. He supported me and led my work to the right direction.

I say thanks to Dipl.-Ing. Jan Löser, who offered me the possibility to take part in a really interesting meeting with Caleffi's representatives.

I am really thankful to my family, my girlfriend and my friends in Verona for their support.

Finally, I must be thankful to the Erasmus program. I would recommend this experience to everyone as an opportunity to grow and to know a different culture.

Table of contents:

Figures:

Symbols

ϑ	°C	Temperature
σ	-	Power to heat ratio
η	-	Efficiency
ρ	Kg/m^3	Density
Δ	-	Difference
τ	s	Time constant
ω	s^{-1}	Pulsation
f	Hz	Frequency
ε	-	Coefficient of air excess
P	W	Power
E	J	Energy
Q	J	Heat
$\dot{Q}$	W	Thermal power
W	J	Work
H	J/Kg	Calorific power
h	J/Kg	Specific enthalpy
β	-	Condensation ratio
p	Pa	Pressure
c	kJ/Kg·K	Thermal capacity
$\dot{V}$	m^3/h	Volume flow
$\dot{m}$	Kg/h	Mass flow
s	J/K	Entropy
t	s	Time
DN	mm	Nominal diameter
Vs	m^3/h	Valve ratio
φ	rad	Electrical phase

Abstract

This thesis has been developed at the “Technische Universität” of Dresden, at the “Energie Technik” institute. It has been supported by the Erasmus program. All the activities, included the measurements, have been made in the “Merkelbau” building, under the supervision of Dr.-Ing. habil. Joachim Seifert and of Dipl.-Ing. Paul Seidel during the summer semester of the year 2014. All the devices and instruments of K06 laboratory have been completely available.
During the measurements the structure and the performance of the micro-CHP Kirsch L 4.12 generator, provided by KIRSCH HomeEnergy GmbH, have been studied.

The aim

With this document the performances of the micro-CHP L 4.12 generator from KIRSCH will be investigated in different conditions. The tools for the measures and computers for monitoring are provided from the laboratory and the micro-CHP L 4.12 generator is completely accessible.

With a hydraulic structure, the heat load of a standard building will be emulated, in order to be allowed to study the coupling between the examined generator and a conventional house.

The measurement will be gained in two different operating conditions of the machine: steady state conditions and transient conditions.

Dealing with the stationary mode, the measures have been taken for different values of volume flow and back flow temperature. They have been considered all the three electrical power steps of the generator: 2kW, 3kW and 4kW. They will be analyzed the diagrams of the electric and heating power produced by the machine as function of the back flow temperature. The diagrams of the overall, the electrical and the thermal efficiency will be plotted as well. Furthermore will be considered also the diagrams regarding the condensation mass to comprehend how much latent heat is subtracted from the output exhaust gas.
All the measures are functions of the back flow temperature because it indirectly represents the amount of thermal energy absorbed by the load of the building.

In the chapters dealing with the transient conditions it is analyzed the operation of the machine during the variation of time. This chapter is useful to understand how the machine reacts to the load variations, considering the whole hydraulic circuit with its own inertia.
The second part of this chapter is aimed to calculate the standard efficiency in a 24 hours measurement. Actually the purpose is to consider the behavior of the whole coupled system generator-load, through the use of a storage.

All the numerical values obtained will be tabulated and compared with the already achieved results of the previous CHP model from Kirsch and with the prototype as well.

1 Introduction

1.1 Cogeneration: general features

Cogeneration, also known as combined heat and power (CHP), refers to a group of proven technologies that operate together for the concurrent generation of electricity and useful heat

in a process that is generally much more efficient than the separate generation of electricity and useful heat.

The fundamental principle on which CHP technology is based, is the following: in any direct thermodynamic cycle, thanks to which it is possible to extract useful work (mechanical or electrical energy), part of the heat at higher temperature entering the cycle must necessarily be transferred to a lower temperature. This portion of transferred heat represents the amount of high-temperature heat that, because of the limits imposed by thermodynamics, is not converted into useful work. Thus, it results an energy loss in the conversion process. In the case in which exists a user who requires thermal heat at low temperature, it would be achieved a cogeneration process.

For the same output of useful energy, cogeneration uses far less fuel than does traditional separate heat and power production; this means lower emissions.
Separate heat and power production, instead, refers to an electricity's central generation in large-scale power plants and separately heat generating onsite. This heat is used in applications such as industrial processes and water heating. This leads to energy losses in both processes. Typical separate heat and power production has a combined efficiency of about $\eta \approx 55\%$ while cogeneration systems can have up to $\eta \approx 90\%$ [1]. Furthermore, cogeneration takes place on-site or close to the facility and has less energy losses during the transmission and distribution process.
As it is shown in Fig.1.1.1, with this combined heat and power configuration (40 unit of electricity and 50 of heat) can be saved an amount $E = \frac{172-100}{172} \cdot 100\% \approx 42\%$ of primary energy thanks to a higher overall efficiency. The boiler here analyzed has an efficiency of roughly $\eta_{boiler} \cong 80\%$. The delivering process of the electricity up to the utility has an efficiency of $\eta_{delivering} \cong 36\%$.

The type of cogeneration systems analyzed in this text is "topping cycle", where fuel is first used to generate electricity or mechanical energy and a portion of the wasted heat coming from power generation is then used to provide useful thermal energy.

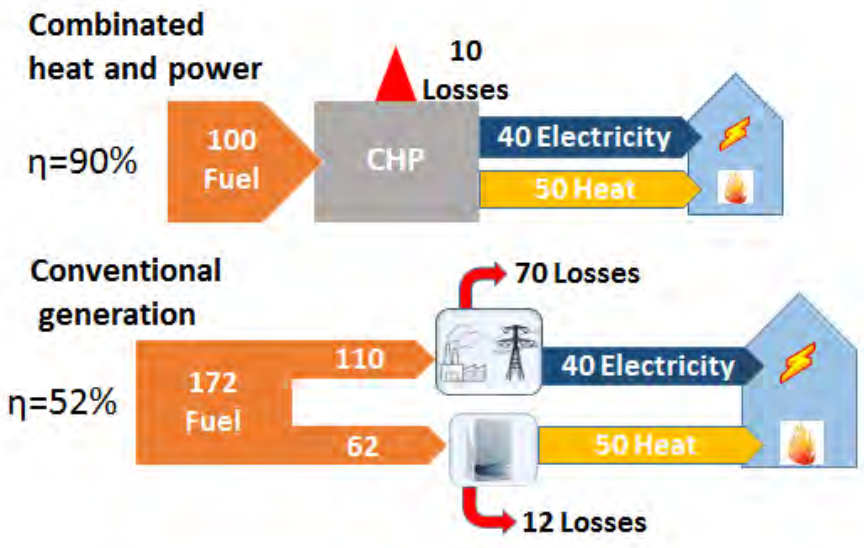

Fig.1.1.1 - Numerical comparison between CHP and a conventional power plants

1.1 Cogeneration: general features

The interest is focused on the micro-cogeneration, that means that the electrical power produced is lower than $P_{el} = 15\ kW$. In this way this technology refers to residential and light commercial users.
As it is shown in Fig.1.1.2, the CHP systems can be distinguished for:

- Size
- Type of fuel
- Type of generation plant

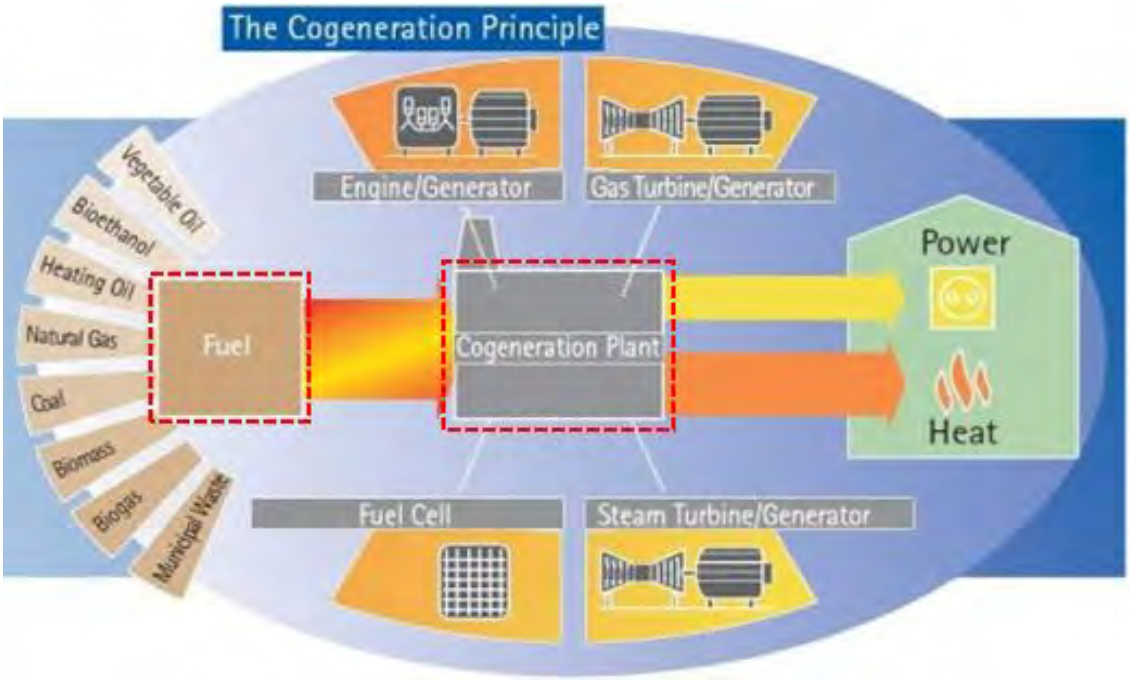

Fig.1.1.2 - Overall illustration of cogeneration [2]

The power size is determined by the demand of the facility and can be formally divided in 4 groups [3]:

- P $\leq$ 10 MVA – Big power stations for the distributed generation
- P $\leq$ 1 MW – Small power plants
- 15 kW $\leq$ P $\leq$ 50 kW – Mini CHP
- P $\leq$ 15 kW – Micro CHP

Dealing with the fuels there are a lot of choices that can be adopted. The solid fuels, such as coal, wastes and contaminated liquid or gaseous fuels, would damage the prime mover and can not be burned in a prime mover. In these instances the fuel is burnt in a combustion chamber and the heat released from the fuel raises pressurized steam. The steam is then used to drive a turbine or other kind of generators. In general, the flexibility of its supply, storage and use influences the cost of a fuel. For example natural gas and the lighter oils are highly valued and viewed as premium quality fuels as a result they are relatively expensive but do not require expensive handling equipment. In a decentralized power generation scenario, where stringent pollutant emissions regulations are increasing, the gas fuelled engines are more and more often used. As their efficiency is lower than the one of comparable diesel engines, the premixed Otto cycle gas engines have less harmful emissions [4].
Non-premium fuels, such as coal, heavy oils and alternative-fuel materials, are cheaper but incur significant costs for handling, burning and reaching environmental standards. These fuels

are sometimes produced by industrial processes or domestic activities and are only economic available for the local use because of the high transport costs.
Commercial fuels are normally natural gas, distillate oils, heavy fuel oils and coal. Examples of renewable fuels instead are: biogas, liquid biofuels, wood fuels, biodiesel, geothermal sources and biomasses.

The plant typologies can be combustion engines, Stirling engines, fuel cells, steam turbines or gas turbines.

If the aim of a cogeneration plant is to obtain a bigger saving of primary energy than a separated heat and power plant normally does, the plant must work mostly in nominal conditions to have a higher efficiency. Normally a small facility has a really variable electric load and this means that the generator must work in off-design conditions. Furthermore the thermal energy, storable for a limited time, is unlikely not required simultaneously. In order to maximize the many benefits that arise from it, micro CHP systems should be based on the heat demand. In this way they are thermal-regulated and the public electric net is used as a huge storage. Thus, the small-sized cogeneration is convenient if the electric energy produced and not self-consumed is well remunerated.
Depending on the load profile of the building, an appropriate heat-to-power ratio must be selected depending on the demand; for the most newly-building with a good thermal insulation the ratio should be low.

1.2 Operating strategies

According to the technical specifications of each technology, it is really important to adopt the most convenient control strategy in order to satisfy the on-site load trends.
The operating strategies can be mainly three [6]:

- Heat-led operation:

The micro-CHP unit operates to feed completely the thermal load. Additional heat requirement can be satisfied by a supplementary heating system. The electricity production is directly depending on the variations occurring in the prime mover. The electric output feeds at first the on-site utilities, and the excess is delivered into the grid.

- Electricity-led operation:

The micro-CHP system follows the electric load demand. The thermal power produced feeds the utilities of the building and the excess is wasted in the ambient.
It is possible to adopt a pick-shaving strategy too. With this strategy the machine operates only during the hours of electric peak demand. This means that the base electrical production is guaranteed by another system. This strategy is attractive when the prices of the electricity during these periods are high.

- Least-cost operation:

With this strategy both the electrical and thermal loads are followed. The electrical output will be controlled according to a combination of fuel prices, electricity import/export prices, and their interaction with the overall efficiency profiles.

For both the heat-led and the electricity-led control there are three possible operating conditions [7]: if there is no demand, or if the demand is lower than the minimum

electrical/heating output, the machine dispatches at minimum capacity. If the demand is higher than the maximum capacity of the system, the engine will dispatch at maximum capacity. Finally, if the demand is higher than the minimum capacity and lower than the maximum one, the system will follow the demand in a continuous way.

1.3 The advantages

Thanks to a better heat recovering and to on-site electricity generation, the CHP technology guarantees a higher overall efficiency, and so a large primary energy saving. Lower emissions, in particular of CO_2, are waste to the environment.
It is an opportunity to move towards more decentralized forms of electricity generation, where plants are designed to meet the needs of local consumers, providing high efficiency, avoiding transmission losses and increasing flexibility of the system used. Even though the investment is often high, CHP provides in some cases a long-term costs saving becoming a competitive solution for industrial and commercial users. Furthermore, the local generation can reduce the risk of consumers being left without supplies of electricity or heating.

1.4 Economic evaluation

In order to define a correct system sizing according to the energy demand, it is necessary to develop an economic optimization method. This numerical method involves an objective function, whose main purpose is:

- Maximize micro-CHP overall efficiency η_0 by meeting the energy demand;
- Maximize the annual worth AW of micro-CHP system operation.

The function belongs to non-linear models; it is defined by the equation (1.4.1), [5]:

$$Max\{k_1 \cdot \eta_o + k_2 \cdot AW\} \quad (1.4.1)$$

where k_1 and k_2 are weighting parameters and vary between 0 and 1.

The AW annual worth results from the difference between the annual revenues and annual costs:

$$AW = \sum Revenues - \sum Costs \quad (1.4.2)$$

The most significant revenues are represented by the sell of the electrical energy excess to the grid and by the electrical energy self-consumed. Considering the actual sell and purchase price of the electric energy p_{sell} and $p_{purchase}$, the revenues result:

$$R_{sell} = E_{el,excess} * p_{sell}$$

$$R_{self\ cons} = E_{el,self\ consumed} * p_{purchase} \quad (1.4.3)$$

Finally, the residual value of the equipment R_{end} at the end of its useful lifetime should be considered as revenue.

In this way the revenues are:

$$\sum Revenues = R_{sell} + R_{boiler} + R_{end} \quad (1.4.4)$$

Dealing with the costs, the main terms correspond to the investment costs C_{inv}, including the installation of the equipment, and the cost of the fuel C_{fuel} for the operation of the CHP system. Other less relevant costs can arise from the maintenance C_m, from the acquisition of a backup boiler C_{boiler} and from the electrical power needed to start the prime mover, C_{start}.

$$\sum Costs = C_{inv} + C_{fuel} + C_m + C_{boiler} + C_{star} \quad (1.4.5)$$

The critical part of this mathematical model consists in the selection of the most convenient operating strategy that face the demand, has the lowest consumption, and has the highest economic revenues.

2 Kirsch L 4.12 generator

2.1 General features

The micro CHP L 4.12 from KIRSCH is an autonomous natural gas-fuelled generator that allows the production of heat and electric power together, through the CHP principle. This means that the gas-fuelled engine transmits its mechanical power to a generator and its heat to a thermal circuit. The electrical power can be modulated from P = 2kW to P = 4kW by steps of P = 1kW, and the heat power reaches up to $\dot{Q} = 12\ kW \pm 2\ kW$.

The overall efficiency is roughly η_o = 95-100% and can reach values over 100% in particular conditions; the electrical efficiency is about η_e = 20-25 %.

The current produced feeds the home net and the excess is delivered to the public net.

Fig.2.1.1 - Kirsch L 4.12 [8]

Micro CHP L 4.12 from KIRSCH has a compact size and a weight of only 200 Kg. Furthermore it is equipped with a 17,8 cm color monitor that shows all the operating conditions, actual values and setting data.

It needs a gas connection to a grid, an electric wiring to the sub distribution net with an inverter and an electric meter, closed central domestic water heating and a single or two-family building heat demand of roughly 20000-50000 kWh/y [8].

The micro CHP L 4.12 is equipped with a sound and heat insulating encapsulation. It enables a sound pressure level of approximately 55 dB at 1 meter distance. Vibrations are largely eliminated through the use of very soft joints.

Kirsch sells this product for about 16.000 € and guarantees a service life up to 20 years long.

Fig.2.1.2 - Right side of Kirsch L 4.12

Fig.2.1.3 - Left side of Kirsch L 4.12

2.2 The engine

Nowadays there are different kind of engine that can be used for the simultaneous production of heat and power. Mainly they can be:

- Stirling engine
- Internal combustion engine
- Fuel cells
- Gas and steam turbines

The micro CHP L 4.12 owns a two cylinders internal combustion V-Twin engine with a cylinder capacity of 479cc and a 15.7 HP power. It is powered by gas and its operating speed is 1900 min^{-1}. It has two separated oil circuits and is chilled with air. With this device is possible to work producing three different powers, P = 2kW, P = 3kW or P = 4kW with an electrical efficiency of η_e = 20-25%. This is possible by changing the gas input amount.

Fig.2.2.1 - Briggs & Stratton Vanguard engine [8]

The V-Twin technology with top valves ensures a better balance, low vibrations, lower emissions, a greater durability of the valves, reducing consumption of fuel and a higher power to weight ratio. It has a Dura-Bore cast iron motor block that extends the engine's life and allows better control of the oil. The starting with electronic ignition is fast and reliable and does not require maintenance.

2.2.1 Internal combustion engine

As a largely widespread system, the internal combustion engine is nowadays available with power size from kW to MW. The internal combustion engines can work with the so-called “Otto cycle” or “Diesel cycle”. This chapter is only focusing on the first typology.

The Otto cycle consists of 4 phases, showed in Fig.2.2.2:

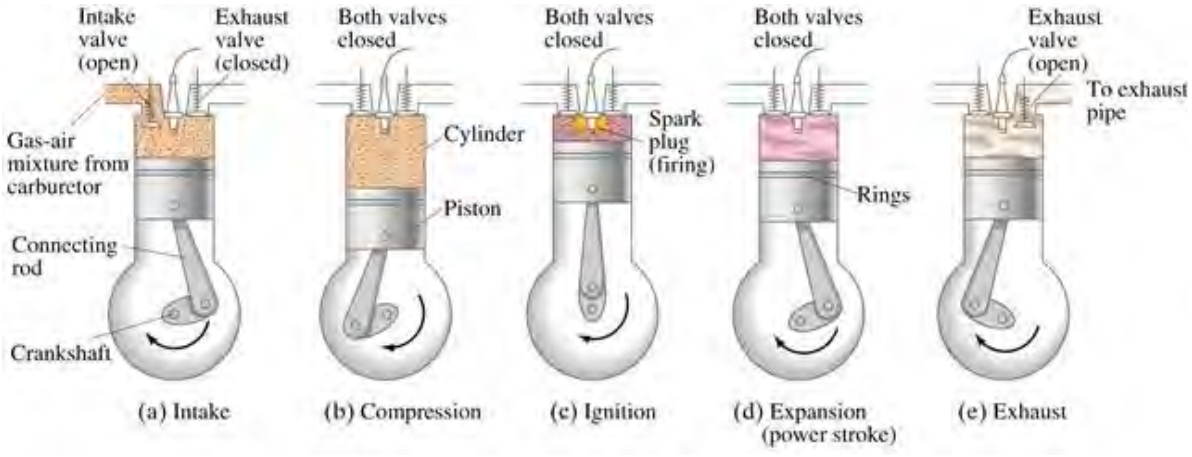

Fig.2.2.2 - Four strokes engine [9]

- The piston, moving from the top to the bottom, draws the gas-air mixture coming from the carburetor in the cylinder. The intake valve is opened.
- The drawn fresh charge is compressed in the combustion chamber. Both the valves are closed.
- Towards the end of the compression stroke begins the charge combustion, triggered by an electric spark. Combustion causes a sudden increase in pressure and temperature of the fluid contained in the cylinder, which performs useful work during the down stroke of the piston. Both the valves are still closed.
- Shortly before that the expansion stroke terms, the exhaust valve opens and the burnt gases are expelled from the cylinder.

In order to correctly express the efficiency and make power balances, it is necessary to refer to the theoretical Otto cycle. In this kind of cycle some simplifications have been made.
This cycle is considered completely closed without direct interactions with the ambient. The heat is given to the fluid in specific moments and in an instantaneous way. Furthermore the fluid is considered an ideal gas and the compression and expansion strokes take place adiabatically.

2.2 The engine

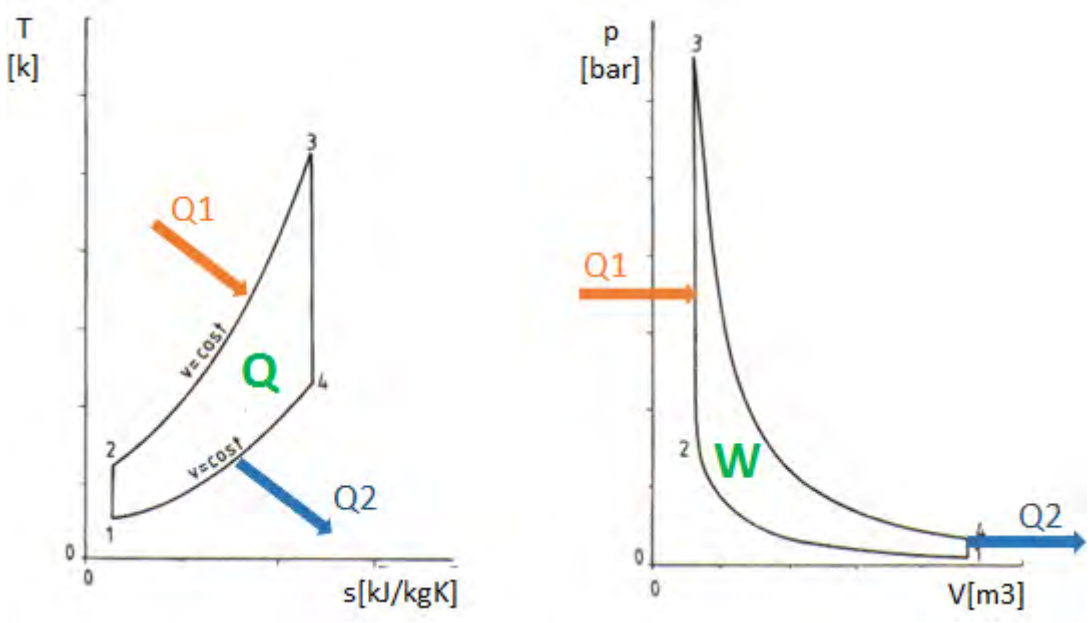

Fig.2.2.3 - Theoretical Otto cycle

Theoretical Otto cycle phases are:

- 1-2: isentropic compression
- 2-3: isochoric heat receiving
- 3-4: isentropic expansion
- 4-1: isochoric heat expulsion

In the two diagrams of Fig.2.2.3 is showed the same result of the process with different units of measurement.
For the second law of thermodynamics the available work of the process must be:

$$W = Q_1 - Q_2 \tag{2.2.1}$$

In particular in the T-s diagram the useful work is given by:

$$Q = \int_{s1}^{s4} T ds \tag{2.2.2}$$

In the p-v diagram the work is represented by the area 1234 and results:

$$W = \int_{v2}^{v1} p\, dv \tag{2.2.3}$$

The efficiency of the theoretical Otto cycle can be express with this equation:

$$\eta_{th,id} = \frac{W}{Q_2} = \frac{Q_1 - Q_2}{Q_2} = \frac{c_v\,(T_3 - T_2) - c_v\,(T_4 - T_1)}{c_v\,(T_3 - T_2)} = 1 - \frac{T_1}{T_2} =$$

$$= 1 - \left(\frac{V_1}{V_2}\right)^{\gamma-1} = 1 - \left(\frac{1}{r}\right)^{\gamma-1} \quad (2.2.4)$$

Where r is the geometric compression ratio, or rather the ratio of the two total volume V1 and V2 of the process, and γ is the adiabatic expansion coefficient.

The real Otto cycle is showed in Fig.2.2.4. It has been plotted measuring the pressure in the cylinder during a cycle as a function of the position of the piston.

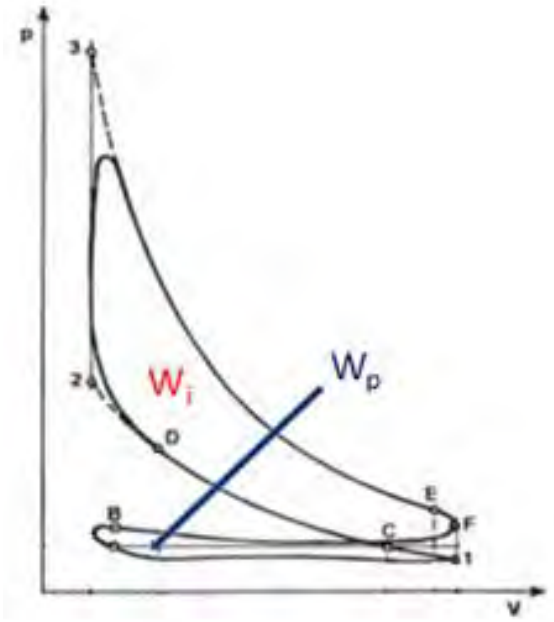

Fig.2.2.4 - Real Otto cycle

As it is clear in the picture, in the real cycle the compression and expansion phases are not adiabatic and the combustion does not take place with a constant volume.
The working fluid is not an ideal gas and so it changes composition during the four strokes. Moreover the piston performs a W_p amount of work to replace the charge and this has a negative sign in the energy balances.

In order to quantify the difference between the two theoretical and real process the η_i has been defined:

$$\eta_i = \frac{W_{real}}{W_{ideal}} \quad (2.2.5)$$

If the engine shaft work (effective work W_e) is measured, it would be smaller than W_i , since not all of the indicated work developed by the gas is transferred to the shaft: part of it is lost to mechanical friction, some is absorbed by auxiliaries (for example, pumps) and part is lost for the replacement of the charge (pumping). Overall, the work lost due to passive resistances is W_p:

$$W_e = W_i - W_p \quad (2.2.6)$$

The mechanical efficiency is:

$$\eta_m = \frac{P_e}{P_i} \tag{2.2.7}$$

Finally the overall thermal efficiency can be written as:

$$\eta_{th,o} = \frac{W_e}{Q_f} = \frac{P_e}{\dot{Q}_f} = \eta_{th,id} \cdot \eta_i \cdot \eta_m \tag{2.2.8}$$

where $\eta_{th,id}$ represents the ideal heat to work conversion, η_i considers the transition from the theoretical process to the real one, and η_i is referred to the passive resistances.

2.2.2 Supply air

Thanks to a fan inside the micro CHP L 4.12, the correct amount of oxygen for the combustion of the gas fuel is sucked into the engine with ambient air.

The minimum quantity required for the complete combustion is $(m_a)_{st}^*$, where "*" means that the quantity is referred to a single fuel mass unit. This is the stoichiometric value for the supply air. This means that with a $(m_a)_{st}^*$ quantity of air all the particles of the fuel gas are surrounded by the right amount of air to complete the whole combustion.

Usually, to obtain the complete oxidation of the whole fuel mass, is used more air than the stoichiometric balance requires, in order to avoid a big amount of unburnt in the exhaust and to exploit the total potential energy contained in the fuel.

From a theoretical point of view, a complete combustion could be reached using a stoichiometric amount of comburent air; practically, operating with finite times, industrial liquid fuels need a comburent air amount m_a^* bigger than the stoichiometric one.

The *coefficient of air excess* is defined as:

$$\varepsilon = \frac{m_a^* - (m_a^*)st}{(m_a^*)st} \tag{2.3.1}$$

In the measurements here analyzed, as it is normally required for the gas fuels, for the natural gas is used:

$\varepsilon = 1$

2.2.3 Stoichiometry

Natural gas used by micro CHP L 4.12 is a mixture of several components. Mainly they are carbon monoxide CO, carbon dioxide CO_2, methane CH_4 and other hydrocarbons C_mH_n. Normally the chemical composition of a gas fuel is preferred to be express as mole fraction of each gas contained in the mixture.

2.2 The engine

Let's suppose that the fuel is an ideal mixture of ideal gasses. If the volumetric analysis of the different gasses is known, it is possible to calculate the stoichiometric air quantity needed for the combustion.
Furthermore, it must be considered that one volume unit of oxygen is contained in 1/0,21 = 4.76 units of air, because the oxygen percentage in the air is about $O_{2\%} = 21\%$.

Let's consider the complete oxidation elementary reactions of the single component:

$$CO + \frac{1}{2} O_2 = CO_2 \qquad (2.3.2)$$

$$1\ vol\ (CO) + \frac{1}{2}\ vol\ (O_2) \rightarrow 1\ vol\ (CO_2)$$

where the volumes are supposed to be at the same temperature and pressure conditions.
As it is shown in the reaction (2.3.2), one vol_{CO} needs $vol_{a,d} = 0{,}5 \cdot 4{,}76 = 2{,}38$ volumes of dry air for a complete oxidation.

The complete reaction of oxidation of hydrocarbons can be written as:

$$C_mH_n + \left(m + \frac{n}{4}\right) \cdot O_2 = m \cdot CO_2 + \frac{n}{2} H_2O \qquad (2.3.3)$$

$$1\ vol\ (C_mH_n) + \left(m + \frac{n}{4}\right)\ vol\ (O_2) \rightarrow m \cdot\ vol\ (CO_2) + \frac{n}{2}\ vol\ (H_2O)$$

One vol_{CmHn} volume needs $vol_{a,d} = 4{,}76 \cdot \left(m + \frac{n}{4}\right)$ volumes of dry air to do the complete stoichiometric combustion.

It is now possible to write the general formulation of the relative stoichiometric volume of air needed for a gas fuel to complete oxidation:

$$(V_a^*)_{st} = 2{,}38 \cdot x_{CO} + 9{,}52 \cdot x_{CH4} + 4{,}76 \sum \left(m + \frac{n}{4}\right) \cdot x_{CmHn} \qquad (2.3.4)$$

where the term related to methane, the main component in natural gas, has been separated to the general one (C_mH_n) to make the equation more clear. The summation Σ is referred to all the other hydrocarbons.

Finally, the relative stoichiometric amount of air can be express like:

$$(m_a)_{st}^* = (V_a^*)_{st} \cdot \frac{\bar{M}_a}{\bar{M}_c} \qquad (2.3.5)$$

$\overline{M}_a$ and $\overline{M}_c$ are respectively the equivalent molecular mass of dry air and fuel.

2.2.4 Combustion

To better understand what happens during the combustion process, in this chapter the engine is considered as a system with input and output where energy is produced.
The combustion reaction occurs in a system with permanent regime outflow, fed by a flow $\dot{m}_f$ of fuel at a t_f temperature and by a flow $\dot{m}_a$ of comburent at a t_a temperature. There is a $\dot{m}_e$ flow of flue gas outgoing the system with a t_e temperature and:

$$\dot{m}_e = \dot{m}_f + \dot{m}_a \qquad [kg/s] \tag{2.3.6}$$

The quantity E_n is transferred outside the system.
Let's consider negligible the variations of kinetic and potential energy and suppose complete the oxidation of the fuel and so:

$\varepsilon \geq 0$

If the first law of thermodynamics is used, this balance is obtained:

$$\dot{m}_f \cdot h_f(t_f) + \dot{m}_a \cdot h_a(t_a) = En + \dot{m}_e \cdot h_e(t_e) \qquad [Kg \cdot J/s] \tag{2.3.7}$$

The same equation written respect the fuel flow mass unit is:

$$En^* = h_f(t_f) + (1+ \varepsilon) \cdot (m_a)_{st}^* \cdot h_a(t_a) - m_e^* \cdot h_e(t_e) \qquad [J] \tag{2.3.8}$$

Let's consider now the particular condition in which the fuel, the comburent and the flue gas temperature are equal:

$$t_f = t_a = t_e = t_0 \qquad [K] \tag{2.3.9}$$

The balance becomes:

$$En_0^* = h_f(t_0) + (1+ \varepsilon) \cdot (m_a)_{st}^* \cdot h_a(t_0) - m_e^* \cdot h_e(t_0) \qquad [J/kg] \tag{2.3.10}$$

The last term of the equation (2.3.10) can be expressed as sum of a term referred to the stoichiometric flue gas and the exhaust due to the air surplus ε:

$$m_e^* \cdot h_e(t_0) = (m_e)_{st}^* \cdot [h_e(t_0)]_{st} + \varepsilon \cdot (m_a)_{st}^* \cdot h_a(t_0) \qquad [J/kg] \tag{2.3.11}$$

Introducing the equation (2.3.11) in the (2.3.10), finally the expression of the calorific power is given:

$$H = En_0^* = h_f(t_0) + (m_a)_{st}^* \cdot h_a(t_0) - (m_e)_{st}^* \cdot [h_e(t_0)]_{st} \qquad [J/kg] \qquad (2.3.12)$$

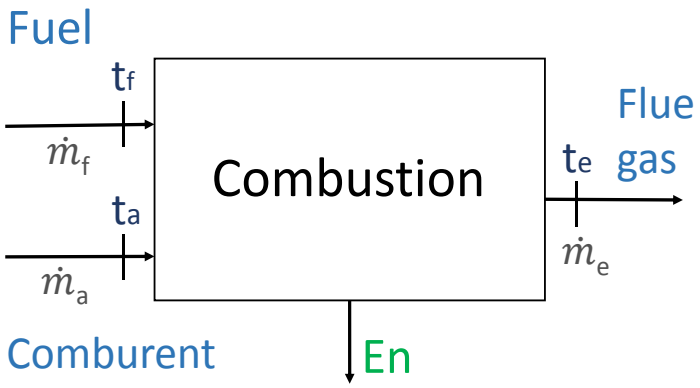

Fig.2.3.2 - Combustion scheme

H is "the amount of heat recoverable from the products of a complete combustion with outflow, respect to the fuel mass flow unit, when the products are cooled to the initial temperature of the common reagents", [10].

From the equation (2.3.12) it is clear that the calorific power En_0^* at the t_0 temperature is not depending on the air surplus ε, if the oxidation process is complete. In fact, the calorific power depends only on the type of each fuel.

In order to give an univocal definition of calorific power the following parameters must be specified:

- The temperature t_0;
- The initial state of the fuel;
- The state (liquid or vapor) of the water in the flue gas.

Depending on this last parameter, as is better clarified in the next chapter, there are two calorific powers, the inferior and the superior.

They are related by this equation:

$$H_s - H_i = (m_w)_s^* \cdot r_0 \qquad [J/kg] \qquad (2.3.13)$$

where $(m_w)_s^*$ is the water contained in the exhaust in a stoichiometric combustion referred to the fuel flow mass unit, and r_0 is the latent heat of vaporization of the water at the t_0 temperature (r_0 = 2465 kJ/kg at 15 °C).

2.3 The generator

The VEM G21R 132S is an asynchronous generator that makes the reactive power compensation. It has three 230/400 AC phases and works at 50 Hz. It has a high efficiency, a long lifetime, a good reliability and thermal overload capacity. It owns an environmental compatibility due to the use of a low-noise and bi-directional ventilation system.

This type of generator has this main features:

Tab. 2.3.1 - Main features of VEM G21R, [11]

Efficiency, η	82,3%
Power factor	cosφ = 0,66
Electric power	5,5 kW
Nominal current	12 A at 400 V
Noise intensity	+3 dB
Weight	65 Kg
Speed	1531 min^{-1}
Number of poles	4 p
Operating temperature	From -35°C up to 45°C

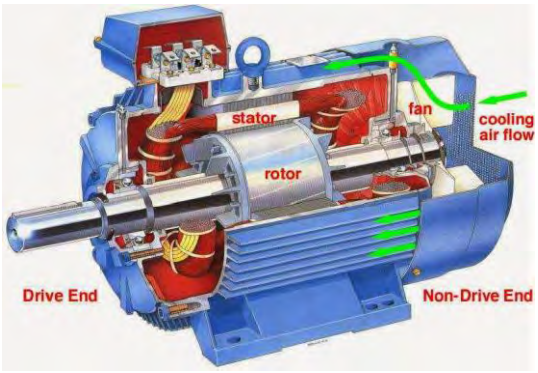

Fig.2.3.1 - Asynchronous generator [12]

Asynchronous three-phase generators, or induction generators, are one of the AC categories among the most popular in industrial applications, with fixed or variable speed. The electromechanical conversion that they implement follows the principle of the induction systems by direct application of the rotating magnetic field. An induction motor therefore does not require mechanical commutation, separate-excitation or self-excitation as DC and synchronous motors.

It includes a fixed part, the stator, and a moving part, the rotor, both in the shape of cylindrical crown of ferromagnetic material and separated by an air gap. On the cylindrical surfaces facing the air gap are formed the stator and rotor slots which are intended to hold the windings. The stator windings consist of three phases with the same number and distribution of turns, and shifted 120 degrees from each other.
There are two main kind of rotor windings: wound rotor and squirrel-cage rotor. The first type of circuit can be realized with a three-phase distributed winding. They are completely analogous to that of the stator and their terminals are owned by three rings on which slide three brushes that allow to connect rotor winding to an external circuit. In the second typology, the one concerning the CHP Kirsch L 4.12 generator, the rotor is realized by means of a set of bars of aluminum, one for each slot, all connected at the two ends by two rings.

2.3.1 The Operation

To understand how these machines work, it will be considered an open wound rotor, in order to neglect, at first, the effect of the currents in the rotor. The electrical quantity are sinusoidal, with constant current amplitude, fixed frequency and with engine running at a constant speed.

If the stator windings are fed by a system of three-phase balanced currents with pulsation ω_s, a rotating magnetic field is created in the air gap with speed :

$$\omega_0 = \omega_s / p = 2\pi \cdot f / p \qquad (2.3.1)$$

where *p* is the number of magnetic poles and *f* is the frequency in Herz.
Each stator's phase concatenates therefore a magnetic flux $\lambda(t)$ with a ω_s alternating pulsation.
The terminal stator's voltage has to balance the resistive voltage drop at the pulsation ω_s and the electromotive force $e = d\lambda(t)/dt$ induced by changes in the flux linkage.
Considering $0<\omega_m<\omega_0$, where ω_m is the mechanical speed of the rotor, the magnetic rotating field rotates with respect to the rotor with speed $\omega_0 - \omega_m$, also equal to $s \cdot \omega_0$ where *s* is the slip:

$$s= (\omega_0 - \omega_m)/ \omega_0 \qquad (2.3.2)$$

At full rated load, slip varies from more than s = 5% for small or special purpose motors to less than s = 1% for large motors, [13].
The difference of pulsation between rotor and stator allows to induce the electromotive force and so the currents in the rotor. Therefore in the opened rotor windings are induced a set of symmetric alternate potential differences with a pulsation $\omega_r = s \cdot \omega_s$.

Let's consider now the rotor windings closed; in the rotor now circulate three alternating balanced currents with a pulsation ω_r. The rotating magnetic field due to this set of currents rotates with respect to the rotor with positive speed proportional to the sliding pulsation equal to $\omega_{r0} = s \cdot \omega_0$ and then with respect to the stator speed with a pulsation $s \cdot \omega_0 + \omega_m = \omega_0$.

2.3 The generator

The rotating sinusoidal fields supported by the stator and rotor currents are synchronous and then fixed to one respect to each other. In this way is generated a constant torque which acts on the rotor with the same direction as the rotation of the magnetic field. In this way, the rotation of the rotor is supported [12].

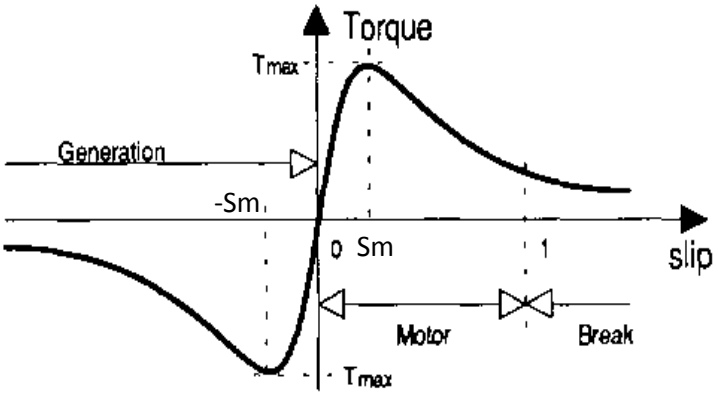

Fig.2.3.2 - Torque diagram of an induction motor [12]

As it is shown in Fig.2.4.2, there are many possible working condition:

- $\omega_m = \omega_0$; s = 0. The rotor speed is equal to the one of magnetic field, no electromotive forces are induced and no torque is produced.
- $\omega_m > \omega_0$; s < 0. The rotor speed is higher than the one of magnetic field. The machine works as a generator.
- $0 < \omega_m < \omega_0$; 0 < s < 1. The machine works as a motor and the torque produced is positive.
- $\omega_m < 0$; s > 1. The rotor rotates in the opposite direction of the one of magnetic field and the machine works like a break.

The machine runs in stable conditions when the slip is included between zero and s_m , where s_m is the slip corresponding to the maximum torque. In this area, when any increase in resistance torque occurs, the motor slows down and goes to work permanently to a new slide. This slide corresponds to a higher torque, with a value equal to the new value of the resistant torque request. This new condition of equilibrium will be reached after a series of oscillations around the equilibrium point; oscillations' trend depends on the rapidity of change in load, on the inertia of the rotating masses and on the presence of friction and damping of the motion. In the instability section, instead, for each increase in resistance torque, the engine slows down with a lower torque. In this way, after a while, depending on the kinetic energy of the rotating masses, the motor stops. The same happens in the generator working conditions.

The VEM G21R is used as a generator. This means that the rotation of the shaft induces alternate voltages in the stator windings. During the transient operation these voltages have variable frequency and amplitude. For this reason an inverter is required in order to give standard electrical quantities as output.

2.3.2 Variable-frequency drive

The generator of micro CHP L 4.12 is linked to the low voltage electric power net by means of a variable-frequency drive. This device allows the generator to work with variable frequency and voltage values. In this way, the system can feed the public net following the standard requirements related to the frequency and the amplitude of the voltage; this is possible in every operating conditions.
This particular drive device allows a bidirectional electric power flow with every combination of current-voltage polarity. It has been installed because, every time the machine has being switched on, the generator needs an input electric power to start the engine. Thus, the electric flow has the opposite sign because, during the starting, the electrical power is absorbed by the machine and not generated. The same thing occurs when the engine is switched off and the gas stops to flow.

The conversion system consists in three distinct sub-system: a rectifier bridge converter, a direct current link with LC filter, and an inverter.

This drive can work in every four quadrant of the speed-torque chart. This means that speed and torque may be in any direction, as is shown in Fig.2.3.3.

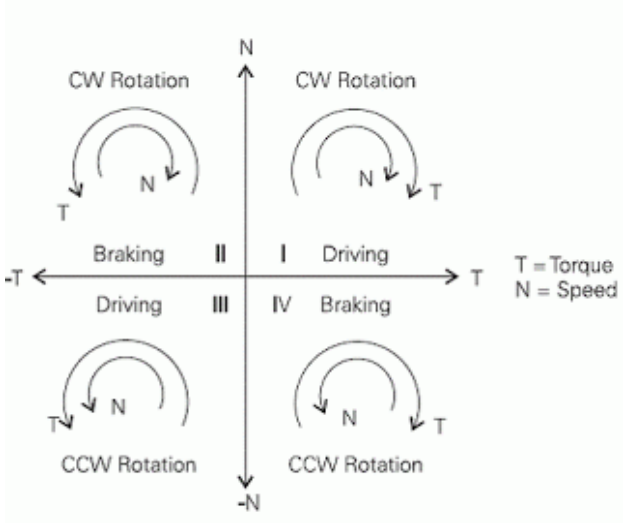

Fig.2.3.3 - Speed-torque chart [12]

2.4 Other components

In addition to the components mentioned above there are many other components with important features that have not been investigated in detail.
The structure without the heat insulated encapsulation is clearly showed in Fig.2.5.1:

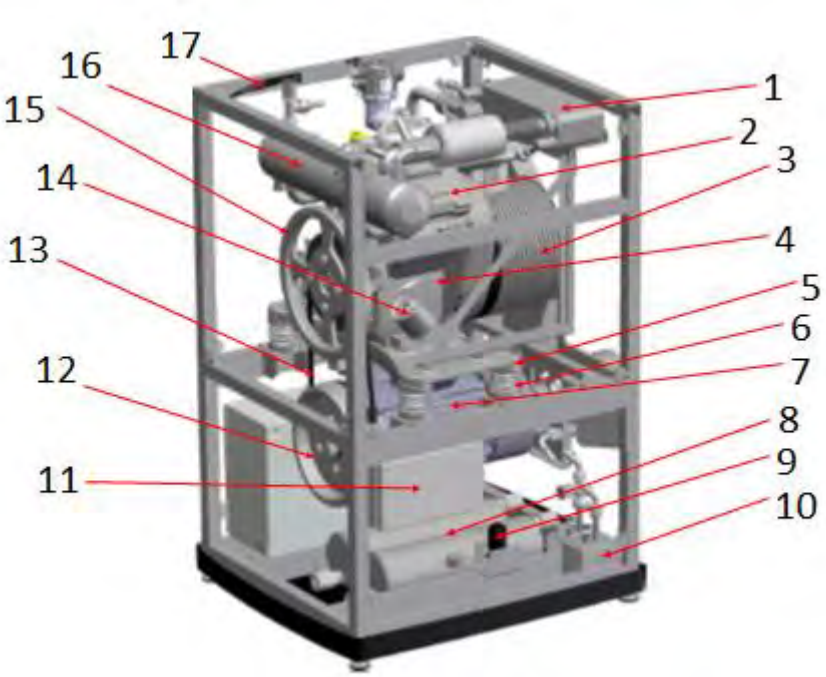

Fig.2.4.1 - Kirsch's structure [8]

1 Exhaust gas heat exchanger
2 Valve cover
3 Engine exhaust heat exchanger
4 Engine
5 Mounting plate
6 Spring elements
7 Generator
8 Oil tank
9 Oil Pumps
10 Oil heat exchanger
11 Terminal box
12 Flywheel of the generator
13 Ribbed belt
14 Oil filter
15 Flywheel of the engine
16 Back gas cooler
17 Gas sensor

2.5 The operation

Considering the heat transfer, it has the same system of a normal vehicle which uses water for cooling. The cold water coming from the utility, enters in the micro CHP system and starts to get warmer first with the heating exchangers at the lowest temperature. The first cylindrical heat exchanger uses the heat owned by the exhaust gas. Then the engine gives its exhaust heat

to the water thanks to a cylindrical air-water exchanger. At the high temperature there is a third heat exchanger facing with the oil circuit. This one has a plate shape.
A scheme of the heat exchange is showed in Fig.2.5.1.

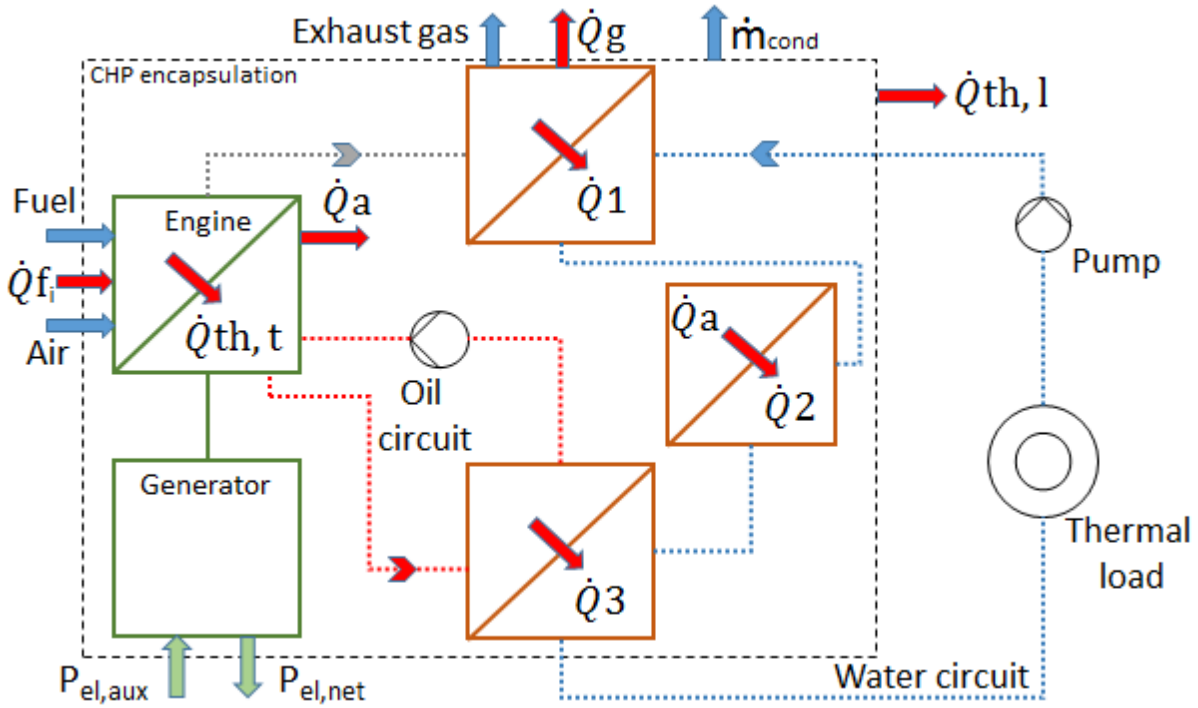

Fig.2.5.1 - Heat exchange scheme

Red arrows represent the thermal power fluxes and the blue ones show input and output of the entire system; the green arrows are related to the electric power.

Here the explanation of the symbols:

$\dot{Q}_{f,i}$= power owned by the fuel referred to the inferior heating value

$\dot{Q}_{th,t}$ = total thermal power produced by the engine

$\dot{Q}_a$ = engine thermal power transferred in the air-water exchanger

$\dot{Q}_g$ = thermal power owned by the exhaust gas

$\dot{Q}_{th,l}$ = thermal losses outgoing the CHP encapsulation

$\dot{Q}_1$, $\dot{Q}_2$, $\dot{Q}_3$ = thermal powers transferred to the water circuit through the three heat exchangers

$\dot{m}_{cond}$= mass flow of the condensing water

$P_{el,net}$ = net amount of electric power produced

$P_{el,aux}$ = electrical consumption of the machine

2.5.1 Calorific power

The input overall power comes into the system through the fuel, which has its own calorific power. This value is not constant and changes continuously during the measurements, depending on the chemical composition of the gas coming in the laboratory. This variation has been detected by the Danalyser Gas Chromatograph so that an accurate calorific power evaluation and a precise energy balance have been done.

The CHP fuel supplied power refers to the inferior calorific power that has roughly a value of:

$H_i = 10{,}01\ MJ/m^3_N$

where:

1 m^3_N = 1 m^3 at t = 0 °C (273,15 K) at an absolute pressure of p = 1,01325 bar.

The input power in the balances refers to the inferior calorific power and is:

$$\dot{Q}_{f,i} = \dot{V}_f \cdot H_i \qquad [W] \qquad (2.5.1)$$

The gas fuel owns also a value that considers the heat coming from the condensation. This value is called superior calorific power and is approximately:

$H_s = 11{,}11\ MJ/m^3_N$

and the power to it referred is:

$$\dot{Q}_{f,s} = \dot{V}_f \cdot H_s \qquad [W] \qquad (2.5.2)$$

The difference between the inferior and the superior calorific power represents the power owned by the condensing water.

$$\dot{Q}_{f,cond} = \dot{Q}_{f,s} - \dot{Q}_{f,i} \qquad [W] \qquad (2.5.3)$$

If the system would use this heat, the efficiency could reach a number higher than 100%.

2.5.2 Electrical power

The micro CHP L 4.12 generator can produce a 2, 3 or 4 kW electrical power. This amount of power has to feed all the auxiliary devices required for the entire generation process. The consumption is mainly due to the circulation pump, the air blower and the electronic control. In this way the power produced by the generator is gross and not net.

$$Pel_{NET} = Pel_{GROSS} - Pel_{AUX} \qquad [W] \qquad (2.5.4)$$

Furthermore the generator is equipped with a central control and regulation unit and with different safety devices. The main electrical consumptions are shown in tab. 2.5.1.

Tab. 2.5.1 - Electrical consumptions [14]

Components	***I* in mA**	***Pel* in W**
Gas valve	80	18.4
Main protection	25	5.75
Condenser protection	90	20.7
Electric control box	135	31.05
ε - regulation	105	24.15

Dealing with the circulation pump, some temperature limits have been followed. Their value depends on the operation conditions of the generator. During the heat-up operation they are higher than the ones in the cooling down operation.
As it is shown in tab. 2.5.2, the allowed temperatures increase with the increasing of the flow through the pump, because the heating exchange is favored by the increasing of the flow; in this way the temperatures can be higher.

Tab. 2.5.2 - Temperature limits of the pump [14]

Pump flow	**Flow temperature °C**	
%	**Warm-up**	**Cool-down**
0	<59	<59
30	<63	<61
50	<68	<66
75	<72	<70
100	<72	

The resulting net power can be measured by an electric meter that is linked to the power line. For the singles phases it can measure the voltage, the current flow, the frequency and phase angle.

2.5.3 Thermal power

The thermal power produced by micro CHP L 4.12 can be minimum $\dot{Q}_{th,net} = 5\ kW$ and reaches a value of roughly $\dot{Q}_{th,net} = 12\ kW$; it depends on the operation of the engine. If a higher electrical power is required, more thermal power is released by the engine and recovered by the thermal exchangers. The warm capacity $c_{p,water}$ of the water is constant and equal to 4189 J/Kg·k.

$$\dot{Q}_{th,net} = \dot{m}_{water} \cdot c_{p,water} \cdot (\vartheta_f - \vartheta_b) \qquad [W]$$

$$\dot{Q}_{th,net} = \dot{V}_{water} \cdot \rho \cdot c_{p,water} \cdot (\vartheta_f - \vartheta_b) \qquad [W]$$

$$\dot{Q}_{th,net} = \dot{V}_{water} \cdot \rho \cdot (h_f - h_b) \qquad [W] \qquad (2.5.5)$$

Where the density ρ is depending on the average temperature ϑm = $\frac{\vartheta f + \vartheta b}{2}$, and hf and hb are the enthalpy depending respectively on flow temperature and back flow temperature.
The portion of the whole thermal power related to condensation water is:

$$\dot{Q}_{cond} = \dot{Q}_{f,cond} \cdot \beta \qquad [W] \qquad (2.5.6)$$

$$\beta = \frac{\dot{m}_{cond}}{\dot{m}_0} \qquad (2.5.7)$$

where $\dot{m}_0$ is the starting portion of water in the exhaust vapor mass and $\dot{m}_{cond}$ is the portion of exhaust gas whose temperature goes under the dew temperature.
The ratio in (2.5.7) is a kind of efficiency of the condensing process and describes how much water can condense in comparison with the overall water in the exhaust.

The useful heat for the process is recovered in the three heat exchangers:

$$\dot{Q}_{th,net} = \dot{Q}_{th,t} - \dot{Q}_g - \dot{Q}_{th,l} = \dot{Q}_1 + \dot{Q}_2 + \dot{Q}_3 \qquad [W] \qquad (2.5.8)$$

where $\dot{Q}_g$ depends on two factors: one related to the difference between the exhaust gas temperature and the temperature of the ambient and the other related to the part of the gas which is not condensed. The term related to the part of the exhaust gas not condensed must be taken in consideration as a loss, because it is part of the superior calorific power and it is not recovered by the system.

$$\dot{Q}_g = \dot{Q}_{gas,th} + \dot{Q}_0 \qquad [W] \qquad (2.5.9)$$

$$\dot{Q}_{gas,th} = \dot{m}_{gas} \cdot c_{p,gas} \cdot (\vartheta_{gas} - \vartheta_{ambient}) \qquad [W] \qquad (2.5.10)$$

$$\dot{Q}_0 = \dot{Q}_{f,cond} \cdot \frac{\dot{m}_0 - \dot{m}_{cond}}{\dot{m}_0} = \dot{Q}_{f,cond}(1 - \beta) \qquad [W] \qquad (2.5.11)$$

2.5.4 Other losses

The remaining heat $\dot{Q}_{th,l}$ missing is due to the losses of the encapsulations of the micro CHP. This amount of heat is released to the ambient through radiation and convection phenomena. Its expression can be indirectly reached thanks to the other quantities:

$$\dot{Q}_{th,l} = \dot{Q}_{f,s} - P_{el} - \dot{Q}_{th,net} - \dot{Q}_{gas} \qquad [W] \qquad (2.5.12)$$

3 The laboratory

The laboratory where the measurements have been done contains, in addiction to other devices, the Kirsch L 4.12 generator, the thermal storage, the hydraulic system and the computers workbench. From there is possible to control the devices through a specific software. All the devices are linked to the computers via a LAN connection.

Fig.3.1 - Laboratory's view

Connected to the laboratory through a valve, a basin is located just behind the building.
Thanks to the large amount of water here contained, it allows to cool the water coming from the generator into the heat module through one of the three heat exchangers. The water from the external basin is first pumped to a roof located tank and then, from here, it flows down to the laboratory through a piping system.

Fig.3.2 - External basin

On the bottom of the basin has been installed a PT-100 temperature sensor to detect the temperature of the water. Furthermore has been installed a heat exchanger and a water-glycol hydraulic piping system between it and the building in order to avoid problems with ice during the winter.

3.1 Hydraulic system

The micro BHKW L 4.12 should not be thought as a stand-alone machine. Actually it is integrated inside the whole hydraulic system with its own inertia. In the simulation here analyzed, the house heating system is represented by some heating exchangers fed with cold water coming from the external basin. The heat power dissipated from these heat exchangers depends on the heat load of the emulated building.

The CHP generator and the heat exchange module are connected thanks to a piping system properly insulated. Before starting the measurements, the connection parts between these tubes and the generator has been insulated rolling them up with a particular insulating material. These movable tubes are represented in Fig.3.1.1 with a dashed line (n. 14).

In the whole hydraulic system there are 10 temperature sensors, 5 of one type, the PT100, and 5 of another type, the PT1000. These sensors measure the temperature with different accuracy. In this way it is possible to make an average of the two different values measured in the same spot. Four of these devices are placed on the generator side and four on the heat exchange module.
In order to analyze the trend of the thermal power and the efficiency changings, two sensors are put, by the generator side, on the front flow (n. 19) and on the back flow (n. 18). By the heat exchange module side, respectively, on the front (n. 20) and on the back flow (n. 17).

The remaining two thermal sensors (represented in the Fig.3.1.1 by the number 12) have been installed to detect exactly the temperature of the flow going out the mix, made from the three-ways valve.
As will be shown in the next chapters, this thermal value is really important for developing the thermal emulation led by the software.

3.1 Hydraulic system

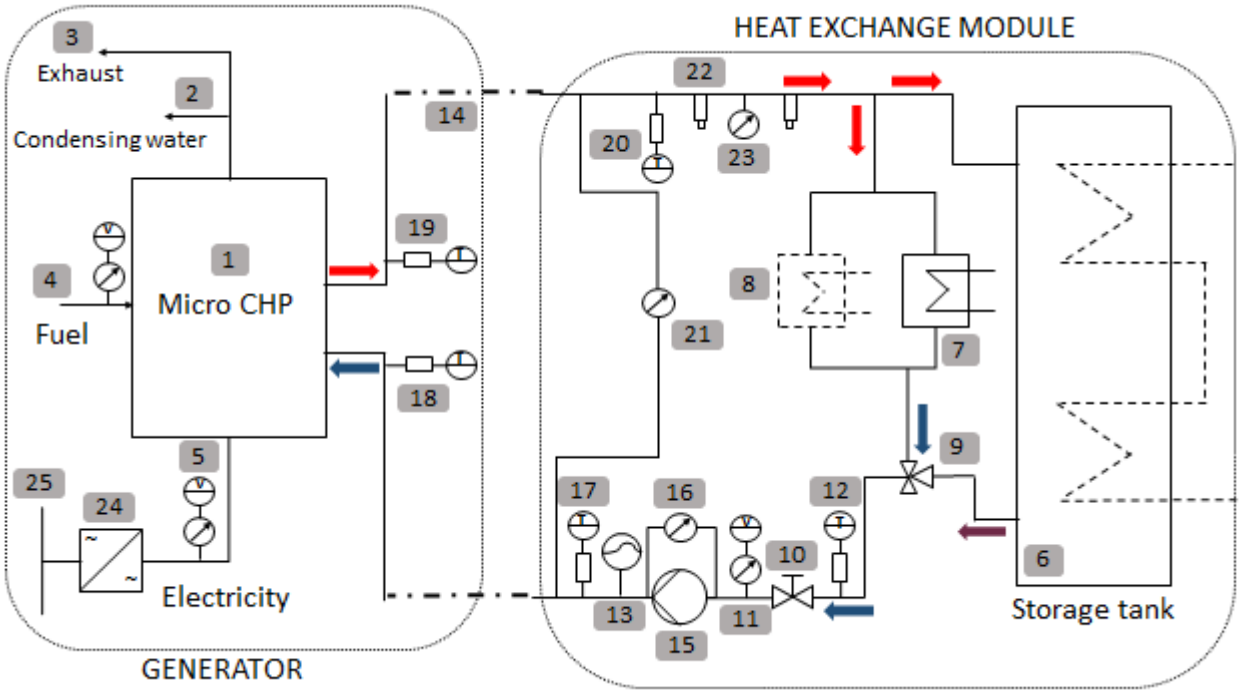

Fig.3.1.1 - Scheme of the hydraulic system

1 Micro-CHP L 4.12
2 Condensing water
3 Flue gas
4 Gas fuel meter
5 Electric power meter
6 Storage tank
7 External basin heat exchanger
8 Secondary heat exchanger
9 Three-ways valve
10 Control valve
11 Flow mass meter
12 PT 100/1000 sensor
13 Expansion vessel
14 Hydraulic binding
15 Water pump
16 Differential pressure meter
17 Back flow temperature PT 100/1000 sensor (heat exchange module side)
18 Back flow temperature PT 100/1000 sensor (generator side)
19 Flow temperature PT 100/1000 sensor (generator side)
20 Flow temperature PT 100/1000 sensor (heat exchange module side)
21 Differential pressure meter
22 Regulation valve
23 Digital manometer
24 Variable-frequency drive
25 Public electric net

3.1.1 Heat exchange module

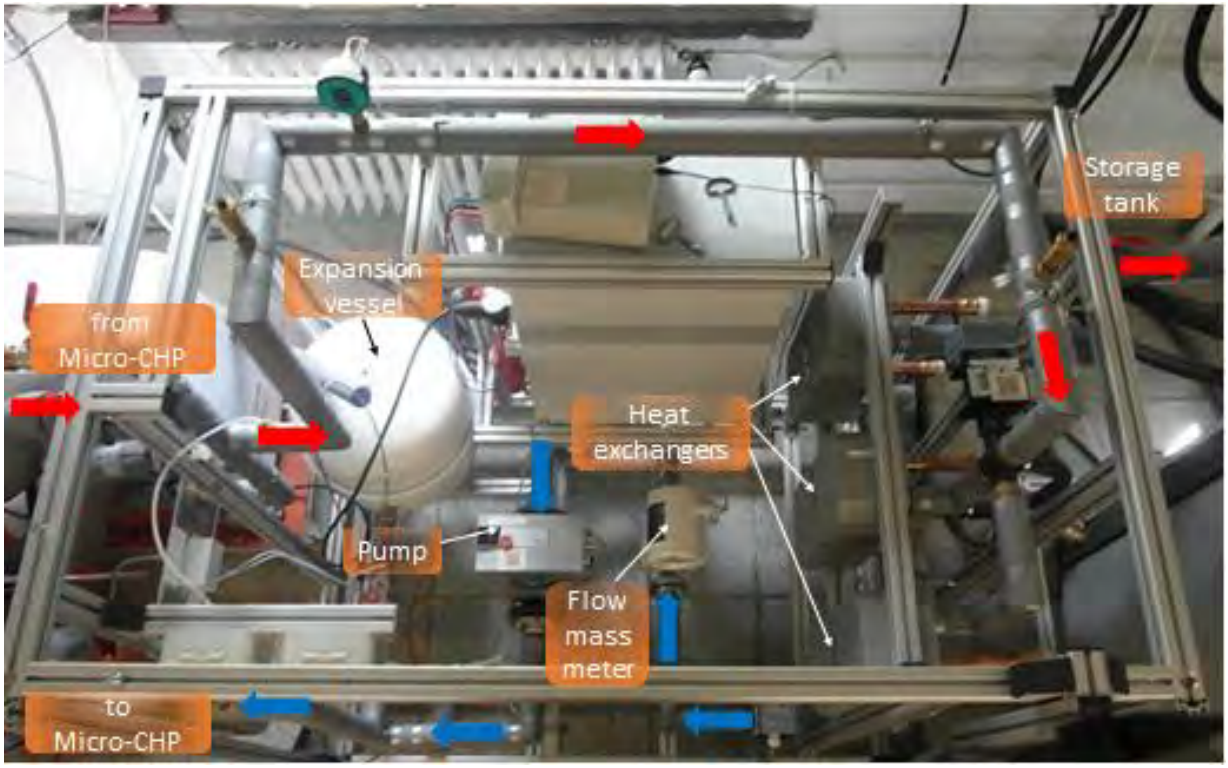

Fig.3.1.2 - Heat exchange module's scheme

Coming from the micro-CHP, the hot water flow splits itself in two parts. One goes to the storage tank, and the other to the two heat exchangers. Actually only one heat exchanger works, and cools the water of the hydraulic circuit through the water coming from the external basin.

The water contained inside the storage tank has a constant value of roughly 70°C because it is warmed thanks to some electrical resistances. Thus, the part of the water coming from the micro-CHP which goes inside the storage tank reaches immediately 70°C mixing itself with the large amount of warmer water.

The other part of the water is completely cooled down by the external basin water to a temperature closed to the one set in the basin.

Thanks to the three-ways valve it is possible to obtain a target temperature in an extremely accurate way. This is possible taking the entire cool flow coming from the external basin heat exchanger and a fraction of the hot water outgoing the storage tank. For different back flow temperatures the opening of the three-ways valve changes, and so the fraction of hot water too.

A part of the incoming water is directed to the storage tank for an obvious reason: without an input the tank would empty down in few hours. The input water incoming the tank is automatically regulated by the opening of the three-ways valve downstream.

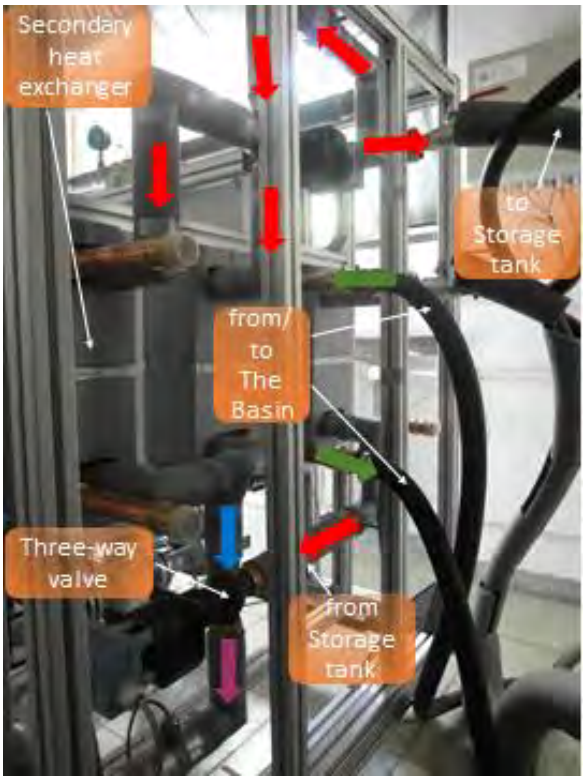

Fig.3.1.3 - Storage tank side of heat exchange module

In Fig.3.1.3 are clearly shown the parts of this system and the route of the water. The green arrows represent the cooling water coming from the external basin.

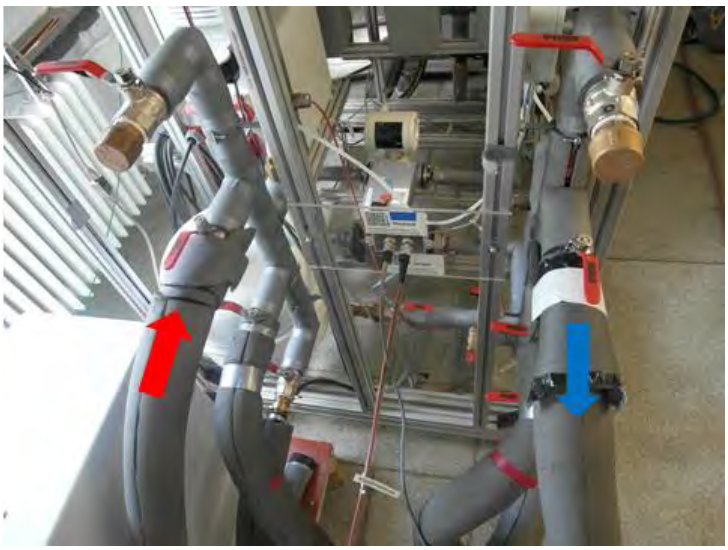

Fig.3.1.4 - CHP's side of the heat exchanger module

On the other side of the module there are eight possible input that allow to link different machines. As is clear from the position of the faucets in Fig.3.1.4 , only two of them are used.

3.1.1.1 Regulation valve

The regulation valve is a device installed in the heat exchange module. It has been used when the module is getting prepared for the measurement. Initially, in fact, the hydraulic circuit was empty and the water had been pumped inside from an external source. During this process some air has been leaked in. To ensure a correct operation of the circulation pump and to preserve the hydraulic circuit avoiding the corrosion, the air has been removed.
The function of this device is actually to remove the air out of the hydraulic system without letting the water going out. The valve is shown in Fig.3.1.5.

3.1.1.2 Digital manometer

In particular during the process described above, and also during the whole measurement, the pressure must be checked. For this reason the LEO 3 digital manometer from KELLER has been installed.
A piezoresistive pressure transducer is the heart of the instrument. The pressure is measured twice per second and displayed. The top display indicates the actual pressure, the bottom display shows the maximum or minimum pressure since the last reset [15].

Fig.3.1.5 - Regulation valve

Fig.3.1.6 - Digital manometer

3.1.1.3 Three-ways valve

For the regulation of the back flow temperature it has been used the MXG461 20-5.0 three-ways valve from SIEMENS.
The valve is suitable as mixed and straight valve. It can be used for the control of cold and hot water systems and its control modulating works thanks to a magnetic system.

Tab. 3.1.1 - Three-ways valve's data [16]

Max_operating pressure	1 MPa
Nominal pressure (PN)	16 bar
Nominal diameter (DN)	20 mm
Operating temperature	-5°C up to 45°C
Type	Equal percentage, linear
Δp_max	300 kPa
k_{vs}	5 m^3/h
Consumption	29 VA

Δp_max is the maximum differetial pressure allowed with valve completely opened. K_v is a typical value of the valves and represents the volumetric water flow at ϑ = 5-30°C which flows through the valve in one hour and with a pressure of P = 1 Pa; it is expressed in m^3/h. K_{vs} is referred to the valve completely opened. The regulation follows a linear characteristic for the straight way and an equal percentage for the other. The regulation characteristics are both shown in Fig.3.1.7.

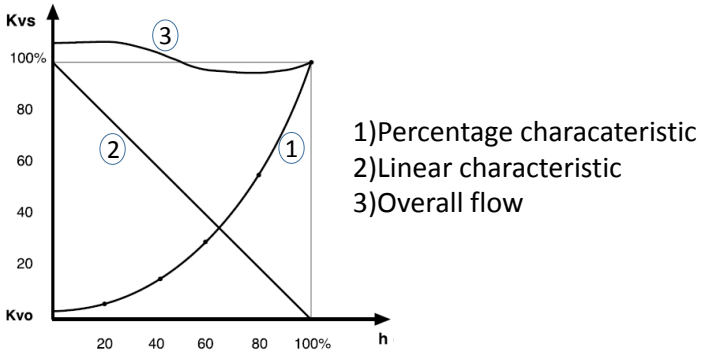

Fig.3.1.7 - Regulation diagram [17]

The curve number 3 is the sum of the two input flows and represents the overall flow outgoing the valve. On the x-axis is represented the opening rate of the valve. K_{v0} is the minimum value for K_v.

3.1.1.4 Volume flow - Control valve

This straight valve is located between the three-ways valve and the circulation pump and its model and data are the same of the three-ways valve. Its function is to regulate the overall flow. During the measurement precise volume flow values have been used, from $\dot{V} = 150\ l/h$ up to $\dot{V} = 450\ l/h$ by steps of $\dot{V} = 50\ l/h$. Thus, this valve has exactly to allow this precise values to pass through with the right opening rate. The current flow value is displayed by the volume flow meter.

3.1.1.5 Expansion vessel

The vessel has an 8 liters capacity and belongs to REFLEX company. The model is “N” and inside has a fixed membrane. The function of this device is to regulate the pressure inside the hydraulic circuit. In a part of the vessel there is nitrogen and in the other the water of the hydraulic circuit. When the pressure of the water changes, nitrogen can compensate the pressure variation elastically deforming the membrane.

Tab. 3.1.2 - Technical data of the vessel [18]

T_max supply	120 °C
T_min	-10 °C
T_max diaphragm	70 °C
Max operating pressure	3 bar
Min operating pressure	0 bar

3.1.2 Storage tank

The tank used is the VITOCELL-B100, type CVB. It is internally electrically heated and made up of steel with Ceraprotect enamel. It is available with a 300, 400 and 500 liters storage capacity. It has two internal coils with the possibility to heat separately the drinkable water. The drinkable water does not get in contact directly with the water in the tank, in order to observe the hygienic regulations.

Fig.3.1.8 - Storage tank VITOCELL-B100

Fig.3.1.9 - Storage tank without external

The tank has these main features [19]:

Tab. 3.1.3 - Main features of VITOCELL-B100

Volume	500 l
Max input temperature	160 °C
Drinkable water temperature	95 °C
Max operating pressure	10 bar
Number of thermal sensors	16

The heating of the entire water content is fast and uniform thanks to a heating coil installed in the bottom of the tank, in addiction to the electric resistances. Low thermal losses are ensured by a high efficiency insulating cladding. The Ceraprotect enamel ensures a long-time corrosion protection.

Dealing with the hydraulic connection between the micro CHP and a generic thermal load of a building, two are the possible configurations [14]:

- Direct heating-side integration
- Heating-side integration through a storage tank

The direct heating-side integration is used if the flow temperature can be adapted relating to the trend of the load. Usually this system is used when the flow temperature can be a function of the external temperature. This means that the machine is allowed to modulate the heat power in a continuous way through its internal pump. A tank is linked to the hydraulic circuit only to heat the drinkable water. This tank should be thought as a heat exchanger where the two fluids do not get in touch.

Let's consider standard building with a conventional operation. If a storage tank has been installed, the generating unit can follow the load trend producing power discontinuously, depending on the size of the tank. The operating is completely equal to the one of a boiler. When the entire volume of water contained in the tank reaches the target temperature, the engine can be switched off until the water's temperature lows under the cutoff limit; thereafter the engine switches on again. In this way the heating demand is decoupled from the generation from an hydraulic point of view.

A storage tank ensures:

- A longer life-time
- A reduction of clock cycles
- An hydraulic decoupling between the generation and the consumption

To determine the volume of the storage, the time constant τ required to reach the target temperature, the difference of temperature of input and output Δϑ, and the thermal power $\dot{Q}_{th,net}$ must be known:

$$V = \frac{\dot{Q}_{th,net} \cdot \tau}{c_p \cdot \rho \cdot \Delta\vartheta} \qquad [l] \tag{3.1.1}$$

Obviously, bigger is the tank and more is the time needed to reach the aim temperature with a constant thermal power. Usually, the temperature difference takes values as Δϑ = 5 – 10K. The warm capacity and the density are constant too. The values are c_p = 4189 J/Kg· K and ρ =

1000 Kg/m^3. Thus, chosen a time constant, the volume is directly depending on the thermal power.

Considering a $\Delta\vartheta$ = 10 K and a τ = 2 h, the volume needed pro kW_{th} is:

$$V = \frac{1000 \cdot (2 \cdot 3600)}{4186 \cdot 1 \cdot 10} = 172 \qquad \left[\frac{l}{kW_{th}}\right] \qquad (3.1.2)$$

This value is useful to understand the dimensions of the storage tank, considering that normally the thermal power takes values of about $\dot{Q}_{th,net} = 10\ kW$.

3.2 Tools

3.2.1 Temperature sensors

To ensure a correct heat accounting for both the generation and consumption side, it has been installed the Pt100 and Pt1000 thermal sensors.

Fig.3.3.1 - Pt 1000 thermal

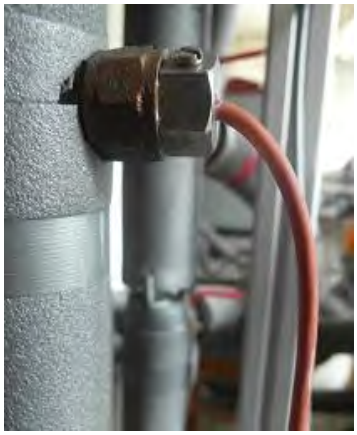

Fig.3.3.2 - Pt 100 thermal sensor

With a platinum sensor material, they detect the temperature thanks to the resistance variation. The platinum's coefficient α of resistance variation from 0°C to 100°C is:

$\alpha_{platinum} = 0.003925$ *[1/K]*

Nominal resistances R_0 at 0°C and the errors are respectively:

Tab.3.3.1 Resistance and errors of thermal sensors [14]

Model	**R_0**	**Error**
Pt100	100 Ω	CLASS B: 0,3°C $\pm$ 0,005 ·ϑ
Pt1000	1 kΩ	CLASS B: 0,3°C $\pm$ 0,005 ·ϑ

where the error has a constant part and a variable one, depending on the temperature's value. Platinum is the best metal for thermal sensors because it has a linear resistance-temperature relationship. This property works over a wide temperature range. It respects the temperature standards over the range of -272.5 °C to 961.78 °C [20].
These sensors are designed for installation in industrial resistance thermometer or in an integrated circuit. Due to their low marginal deviations they are interchangeable without recalibration in most cases.

3.2.2 Volume flow meter

For the volume flow measurement it is used the ABB ProcessMaster FEP 300 flow meter from ABB. It works with a magnetic-inductive operating principle. Perpendicular to the magnetic field are arranged measuring electrodes that induce a voltage depending on the deflective effect.

Its main features are listed in Tab. 3.3.2:

Tab. 3.3.2 - Technical data of ABB volume flow meter [21]

Material	Stainless steel
T_max	130°C
Operating temperature	20°C up to 60°C
Power supply	230V AC, 50Hz
Flow_max	100 l/min
Measured value error $u(\dot{V})$	Standard: 0,4% of rate Optional: 0,2% of rate

Using a higher excitation frequency for the transmitter, it has an especially short response time. With advanced filtering methods, the device improves accuracy even under difficult conditions by separating the noise from the measuring signal. This leads to a maximum measuring error of $u = 0{,}2\%$ of rate. The self-cleaning measuring electrodes enhance the

Fig.3.3.3 - ABB volume flow

device's reliability and performance. Typical values of volume flow are from $\dot{V} = 150l/h$ up to $\dot{V} = 500l/h$.

3.2.3 Circulation pump

For the circulation of water has been installed a 40/1-12 Wilo Stratos pump from WILO.
This device can work with heating water or with a water-glycol mixture and is integrated with the Setra Dp-sensor 231MS1 from SETRA. This device measures the pressure before and after the circulation pump.

Main data are shown below:

Tab.3.3.3 - Technical data of the Circulation pump [22]

Max_flow	19 m^3/h
Flange nominal size	40 mm
Power supply	230V, 50Hz
Max_operation pressure	6/10 bar
Flow temperature range	-10°C up to 110°C
Max_Tamb	40°C
Engine's power	350 W
Consumption	25-470 W

Fig.3.3.4 - Circulation pump

3.2.4 Gas flow meter

To detect the gas mass flow has been used a gas flow rate meter. This device allows to understand the mass flow of the gas through the variation of temperature between the way in and the way out of the device. There are two temperature sensors: a heat sensor and another sensor that measures the temperature of the gas. Mass flow rate is computed depending on the amount of electrical power required to maintain a constant difference of temperature between the two temperature sensors [23]. The error is $u = 0{,}5\%$ of the measurement value.

3.2.5 The balance

The condensing water is measured by Pcb 6000-1 from KERN. The values are sent each second to the software. The error of the measurement is $u = \pm 0{,}01\text{g}$. The tank on the scale contains the water coming from the condensing water valve. The balance can measure only up to 6 liters. Thus, during the measurements the tank must be emptied in order not to go over the limit value.

Tab. 3.3.4 - Technical data of the scale [24]

Readabilty	0,1 g
Weight range	6000 g
Linearity	± 0,3 g
Warm-up time	2 hours
Stabilization time	3 s
Operating temperature	+5°C up to +35°C

3.2.6 Flue gas analyzer

Flue gas have been detected by the gas analyzer J2KN from ECOM. It can analyze the exhaust gas composition, in addiction to the exhaust gas temperature. Inside the tool case there is also a detachable control panel, equipped with a flexible data memory multi-media card, which allows to see the main data moving away from the device, through a radio transmission (Fig.3.3.6). To ensure good long-term measurements, ECOM J2KN is suited by a nearly complete dehumidification of the sample gas.
The device has a $u = 0{,}5\%$ margin of error of measured value.

Fig.3.3.5 - ECOM J2KN gas analyzer

Fig.3.3.6 - Detachable control panel

The modular probe has been installed directly inside the exhaust gas pipe after the condensing water valve (Fig. 3.3.7). It allows to measure the following values:

Tab. 3.3.5 - Technical data of flue gas analyzer [25]

Parameter	Range	Principle
O2	0-21%	Electrochemistry
CO	0-4000 ppm	Electrochemistry
NO	0-1000 ppm	Electrochemistry
NO2	0-5000 ppm	Electrochemistry
CO2	0-CO2max	Calculation
T_gas	0-1000°C	NiCr/Ni
T_air	0-99°C	Semiconductor
Efficiency	0-120%	Calculation
Losses	0-99.9%	Calculation

where *ppm* means parts per-million.

Fig.3.3.7 - Exhaust system

3.2.7 Chromatograph gas analyzer

To analyze the gas incoming the laboratory has been used the natural gas Chromatograph Danalyzer from DANIEL industry, model 500. The possible functions of this device are several: calorific power measurement, trace contaminant monitoring, pipeline integrity, product quality and process control.
For the measurements the gas analyzer it is used mainly to detect the composition of the natural gas and to calculate the variations of the calorific power of the mixture with the variation of time.
The device consists mainly in a *mobile phase* and a *stationary phase*. The *mobile phase* is a carrier gas, usually an inert gas such as helium or an unreactive gas such as nitrogen. The *stationary phase* is a microscopic layer of liquid or polymer on an inert solid support, inside a piece of glass or metal tubing called *column*. The gaseous compounds being analyzed interact

with the walls of the column, which is coated with the *stationary phase*. This causes each compound to elute at a different time, known as the retention time of the compound. In a second time, the software makes the comparison of retention times and analyzes the composition of the gas [26].

The MON2000 software allows to control the analysis, review and modify settings, display multiple chromatograms on the screen for comparison, trend any of the measured results and export data.

Fig.3.3.8 - Chromatograph gas analyzer

3.3 The control software

Inside the whole software which controls the K06 laboratory, a part is dedicated only to Kirsch L 4.12. In this section are available several devices to control the laboratory and to obtain information.
In Fig. 3.4.1 is shown the main dialog, where is possible to see all the devices of the hydraulic system, already sketched in Fig. 3.1.1. The visual representation of the test set with measured values, allows a quick evaluation of the data and simplifies the operation. The internal pump of Kirsch is not represented because is thought as integrated inside the machine.

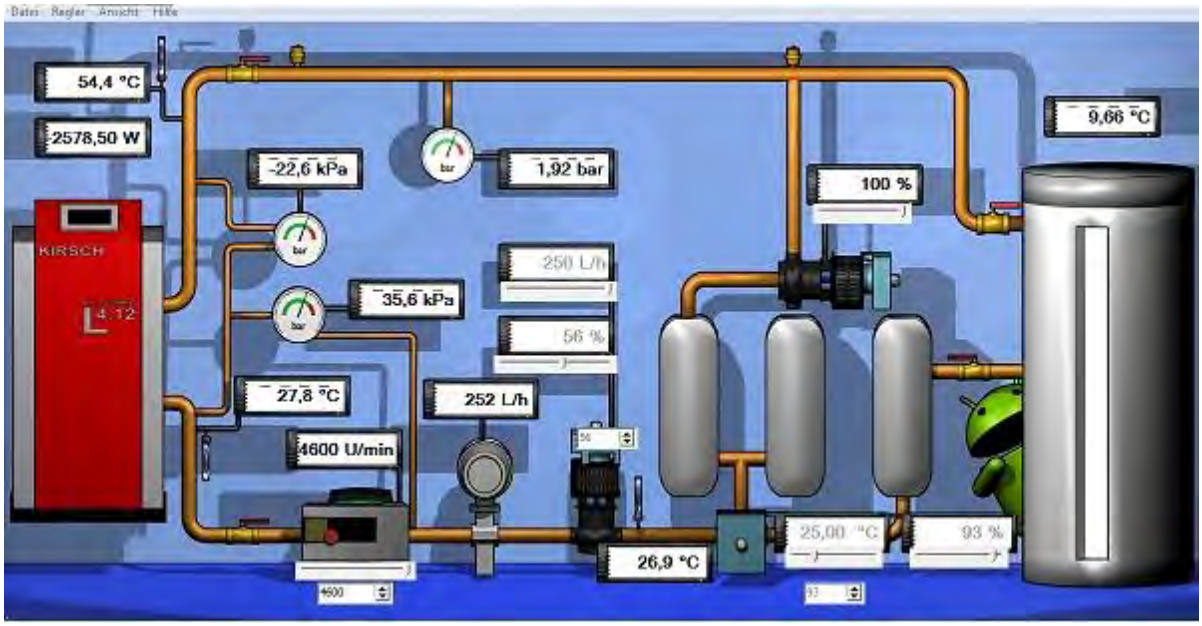

Fig.3.4.1 - Main dialog of K06 datalogger

Furthermore, in the Kirsch micro CHP dialog is possible to analyze the trends of the condensing water in grams and of the electrical power as function of the time. The temperature numerical values of the engine cylinders and of the oil are shown as well. In the left-upper side can be read the exhaust gas values.
In the analyzer dialog it is possible to see the trends of all the quantity involved in the measurement simply dragging them into it.
The storage tank dialog allows to detect the temperature of the storage tank as function of the position along the tank.
There is also a dialog that shows the temperatures gained by the thermal sensors and a dialog referring the volume flow and the calorific power of the gas.
All measured values are permanently recorded internally and saved in CSV file format.

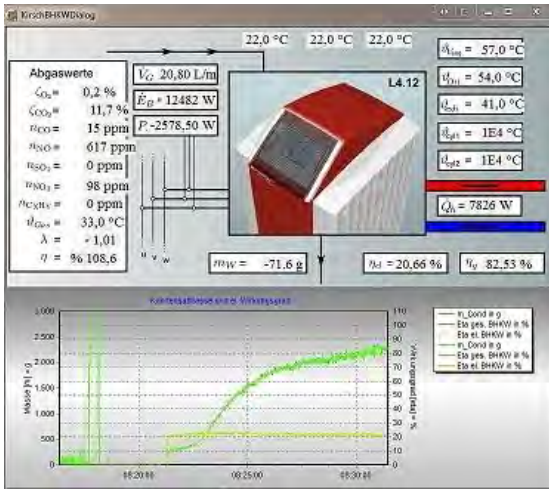

Fig.3.4.2 - Kirsch micro CHP dialog

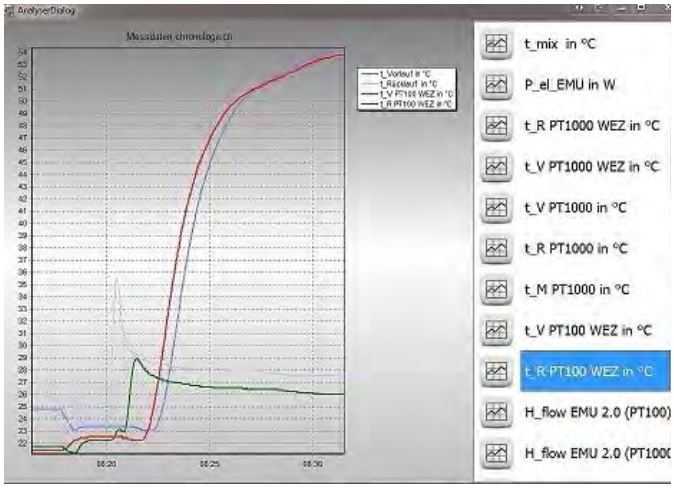

Fig.3.4.3 - Analyzer dialog

4 Measurements

4.1 Theoretical references

In this chapter are shown theoretical values obtained from the measurement of actual quantities. They are mostly instantaneous because referred to power values. Only the standard efficiency is an integral value, and it is useful to comprehend the average trend of the efficiency in a long term period.

4.1.1 Efficiencies

The electrical and heating efficiencies are the most important values for the evaluation of the micro CHP L 4.12 performance. They are calculated referring to the inferior calorific power. For this reason, if water condensation occurs, the overall efficiency can reach values over 100%; using the energy owned by the condensing water, the useful output energy, sum of the electrical and the thermal one, is higher than the inferior calorific power.

Neglecting the internal losses of the system, gross efficiencies would be calculated:

$$\eta_{el,gross} = \frac{P_{el,net} + P_{el,aux}}{\dot{Q}_{fi}} \cdot 100\% \qquad [\%] \qquad (4.1.1)$$

$$\eta_{th,gross} = \frac{\dot{Q}_{th,net} + \dot{Q}_g + \dot{Q}_{th,l}}{\dot{Q}_{fi}} \cdot 100\% \qquad [\%] \qquad (4.1.2)$$

Considering the net quantities, lower values occur. They are so defined:

$$\eta_{el,net} = \frac{P_{el,net}}{\dot{Q}_{fi}} \cdot 100\% \qquad [\%] \qquad (4.1.3)$$

$$\eta_{th,net} = \frac{\dot{Q}_{th,net}}{\dot{Q}_{fi}} \cdot 100\% \qquad [\%] \qquad (4.1.4)$$

The overall efficiency is referred to the total power gained from the chemical power of the gas fuel. It is defined like:

$$\eta_{overall} = \eta_{el,net} + \eta_{th,net} = \frac{P_{el,net} + \dot{Q}_{th,net}}{\dot{Q}_{fi}} \cdot 100\% \qquad [\%] \qquad (4.1.5)$$

4.1.2 Power to heat ratio

This is an import value to understand how the power gained from the fuel is shared between the electrical and the thermal side. It can be expressed as quotient of the respective efficiencies:

$$\sigma = \frac{P_{el,net}}{\dot{Q}_{th,net}} = \frac{\eta_{el,net}}{\eta_{th,net}} \tag{4.1.6}$$

4.1.3 Standard efficiency

The standard efficiency is the integral of the overall efficiency calculated on a determined period. The period of the calculation includes the starting warm-up of the engine and the final shut-down. In this way it can be thought as an average of the overall efficiency over the operation time of the machine. During that period, changings in the user load demand can also occur.

$$SE_{net} = \frac{W_{el,net} + Q_{th,net}}{Q_{fi}} \cdot 100\% = \int_{t0}^{t} \eta_{overall}(t)dt = \frac{\int (P_{el,net} + \dot{Q}_{th,net})dt}{\int \dot{Q}_{fi}\, dt} \cdot 100\% \quad [\%] \tag{4.1.7}$$

4.2 Errors analysis

In order to ensure a complete analysis, precise information about the quality of the measurements must be provided. Considering the errors of the devices used in laboratory coming from the data sheets, the error of the overall efficiency will be calculated.
The uncertainty of the indirect quantities, so the values that depend on more than one other measurement, normally must be calculated with the formulation of maximum error:

$$u(y) = \sqrt{\sum_{i=1}^{N} \left(\frac{\partial f}{\partial x_i}\right)^2 \cdot u^2(x_i)} \tag{4.2.1}$$

where the measurement *y* is a function of different unknowns:

$$y = f(x_1, \dots, x_N) \tag{4.2.2}$$

In order to make easier the explanation, it will be used the law of Gaussian propagation to calculate the uncertainty:

$$u(y) \approx \sqrt{\sum_{i=1}^{N} u^2(x_i)} \qquad (4.2.3)$$

This decision has been done because the quantities considered, in the steady state, are almost constant during the 15 minutes of measurement and the term $\left(\frac{\partial f}{\partial x_i}\right)^2 \cong 1$.

4.2.1 Thermal power

Thermal power depends on other two quantities, the temperature and the volume mass flow. Considering that the error of the Pt-1000 and Pt-100 sensors is:

$$u_{100/1000}(\vartheta) = 0{,}3°C + 0{,}005 \cdot |\vartheta|$$

and that normally the flow and back flow temperatures stay in these ranges:

$$40°C \leq \vartheta_f \leq 80°C \; ; \; 20°C \leq \vartheta_b \leq 50°C$$

the absolute errors, considering for each one the medium temperature, are:

$$u_{100/1000}(\vartheta_f) = \pm 0{,}6K$$
$$u_{100/1000}(\vartheta_b) = \pm 0{,}475K$$

$$u_{rel,100/1000}(\vartheta_f - \vartheta_b) = \pm \frac{\sqrt{u_{1000}^2(\vartheta_f) + u_{1000}^2(\vartheta_b)}}{(\vartheta_f - \vartheta_b)} \cdot 100\% \cong \pm 2{,}55\% \qquad (4.2.4)$$

The quantity $(\vartheta_f - \vartheta_b)$ is variable for every measurement, and normally has values comprehended between $20\ °C \leq (\vartheta_f - \vartheta_b) \leq 40\ °C$.

Regarding the volume mass flow the expression is:

$$u(\dot{V}_w) = \pm 0.005 \cdot \dot{V}_w$$

Finally the uncertainty of the thermal power is:

$$u_{rel}(\dot{Q}_{th,net}) = \pm \sqrt{u_{rel}^2(\vartheta_f - \vartheta_b) + u_{rel}^2(\dot{V}_w)} = \pm \sqrt{0.0255^2 + 0.005^2} \cong \pm 2{,}6\% \qquad (4.2.5)$$

4.2.2 Fuel power

Fuel power depends on the calorific power and on the fuel volume mass flow.
The relative uncertainty of the calorific power is:

$$u_{rel}(H_i) = \pm\frac{u(H_i)}{H_i} = \pm\frac{0{,}0473\ kWh/m_N^3}{10{,}0179\ kWh/m_N^3} \cong \pm 0{,}47\% \qquad (4.2.6)$$

The uncertainty of the fuel volume mass flow is:

$$u(\dot{V}_f) = \pm 0.005 \cdot \dot{V}_f$$

Thus, the formulation of the fuel power is:

$$u_{rel}(\dot{Q}_{f,i}) = \pm\sqrt{u_{rel}^2(H_i) + u_{rel}^2(\dot{V}_f)} = \pm\sqrt{0.0047^2 + 0.005^2} \cong \pm 0{,}67\% \qquad (4.2.7)$$

4.2.3 Overall efficiency

The uncertainty of the electric power is:

$$u(P_{el,net}) = \pm 0.001 \cdot P_{el,net}$$

Considering an electric power of $P_{el,net} = 3kW$ and a thermal power of $\dot{Q}_{th,net} = 10kW$ the relative uncertainty of the overall efficiency can be written as:

$$u_{rel}(\eta_o) = \pm\sqrt{\left(\frac{u(P_{el,net})}{P_{el,net} + \dot{Q}_{th,net}}\right)^2 + \left(\frac{u(\dot{Q}_{th,net})}{P_{el,net} + \dot{Q}_{th,net}}\right)^2 + u_{rel}^2(\dot{Q}_{f,i})}$$

$$u_{rel}(\eta_o) = \pm\sqrt{\left(\frac{0{,}03kW}{3kW + 10kW}\right)^2 + \left(\frac{0{,}26kW}{3kW + 10kW}\right)^2 + (0.0067)^2} \cong \pm 2.12\% \qquad (4.2.8)$$

4.3 Steady state

In this part of the analysis, the measurements have been made in steady state conditions. This means that the performances of the machine have been considered only with a constant power amount, a constant flow and constant temperature values.

It was important to switch off the internal circulation pump of the micro CHP L 4.12 to control the machine directly from the software. Otherwise the machine would have worked in an autonomous way not following the temperature trend imposed by the timetable.

For each of the three electrical level, P = 2kW, P = 3kW, P = 4kW the measure has been done with this following water flow values:

- $\dot{V} = 200\ l/h$
- $\dot{V} = 250\ l/h$
- $\dot{V} = 300\ l/h$
- $\dot{V} = 350\ l/h$
- $\dot{V} = 400\ l/h$
- $\dot{V} = 450\ l/h$

$\dot{V} = 150\ l/h$ value has been investigated only with the $P_{el,net} = 2kW$ level, because with the other levels too high flow temperatures would have been reached.

4.3.1 Measurement start

The procedure to start each measurement consists at first of opening the valve of the water coming from the external basin. Then the micro CHP machine must be switched on in the stand-by mode. After the flue gas analyzer and the scale have been switched on, the software can be started clicking on *K06datalogger.exe*.
To allow the circulation of the water in the hydraulic circuit, the external pump must be set on a sufficient power level. Before switching on the machine to the running mode and starting the timetable of the current measurement, the water flow and the back flow temperature must be set on the values corresponding to the current measurement.

4.3.2 Timelines

Ones switched on, the machine takes about 6 minutes to warm up. During this period the thermal power increases and the electrical power produced settles to the target values after some fluctuations. Then, the running mode starts and the timetables can be started.
Each measurement of each water flow takes about six hours to be carried out. The whole timetable is so split up:

- 105 min: preparation
- 15 min: measure achievement
- 45 min: transient between two measures

For each flow value, the measurement is obtained for several back flow temperatures:

- $\vartheta_b = 25\ °C$
- $\vartheta_b = 30\ °C$
- $\vartheta_b = 35\ °C$
- $\vartheta_b = 40\ °C$
- $\vartheta_b = 45\ °C$

The 45 minutes of transient between the measures, corresponding to each back flow temperature, are taken in order to have a constant temperature value for each measure in order to satisfy the steady state conditions.

During the normal operation of the machine the natural gas amount is almost constant. Remaining the produced electrical power constant, and assuming the losses and the consumptions of the auxiliary devices constant too, the thermal power remain constant as well. Its range is about $8\ kW \leq\ \dot{Q}_{th,net} \leq 12\ kW$.

According to thermodynamics:

$$\dot{Q}_{th,net} = \dot{m}_{water} \cdot c_{p,water} \cdot \left(\vartheta_f - \vartheta_b\right) \qquad [W] \qquad (4.3.1)$$

Considering a whole measurement relative to one distinct $\dot{m}_{water}$, the difference between the flow and the back flow temperature $\Delta\vartheta_{fb}$ is constant. Thus, the trends of the flow temperature and the back flow temperature have the same shape translated one from the other of a constant quantity.

4.3.3 $P_{el,net}$ = 2 kW electrical power

In the next pages are shown the diagrams of the output quantities of the system, the electrical and the thermal power, with the related efficiencies, as function of the back flow temperature. The most important parameter is the overall efficiency, because describes the performance of the whole system considering the losses of both the electrical and thermal sides. Its values are shown in Tab.4.3.1.

Tab.4.3.1 - Overall efficiency values, 2kW

ϑr	**Volume flow, l/h**						
	150	**200**	**250**	**300**	**350**	**400**	**450**
25°C	95,22	97,04	98,45	99,39	100,85	100,49	101,88
30°C	94,02	96,08	97,4	98,14	98,67	99,42	101
35°C	-	94,58	96,27	97,37	97,73	98,41	99,41
40°C	-	93	94,46	96,09	95,96	96,52	98,09
45°C	-	90,94	92,02	93,71	93,96	94,52	95,93

The Fig.4.3.1 shows a decreasing trend of the overall efficiency with increasing back flow temperatures. This is only due to the decreasing values of the thermal efficiency, because the electrical efficiency is almost constant.

As it is written on the top of the diagrams, the trend refers to the average between the values measured with the Pt-100 thermal sensors on the machine side and the ones installed on the thermal exchange module.

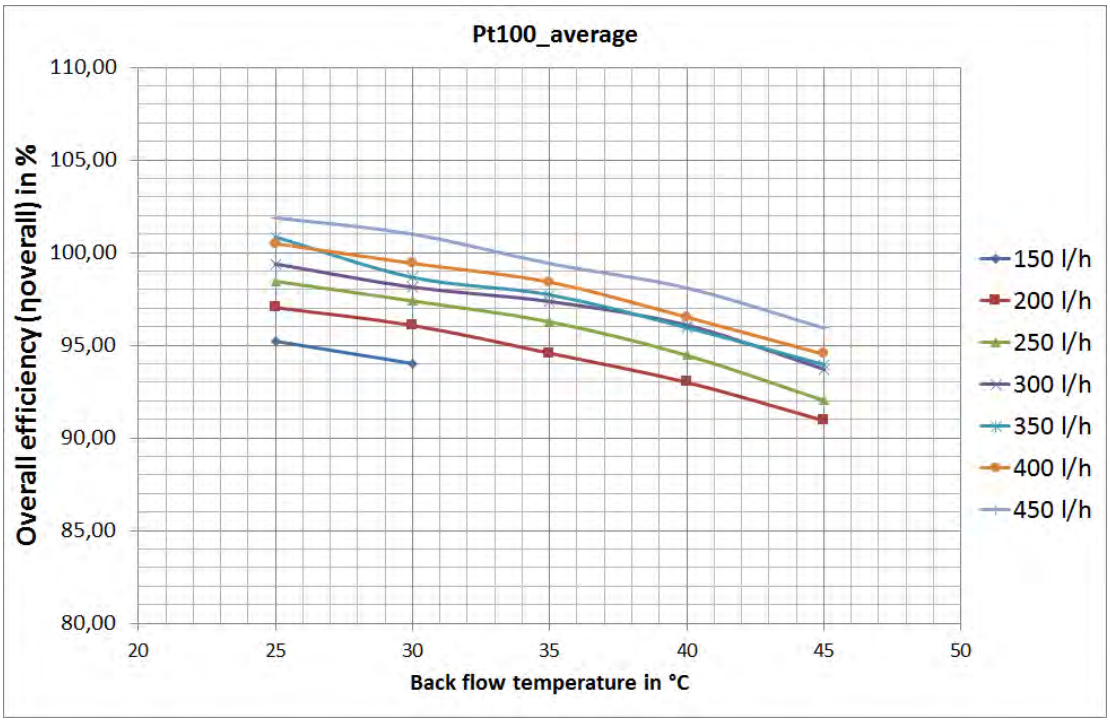

Fig.4.3.1 - Overall efficiency of Kirsch L 4.12, 2kW

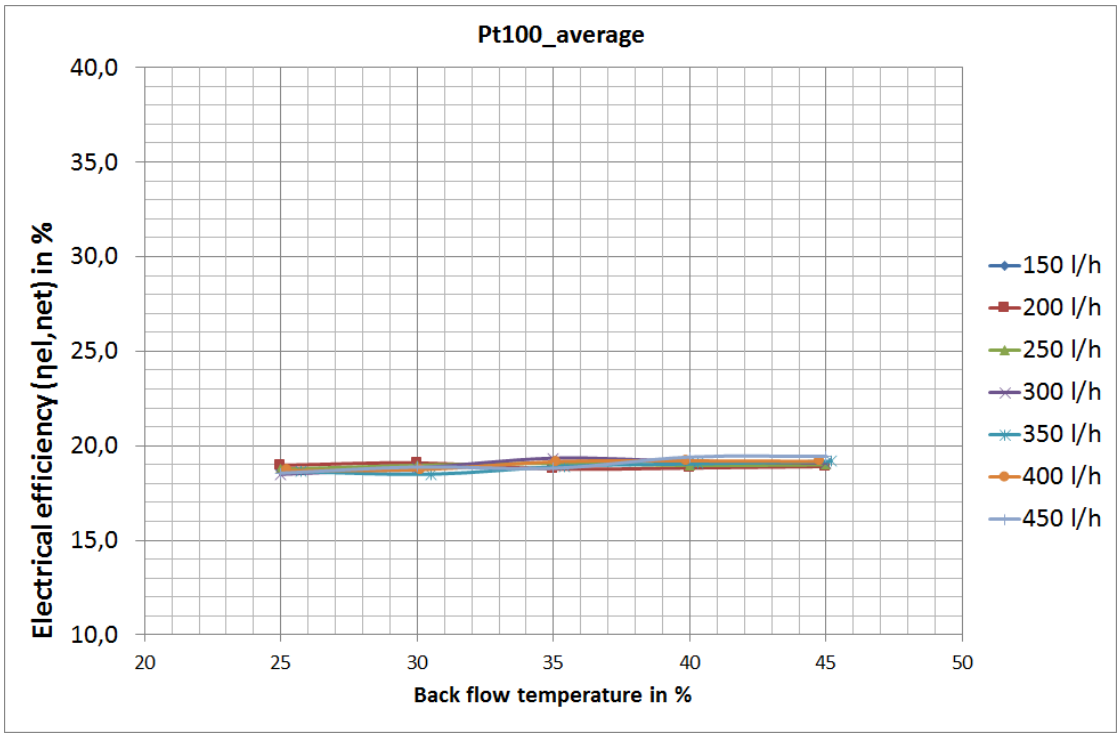

Fig.4.3.2 - Electrical efficiency of Kirsch L 4.12, 2kW

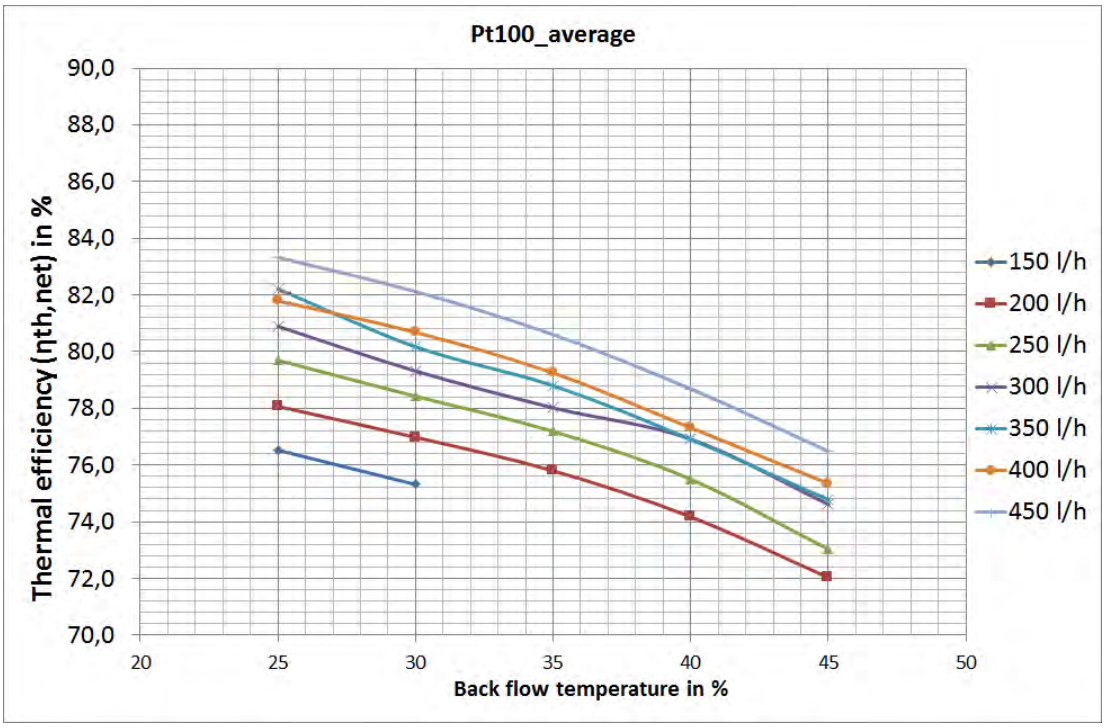

Fig.4.3.3 - Thermal efficiency of Kirsch L 4.12, 2kW

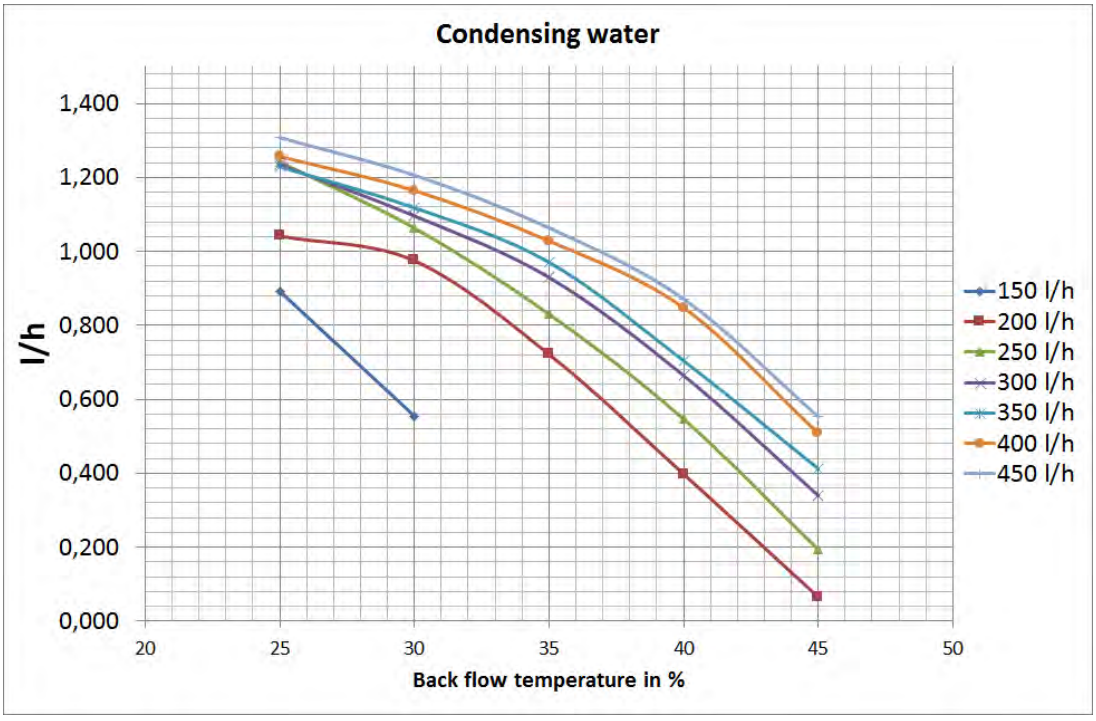

Fig.4.3.4 - Condensing water of Kirsch L 4.12, 2kW

The thermal efficiency decreases with high back flow temperatures because, remaining the incoming fuel power $\dot{Q}_{f,i}$ almost constant, the useful thermal power $\dot{Q}_{th,net}$ decreases. This is due to the increasing of losses depending on different factors. First of all, the most considerable loss: the decreasing condensing water, shown in Fig.4.3.5. If the back flow is higher, less latent heat is recovered from the flue gas, lower is β, and higher is the loss $\dot{Q}_0$. Secondly, the temperature of the outgoing exhaust is higher. So higher become the losses $\dot{Q}_{gas,th}$, due to the difference of temperature between the exhaust and the ambient. Then, also the other losses $\dot{Q}_{th,l}$ increase because the average temperature of the machine is higher. Thus, is higher the convection and radiation exchange with the ambient.

The condensing water, for a constant water flow value, is strongly decreasing with the back flow temperature rise. There is less water in the flue gas which, getting in touch with the pipes of the heat exchangers, has a temperature under the dew value. In this way there is less water in the flue gas which gives his latent heat to the water of the hydraulic circuit, through the heat exchangers.
From another point of view, if it is considered a constant back flow temperature, there is a decrease, slightly weak, of the condensing water with smaller water flow values. This is due to an increasing flow temperature and so of the average temperature of the machine. With a constant thermal power, if the water flow is lowed, the difference between the flow and the back flow temperature becomes bigger.

The same reasoning can be done with the overall efficiency. For constant back flow temperature values, the efficiency rises with higher values of water flows. This is due to a lower flow temperature and so to an increasing thermal efficiency.

The trend of $\dot{V} = 250\ l/h$ curve is different from the other because in that measurement a flow gas variation has been occurred. Anyway, this measurement has not been deleted because the thermal efficiency remained constant.

The power to heat ratio rises up with the back flow temperature because of the decreasing of the thermal power. This means that with high back flow temperature the electric power production prevails over the thermal one.

The values of the overall efficiency for $P_{el,net} = 2\ kW$ operating reaches, in the worst conditions, about $\eta_{overall} \cong 91\%$ and, with low back temperatures and high water volume flows, up to $\eta_{overall} \cong 102\%$.

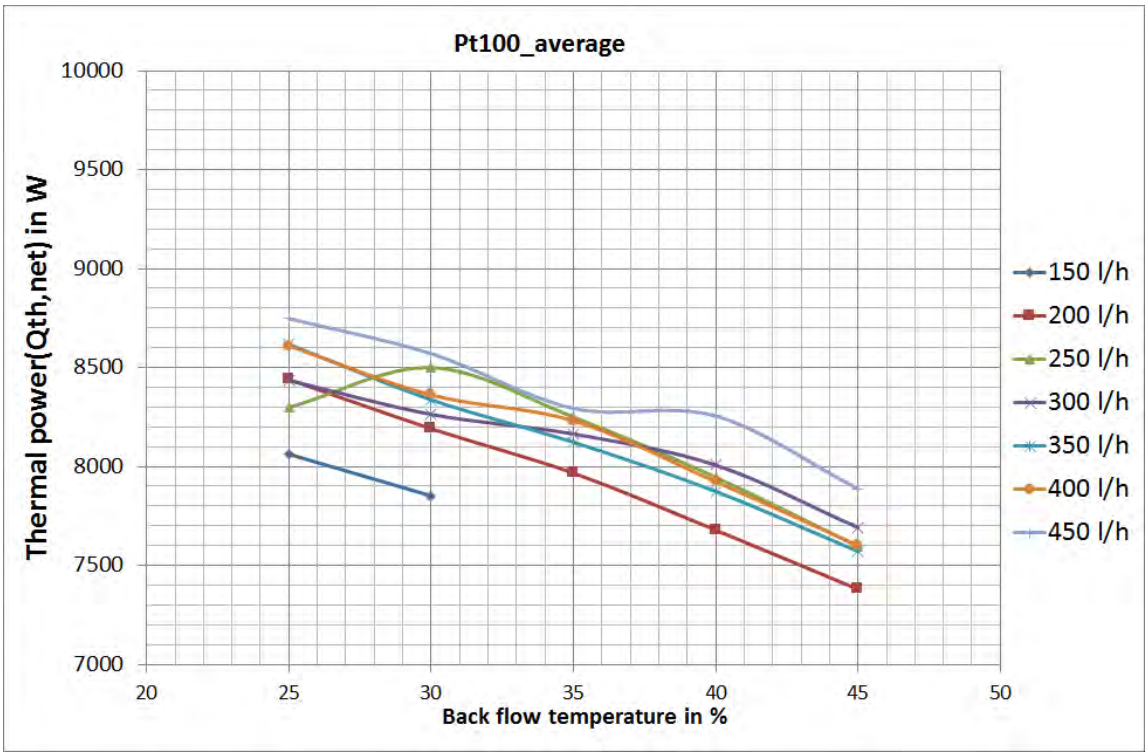

Fig.4.3.5 - Thermal power of Kirsch L 4.12, 2kW

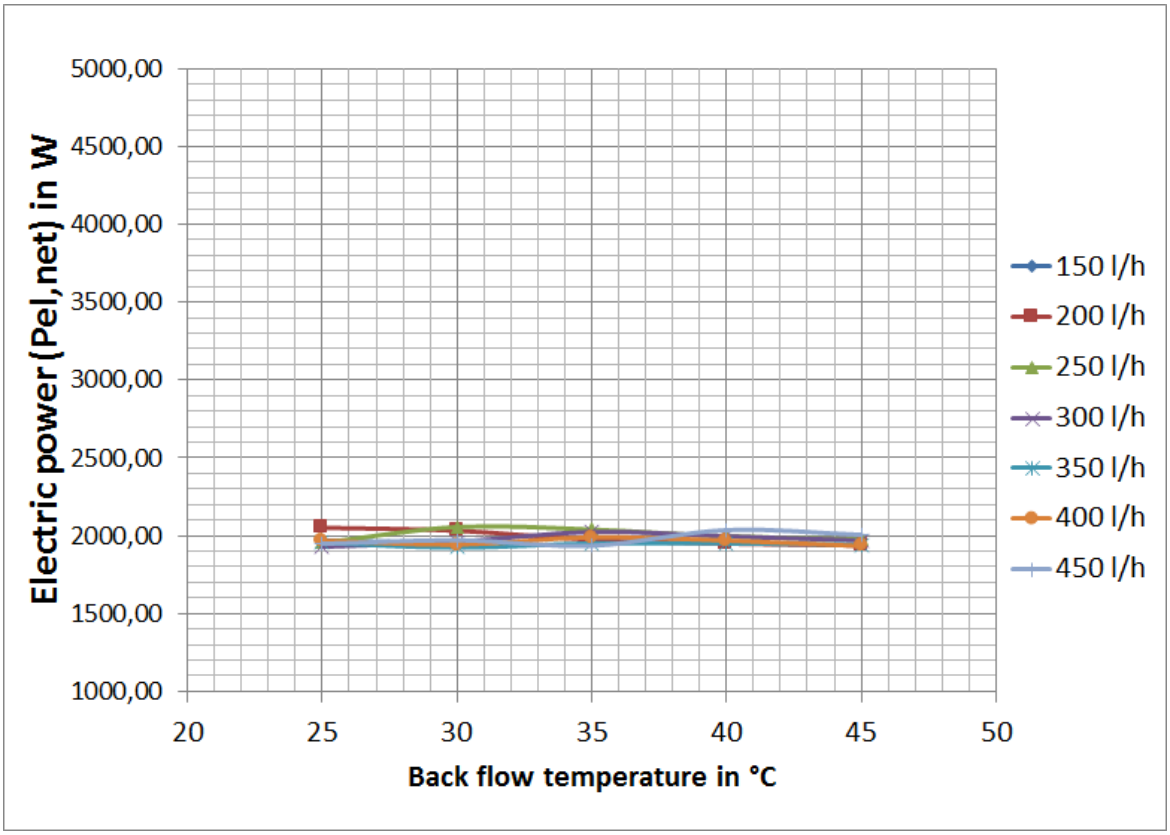

Fig.4.3.6 - Electric power of Kirsch L4.12, 2kW

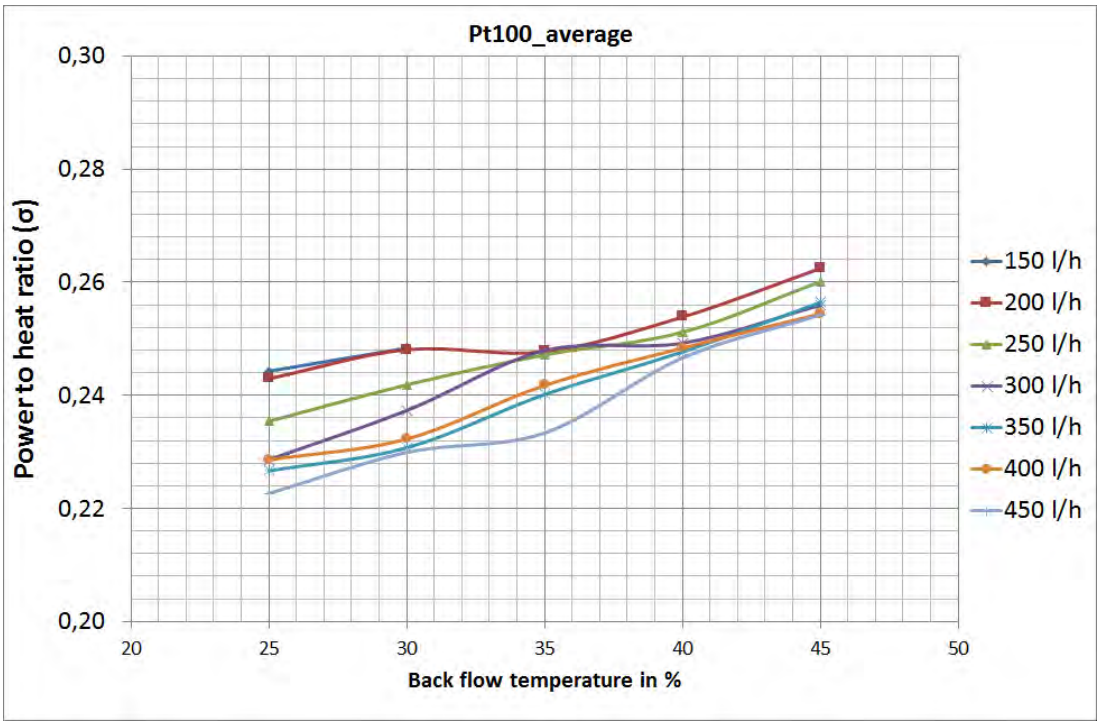

Fig.4.3.7 - Power to heat ratio of Kirsch L 4.12, 2kW

4.3.4 $P_{el,net}$ = 3 kW electrical power

For the $P_{el,net} = 3\ kW$ performance, it is valid the same reasoning made for the $P_{el,net} = 2\ kW$ power's chapter. The diagrams represent the same quantities, considering the average of the Pt-100 sensors, as function of the back flow temperature. So the trends are approximately the same but with different values.

For $\dot{V} = 200\ l/h$ the measurement has been made only for $\vartheta_b = 25°C$ and $\vartheta_b = 30°C$. For $\dot{V} = 250\ l/h$ the measurement has been made for all the temperature except for $\vartheta_b = 45°C$. This because with low volume flows the flow temperature reaches values that the machine can not tolerate.

The Fig.4.3.9 shows that the overall efficiency is grown up in reference to the one of $P_{el,net} = 2\ kW$. It has values between $\eta_{overall} = 95\%$ and $\eta_{overall} = 103\%$.

Tab.4.3.2 - Overall efficiency values, 3kW

ϑr	Volume flow, l/h					
	200	**250**	**300**	**350**	**400**	**450**
25°C	99	100,4	101,9	102,3	103	102,8
30°C	98,2	99,5	100,2	100,5	102,1	101,9
35°C	-	98	99,1	99,1	99,9	100,3
40°C	-	96	96,9	97,2	98,1	98,2
45°C	-	-	94,8	95,6	96	96,1

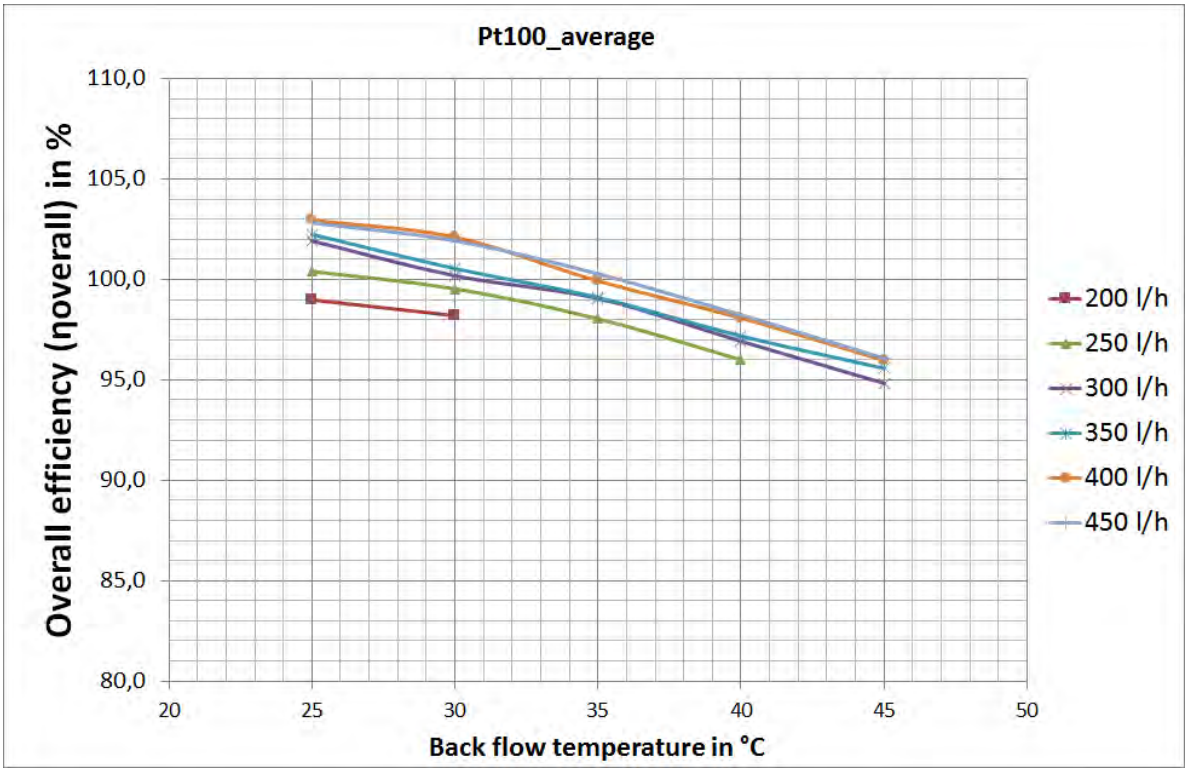

Fig.4.3.8 - Overall efficiency of Kirsch L 4.12, 3kW

The thermal power is risen up to a range of $10kW \leq \dot{Q}_{th,net} \leq 11kW$. In fact the engine, producing more mechanical power at the shaft to feed the generator, has to throw out more heat.

Also the condensing water volume flow is higher than the one of $P_{el,net} = 2\ kW$. It reaches $\dot{m}_{cond} \cong 1{,}7\ kg/h$ for $\vartheta_b = 25°C$. This because a higher fuel input amount involves a higher flue gas output amount, and so higher condensing water.

The electrical efficiency is risen from $\eta_{el,net} \cong 19\%$ of $P_{el,net} = 2\ kW$, up to more than $\eta_{el,net} \cong 22\%$. The generator has a better operating with higher speed of the shaft.

The thermal efficiency got worse. From a maximum value of $\eta_{th,net} \cong 83\%$ with $P_{el,net} = 2\ kW$ it lowed down to $\eta_{th,net} \cong 81\%$. This is due to the fact that the increase of the fuel consumption is grown more than the thermal power produced. The thermal power production moved from an average value of $\dot{Q}_{th,net} \cong 8kW$ to a range of $10kW \leq \dot{Q}_{th,net} \leq 11kW$; the fuel flow, instead, moved from a consumption of about $\dot{m}_{fuel} \cong 17\ l/h$ to a value of roughly $\dot{m}_{fuel} \cong 22\ l/h$. These changings can be more clear analyzing the power to heat ratio's diagram, which shows a higher average value in respect to the $P_{el,net} = 2\ kW$ one.

In the thermal power diagram, the curve related to $\dot{V} = 450\ l/h$ has a particular trend. This is due to a lower gas flow at the beginning of the measurement. In spite of that, the measurement is considered valid because this variation does not influence the thermal efficiency, and so the overall efficiency.

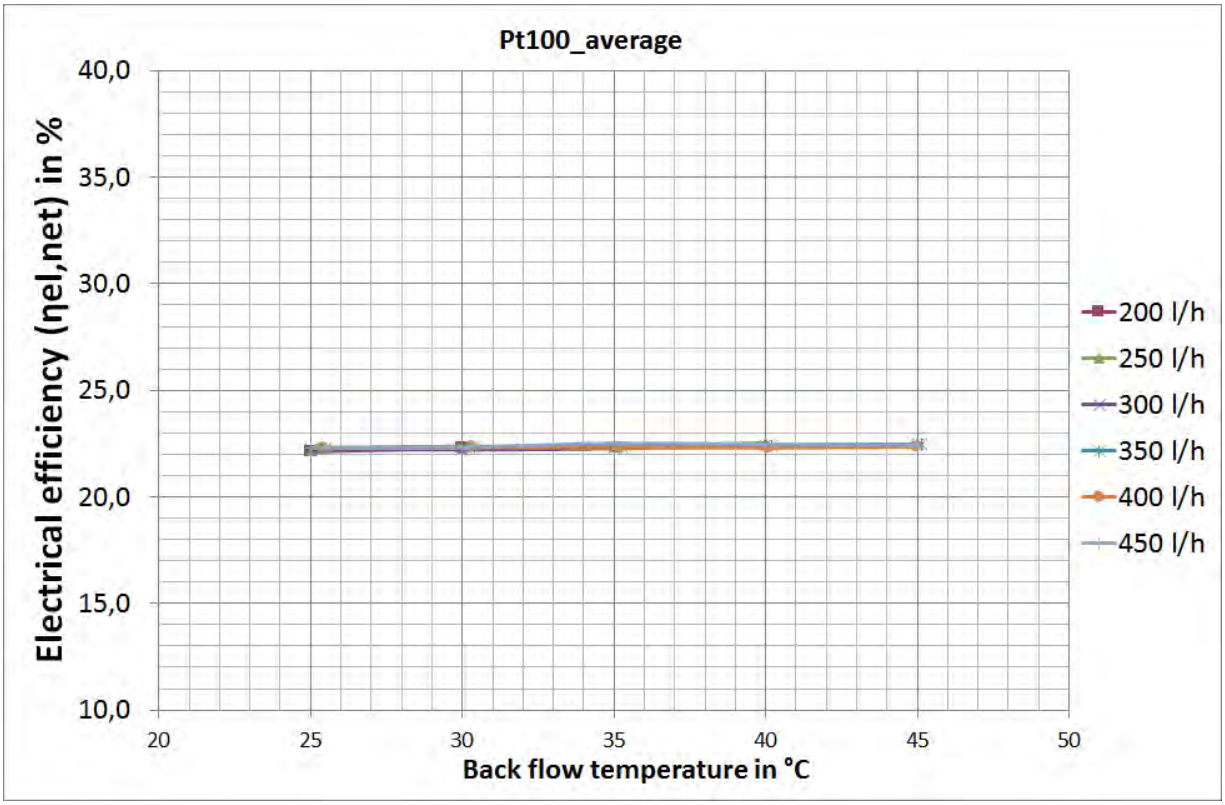

Fig. 4.3.9 - Electrical efficiency of Kirsch L 4.12, 3kW

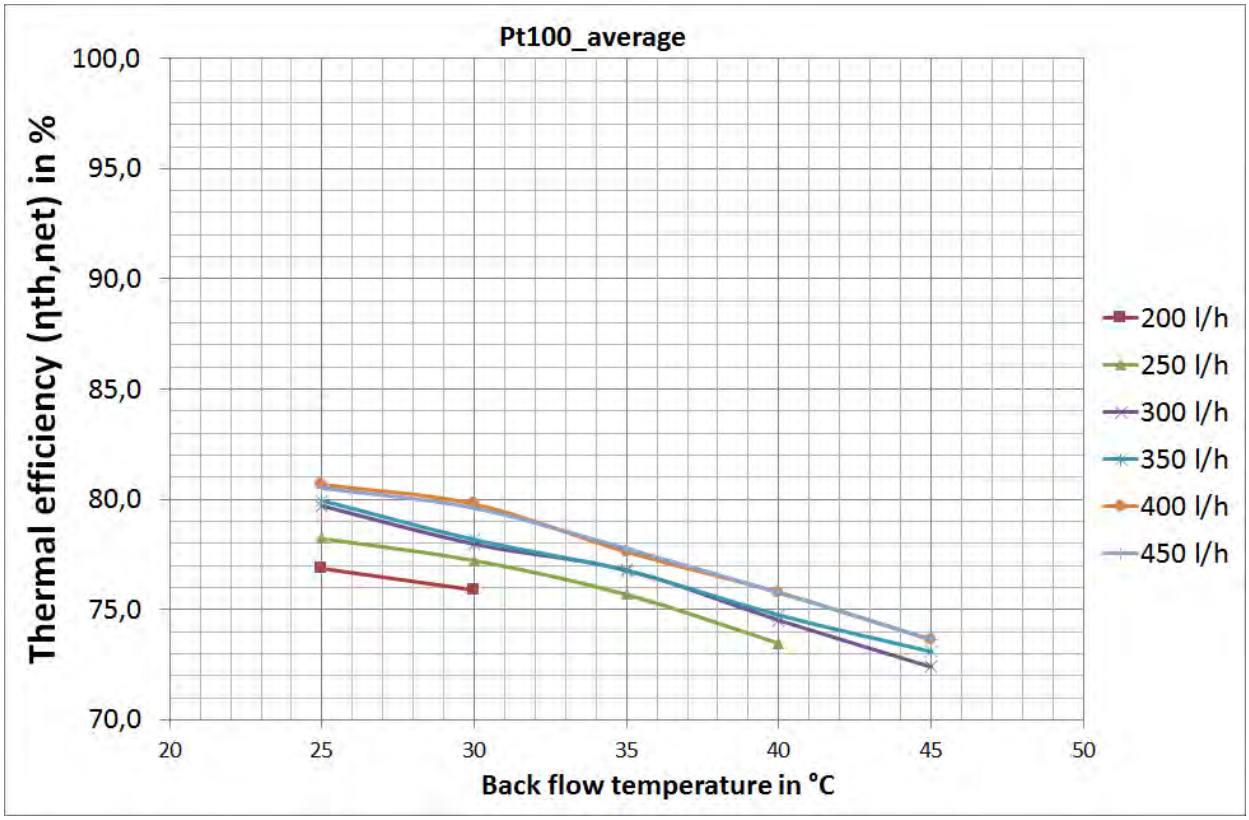

Fig.4.3.10 - Thermal efficiency of Kirsch L 4.12, 3kW

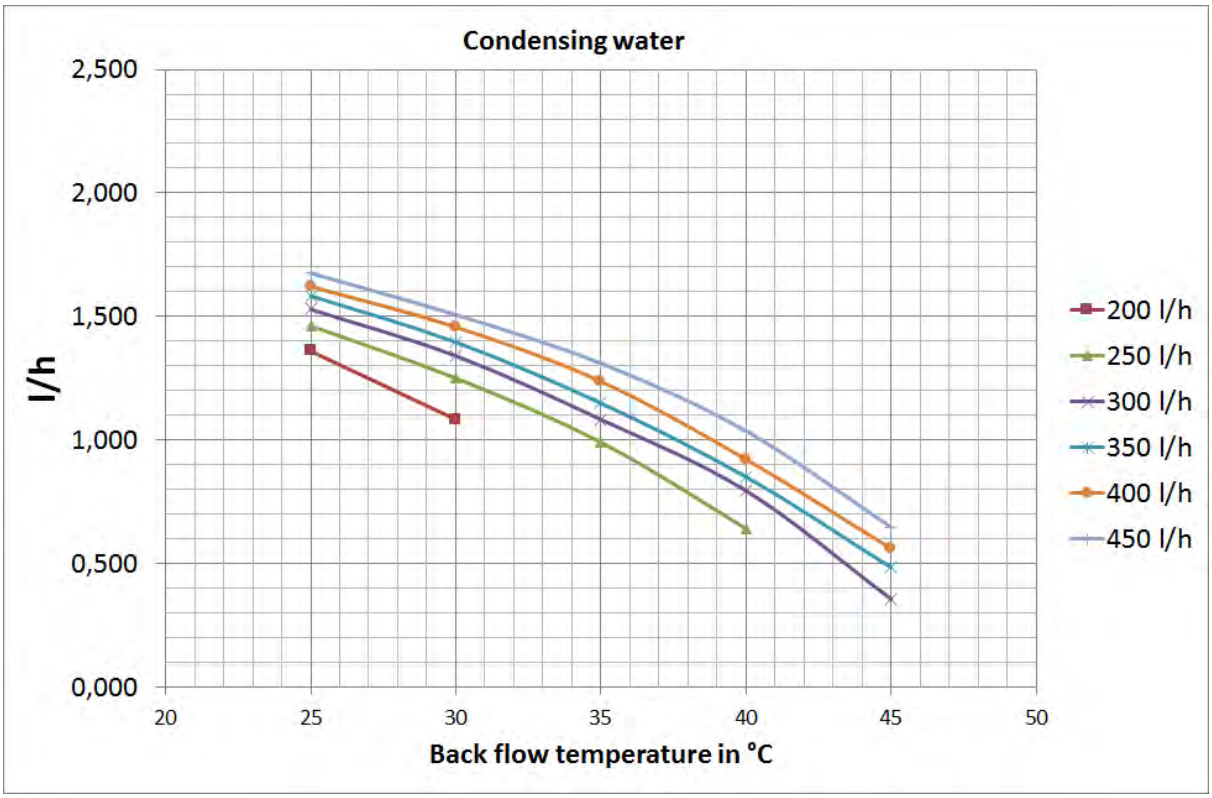

Fig.4.3.11 - Condensing water of Kirsch L 4.12, 3kW

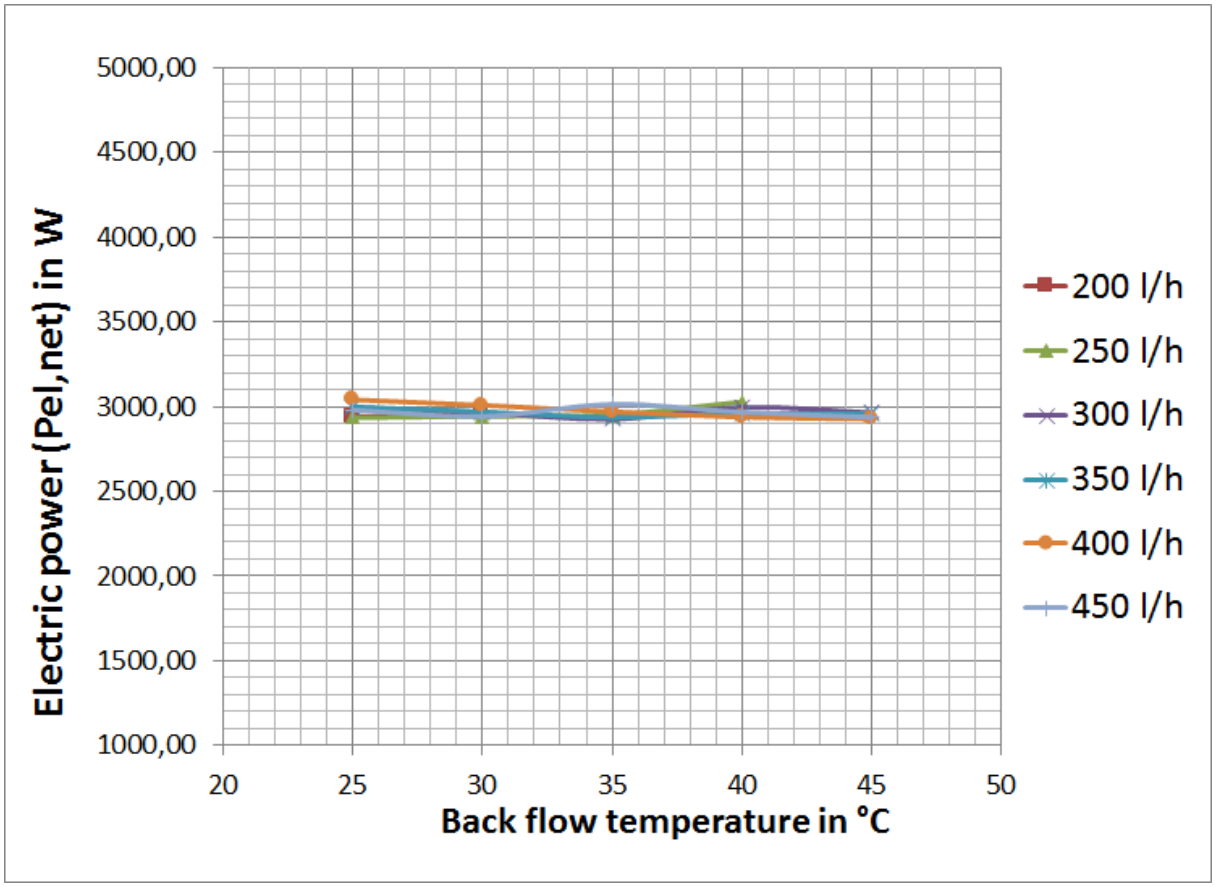

Fig.4.3.12 - Electrical power of Kirsch L 4.12, 3kW

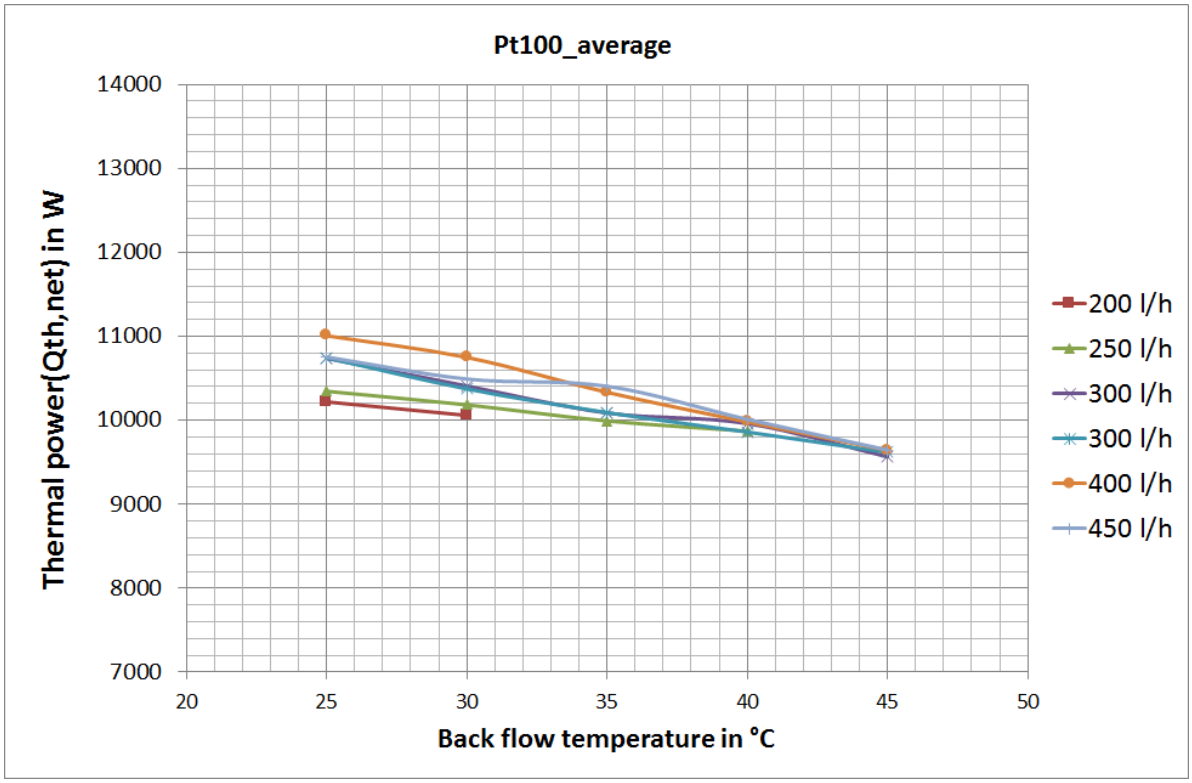

Fig.4.3.13 -Thermal power of Kirsch L 4.12, 3kW

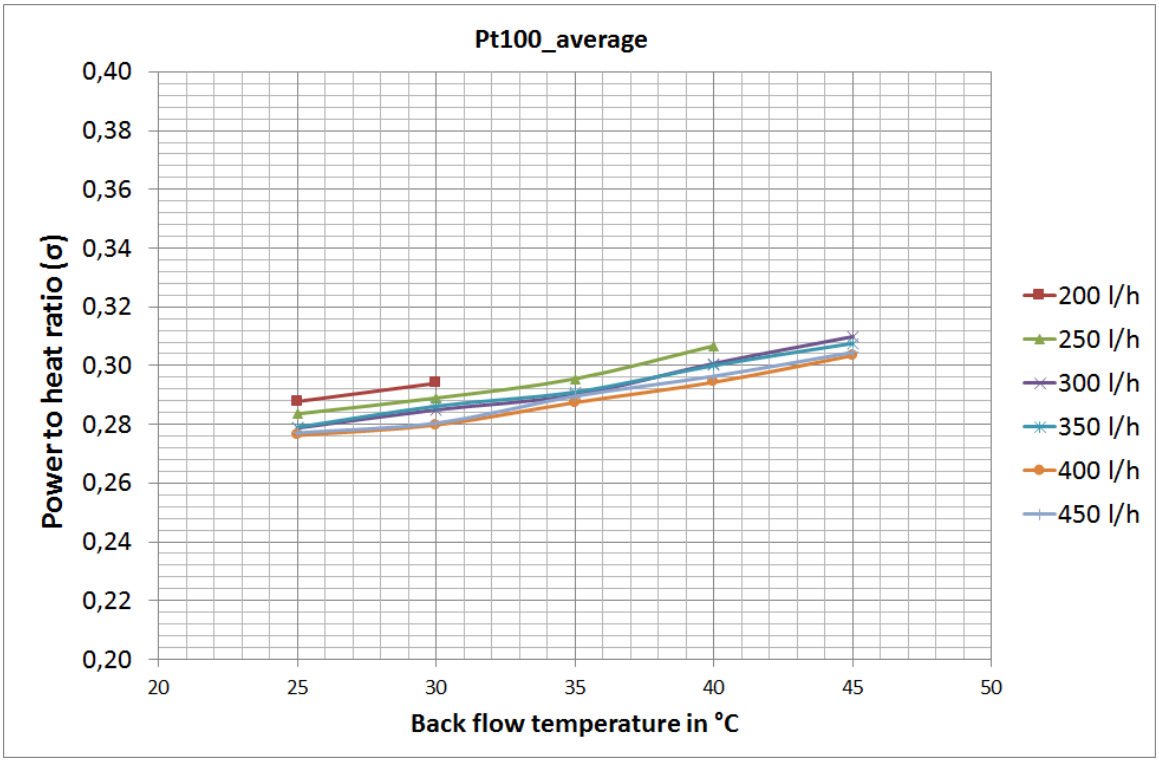

Fig.4.3.14 - Power to heat ratio of Kirsch L 4.12, 3kW

4.3.5 $P_{el,net}$ = 4 kW electrical power

For the $P_{el,net} = 4\ kW$ performance, it is valid the same reasoning made for the other power levels' chapters. Actually, the maximum power developed by the engine is about $P_{el,net} \cong 3{,}6\ kW$. The diagrams represent the same quantities, considering the average of the Pt-100 sensors, as function of the back flow temperature. So the trends are approximately the same but with different values.

Only the measurements related to the volume flows comprehended between $250\ l/h \leq \dot{V} \leq 450\ l/h$ are considered. For $\dot{V} = 250\ l/h$ the measurement has been made only for $\vartheta_b = 25°C$ and $\vartheta_b = 30°C$ for the same reasons presented in the previous chapters.

As it is showed in Fig.4.3.17, the overall efficiency has a minimum value of $\eta_{overall} \cong 96\%$ and a maximum value of more than $\eta_{overall} \cong 104\%$.

Tab.4.3.3 - Overall efficiency values, 4kW

ϑr	Volume flow, l/h					
	200	**250**	**300**	**350**	**400**	**450**
25°C	-	101,8	101,5	101,8	103,5	104,2
30°C	-	101,8	101,4	101,8	102,3	102,5
35°C	-	-	99,9	100,4	101,2	101,5
40°C	-	-	98,5	98,4	100,2	100,1
45°C	-	-	96,1	97,3	98	98,6

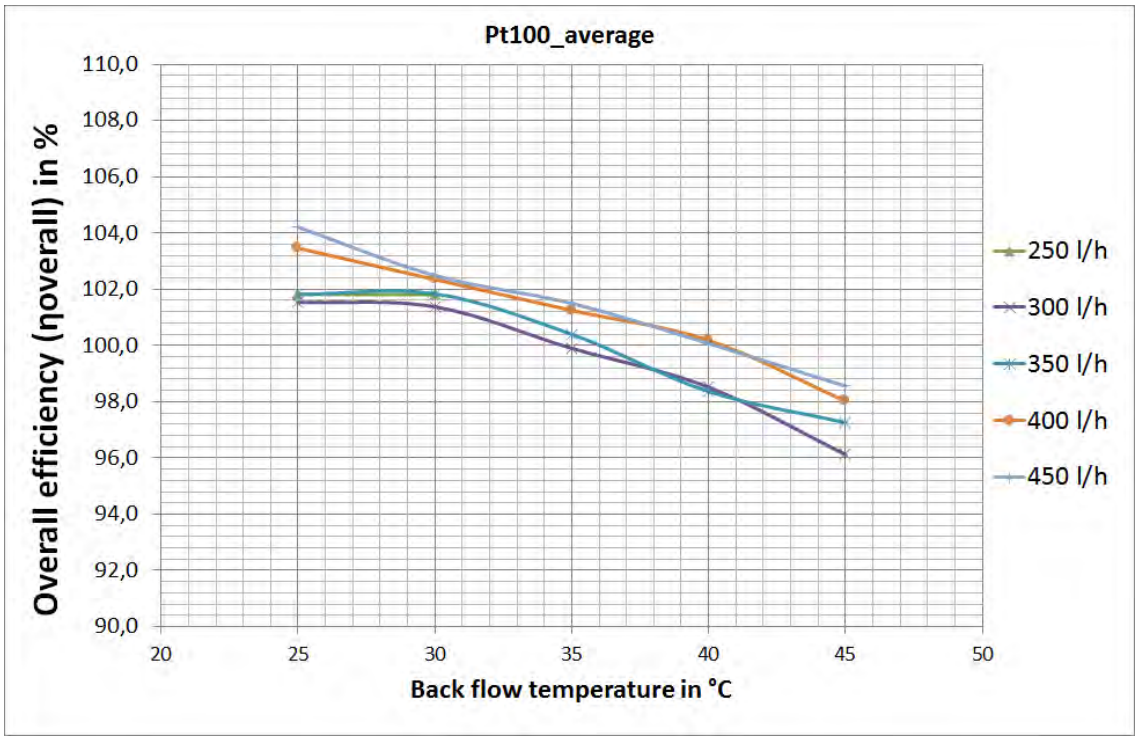

Fig.4.3.15 - Overall efficiency of Kirsch L 4.12, 4kW

The thermal power has values comprehended between $11kW \leq \dot{Q}_{th,net} \leq 12{,}5kW$ and the condensing water amount reaches a maximum value of about $\dot{m}_{cond} \cong 2\ l/h$.
The electrical efficiency reaches a value higher than $\eta_{el,net} = 23\%$. A result much better than the one gained with $P_{el,net} = 2\ kW$. In the $P_{el,net} = 4\ kW$ mode the generator works in almost nominal conditions. The thermal efficiency is remained quite the same of $P_{el,net} = 3\ kW$.

To produce more electric power is obviously necessary a wider amount of input fuel. Considering the $P_{el,net} = 2\ kW$ performance it is risen up from an average value of $\dot{m}_{fuel} \cong 17\ l/h$ up to $\dot{m}_{fuel} \cong 25\ l/h$.

The measurements related to $\dot{V} = 450\ l/h$ and $\dot{V} = 400\ l/h$ have more performing values probably because of the ambient temperature of the days in which they have been made.

Considering the whole steady state measurement, they can be recognized some constant trends with the electric power variation from $P_{el,net} = 2\ kW$ to $P_{el,net} = 4\ kW$: it can be said that the average value of the overall efficiency is increasing with the increasing production of electric power. The electric efficiency is always constant and his value increases thanks to the better performances of the generator. The thermal power amount increases with the increasing of the electrical power. This is due to the fact that the engine hast to throw out more and more heat. Dealing with the thermal efficiency, the trends take lower values with the electric power increasing. In fact, with a higher average temperature inside the machine, the thermal losses become more relevant. Nevertheless the thermal efficiency lows down less than the electric efficiency grows up. The amount of condensing water obviously increases because of the bigger input of fuel volume flow: more is the fuel volume flow and more will be the exhaust gas, and then the condensation. Last but not least, power to heat ratio has a slight increase because the electric production prevails on the thermal one.

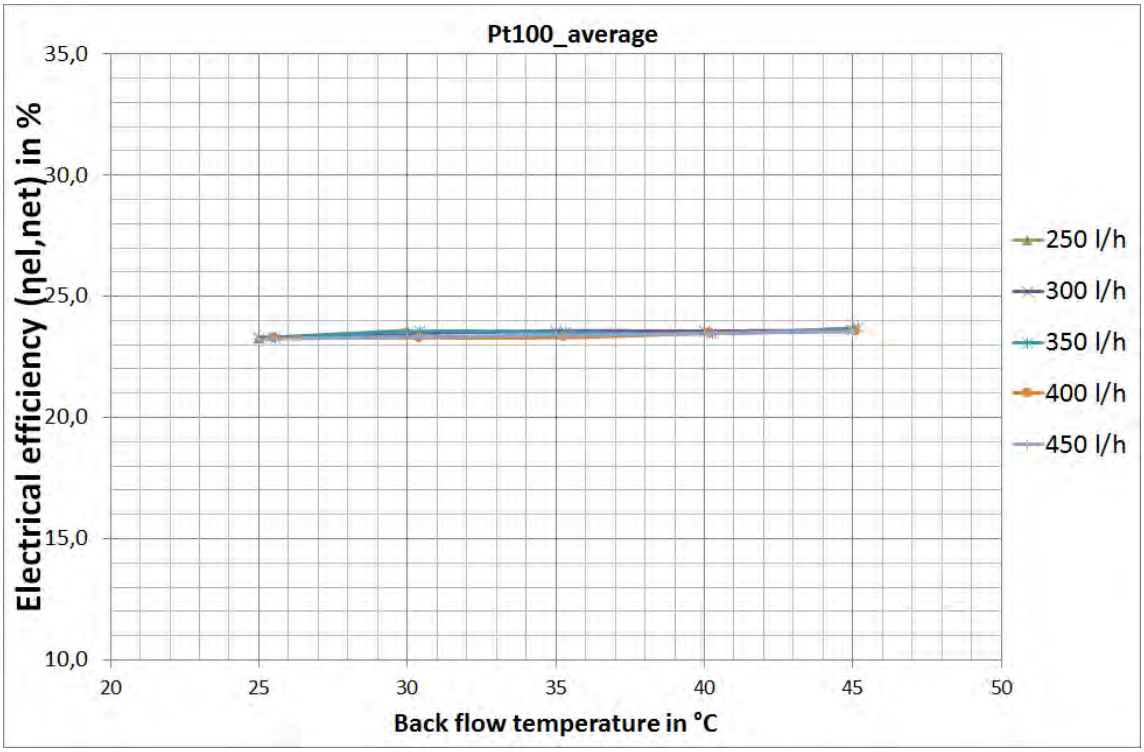

Fig.4.3.16 - Electrical efficiency of Kirsch L 4.12, 4kW

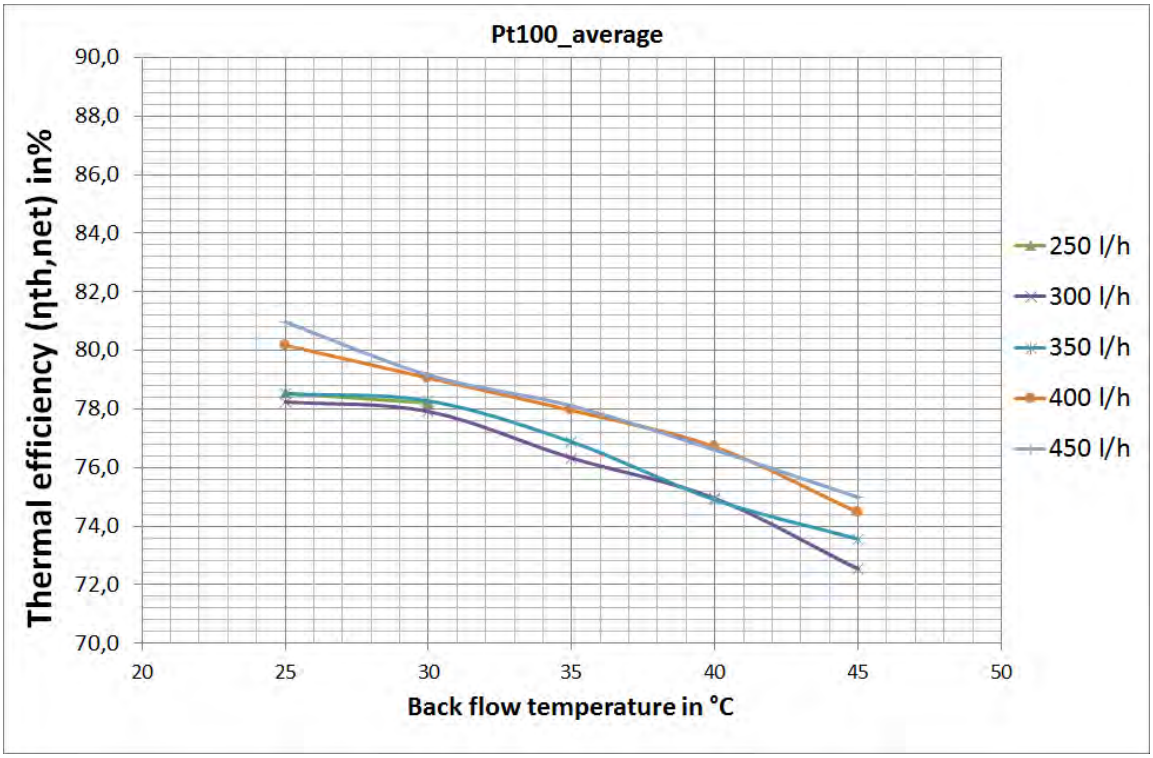

Fig.4.3.17 - Thermal efficiency of Kirsch L 4.12, 4kW

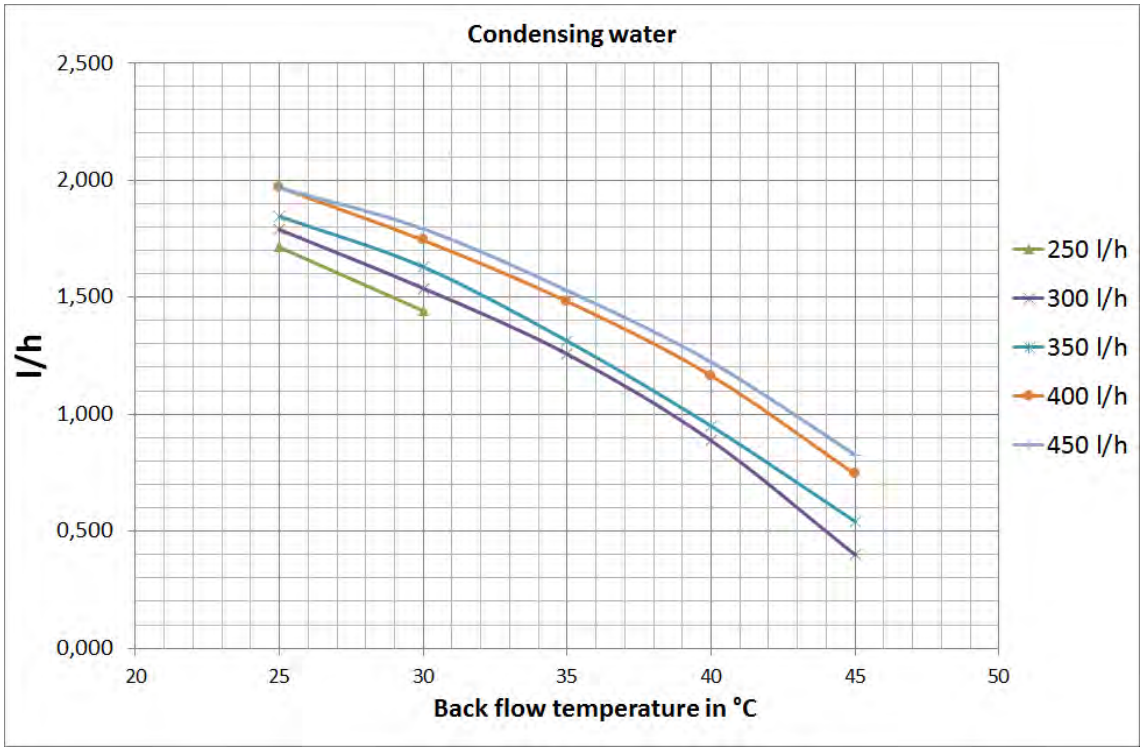

Fig.4.3.18 - Condensing water of Kirsch L 4.12, 4kW

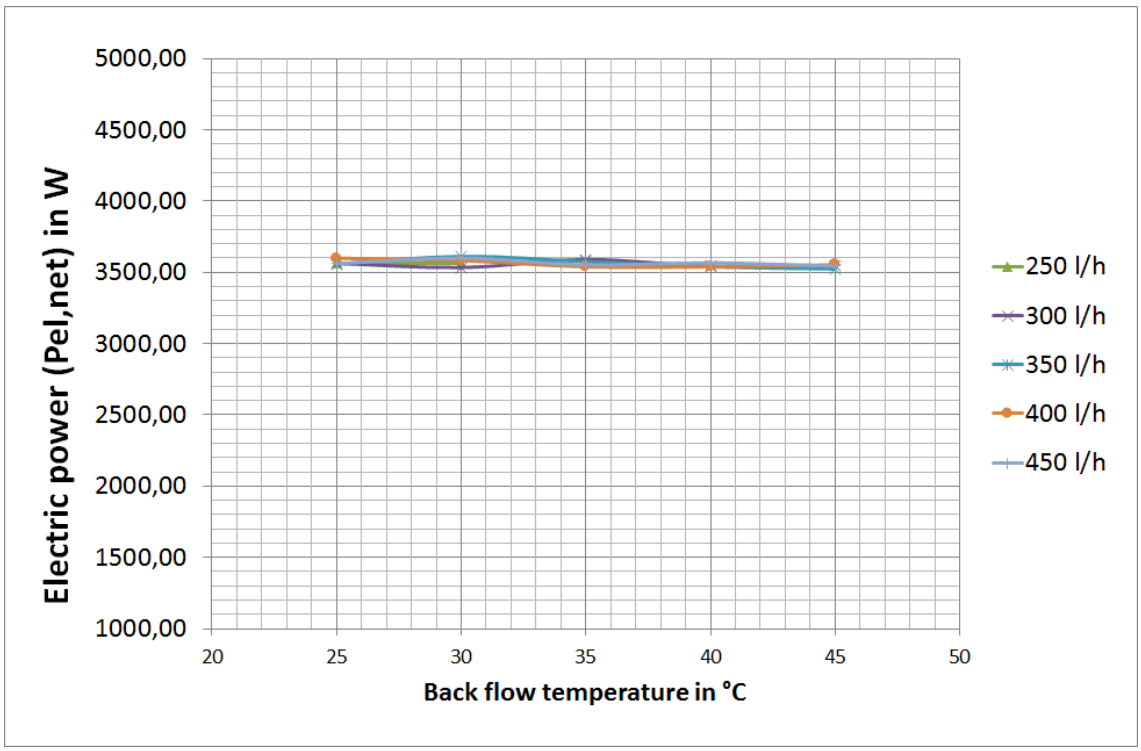

Fig.4.3.19 - Electrical power of Kirsch L 4.12, 4kW

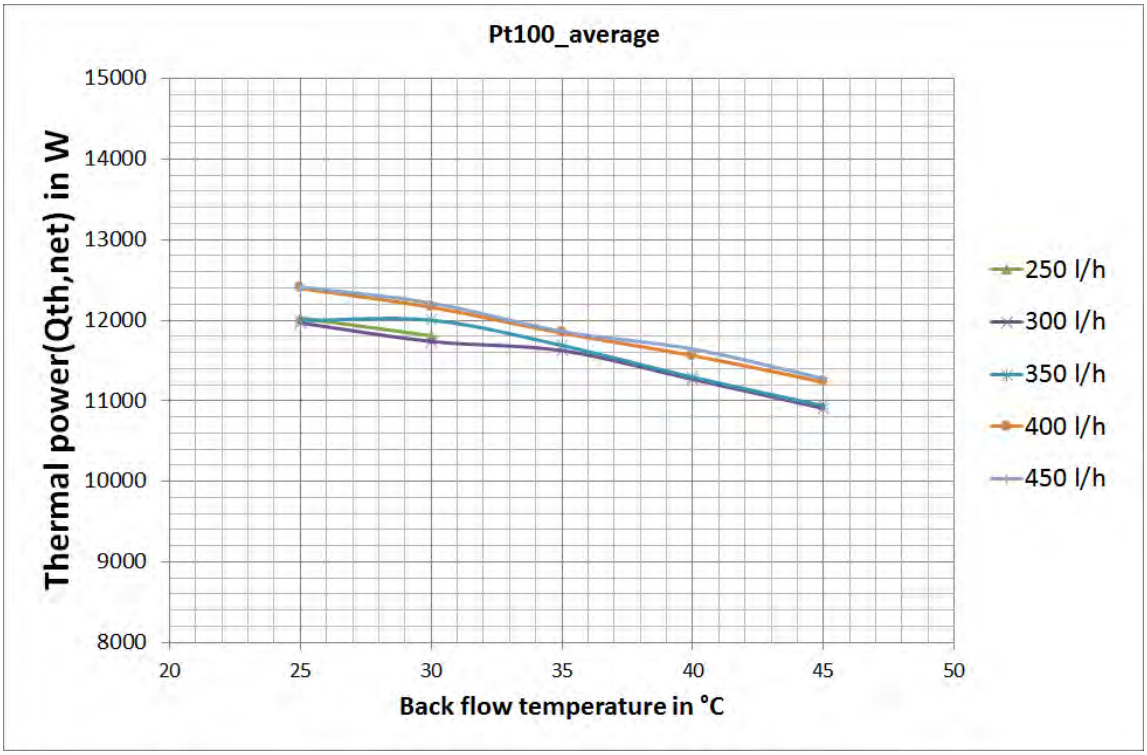

Fig.4.3.20 - Thermal power of Kirsch L 4.12, 4kW

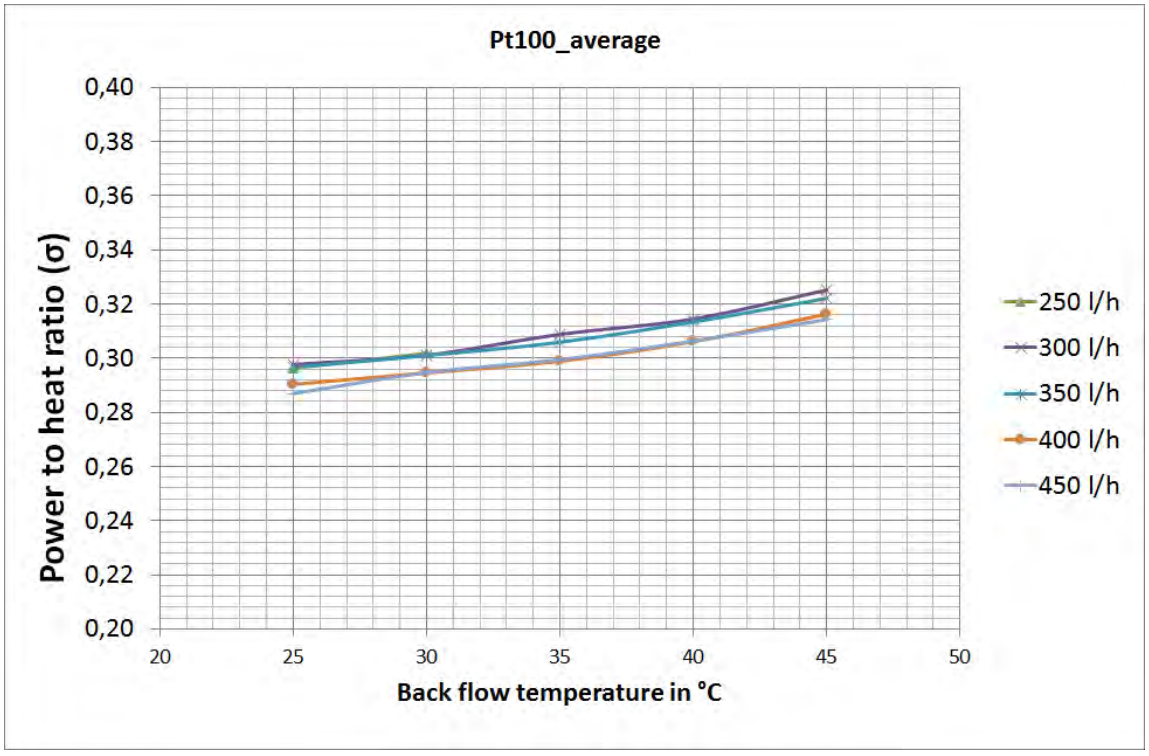

Fig.4.3.21 - Power to heat ratio of Kirsch L 4.12, 4kW

4.4 Transient

In this chapter will be analyzed the behavior of the system in dynamic conditions. Therefore the volume flow and the flow temperature are no more constant and vary depending on the setting of the measures. In the first part, the hydraulic circuit configuration remains exactly the same. In the second part, aimed to calculate the standard efficiency, some changes will occur. The first part consists in four measures: two with the internal pump of the machine and other two with the external pump of the hydraulic circuit.

4.4.1 Internal pump measures

Purpose of this measure is to analyze the response time of the system imposing different electrical power's output. During the measure's achievement has been maintained a constant back flow temperature of exactly $\vartheta_b = 30°C$. This is possible thanks to the three-ways valve opening, set with the software.

To start the measurement is necessary to let the whole circuit reach the aim temperature of $\vartheta = 30°C$. So, while the machine works in stand-by mode, the external pump works for some minutes. Once the temperature is reached by the entire circuit, the external pump can be switched off and the machine switched on to the operating mode. By now, the machine works with its own pump. To proof the good operating of the internal pump, the machine sends some signals to the pump. So, it develops two volume flow picks before starting. Through the touch screen of KIRSCH L 4.12 is possible to set the following power levels with their own duration:

Tab.4.4.1 - Internal pump measure's schedule

Duration h	**Electric power, kW**	**Back flow temperature, °C**	**Volume flow, $\dot{V}$**
2	3	30	Internal
1	4	30	Internal
1	2	30	Internal
1	3	30	Internal
2	0	30	Internal

The two hours set to $P_{el,net} = 0\ kW$ are useful to detect the whole warm-down of the machine. The volume flow is *internal* because varies according to the internal pump. It imposes a volume flow's trend in order to maintain a nearly constant flow temperature.
The back flow temperature is fixed to $\vartheta_b = 30°C$ to be allowed to analyze the trend of the flow temperature during the volume flows' variations. In this way the flow temperature is used as an index of the performance of the machine.
Volume flow makes some step fluctuations when an electric power's changing occurs. Thereafter it settles down to a constant value. For this reason the flow temperature has roughly a saw teeth trend with an average value of approximately $\vartheta_f \cong 67°C$.
The thermal power is calculated using the temperature values measured at the CHP side by the Pt 100 sensors. In this way the thermal power refers directly to the heat outgoing the machine, not taking in consideration the thermal losses of the piping system of the hydraulic circuit.

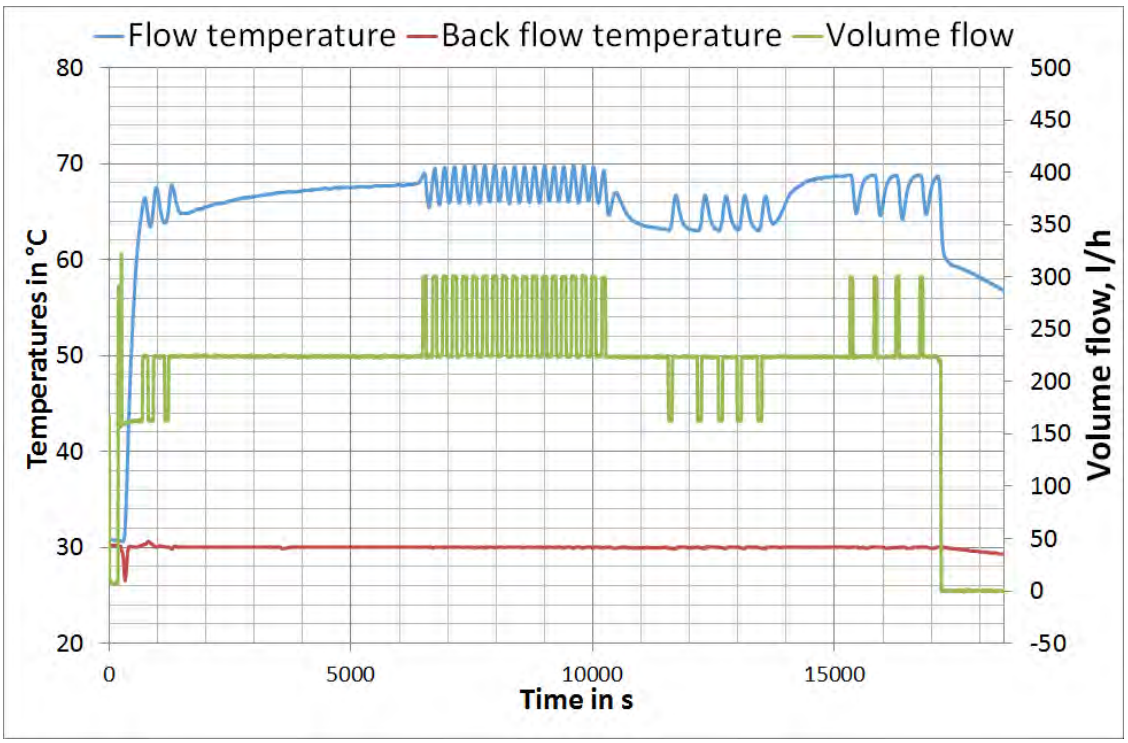

Fig.4.4.1 - Transient with internal pump, temperatures and volume flow

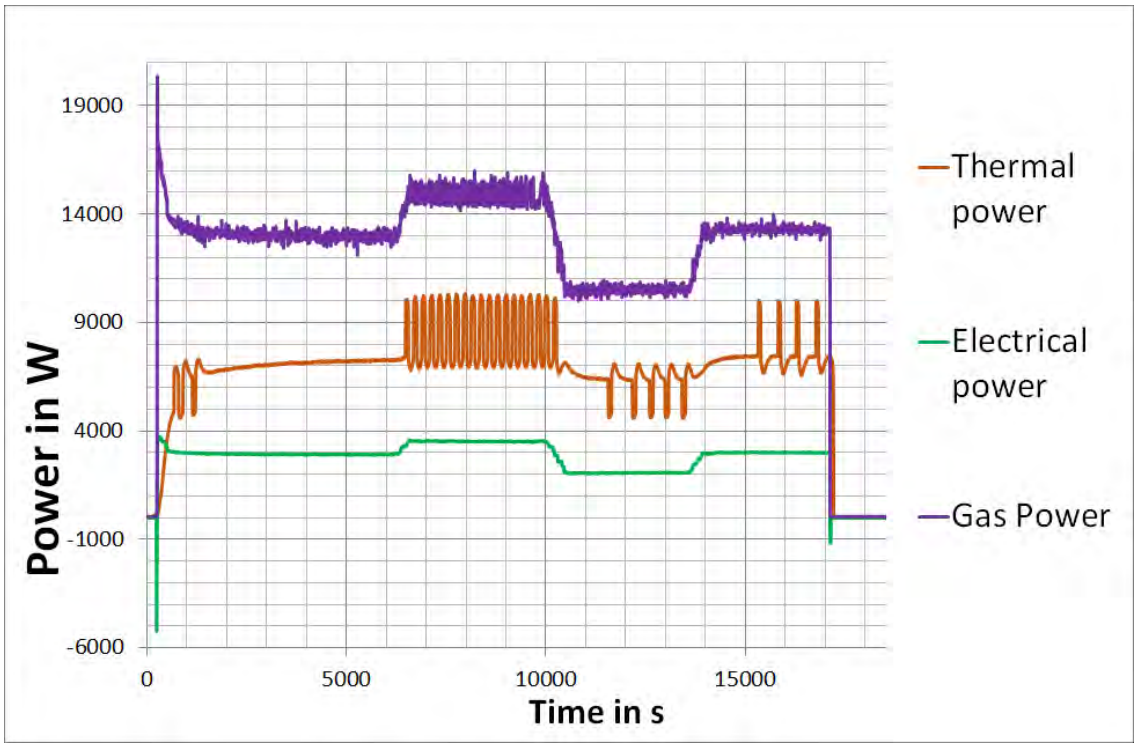

Fig.4.4.2 - Transient with internal pump, powers' trends

In a second part is analyzed merely the warm-up transient of the machine. The electrical power is set to a constant level of $P_{el,net} = 3\ kW$. The volume is imposed by the internal pump again.

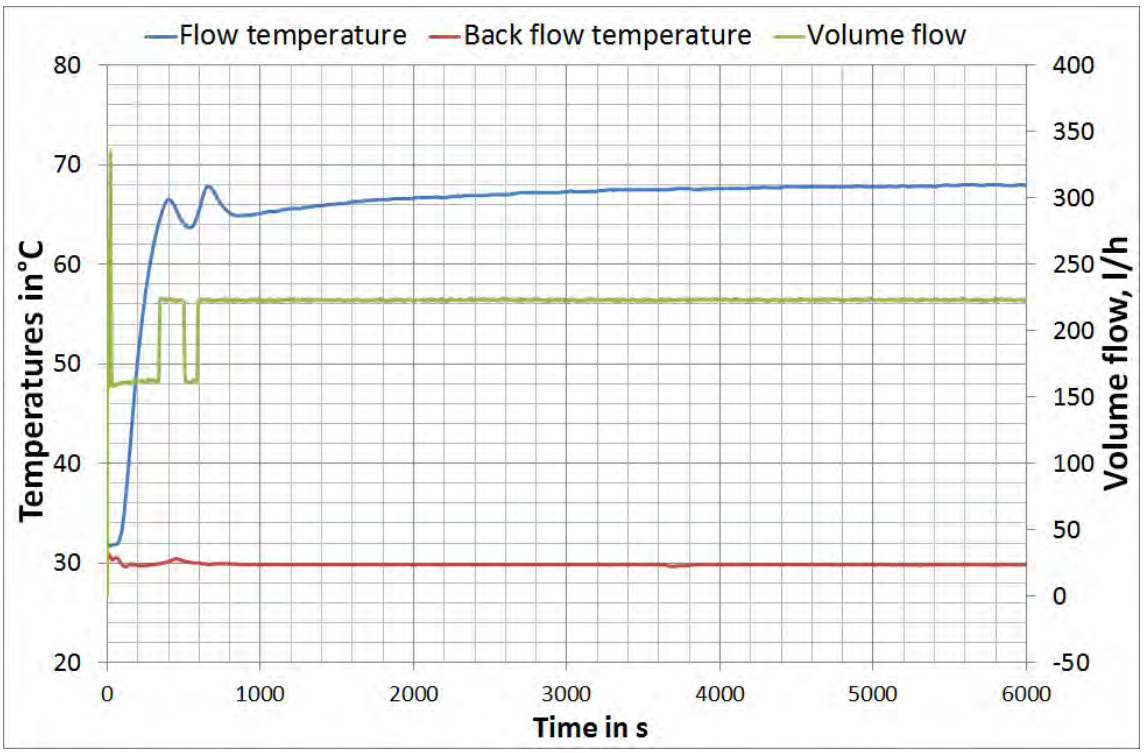

Fig.4.4.3 - Start transient with internal pump, temperatures and volume flow

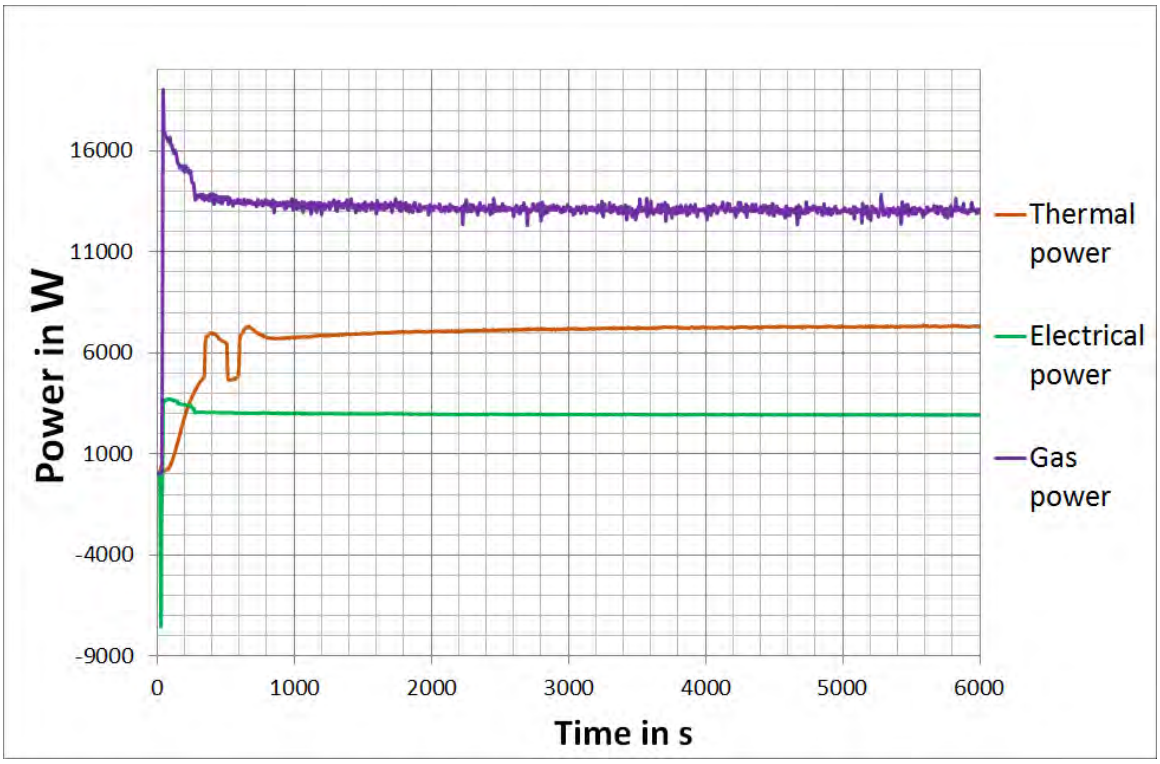

Fig.4.4.4 - Start transient with internal pump, powers' trends

From the diagram it is possible to see that the volume oscillates between $\dot{V} \cong 160\ l/h$ and $\dot{V} \cong 220\ l/h$. Once the transient is passed over, the flow temperature settles to $\vartheta_f \cong 68°C$ and the volume flow remains $\dot{V} \cong 220\ l/h$.

The system belong to non-linear systems according to the control theory. In fact, the flow temperature reaches the steady state value after some oscillations. The system has a rise time of about $t_r = 350\ s$. This means that the flow temperature reaches a value of $\vartheta_{f,rise} = 0{,}9 \cdot \vartheta_{f,MAX} = 62{,}3\ °C$ after $t_r \cong 350\ s$. This time is a precious value to have an idea of how much time the system takes to react.

In Fig.4.4.2 and Fig.4.4.4 is possible to see a negative electrical power's pick. It occurs at the beginning of the measure when the engine needs to be started and the generator receives electrical power from the net. In Fig.4.4.2 is also possible to observe a negative electrical power's pick when the engine shuts down. When the fuel stops to flow, in fact, the generator absorbs some electrical power for few seconds to let the engine shut down.

4.4.2 External pump's measures

The same measurements have been made with the external pump of the hydraulic circuit. During the measure's gaining has been maintained a constant back flow temperature of exactly $\vartheta_b = 30°C$ and a volume flow of $\dot{V} = 300\ l/h$.

To start the measure is now necessary to switch off the internal pump of the machine. Once the whole circuit has reached the target temperature, the machine can be switched on to the operating mode.

The timetable is shown below:

Tab.4.4.2 - External pump measure's schedule

Duration h	**Electric power, kW**	**Back flow temperature, °C**	**Volume flow, $\dot{V}$**
2	3	30	300
1	4	30	300
1	2	30	300
1	3	30	300
2	0	30	300

From the diagrams it can be seen that the curves have more smooth trends. This is due to the constant volume flow. Imposing a constant volume flow with the external pump, the flow temperature assumes quite the same trend of the thermal power produced by the machine. For this reason the flow temperature can not have an about constant trend as occurred with the internal pump operation.

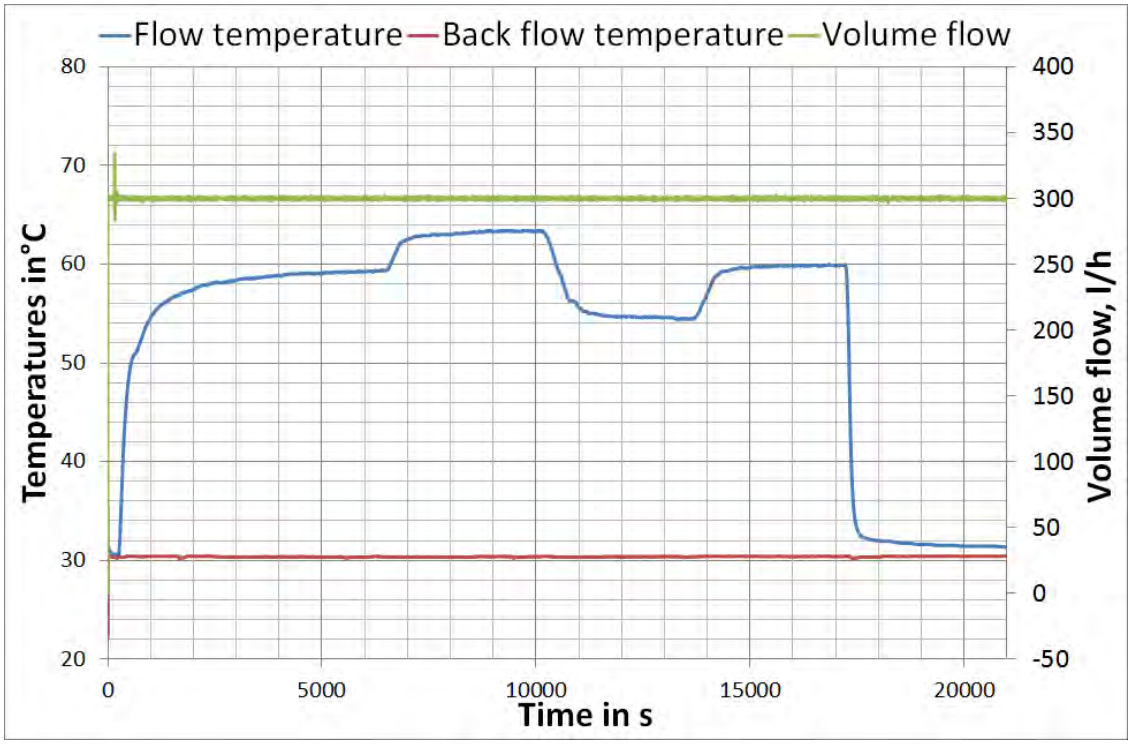

Fig.4.4.5 - Transient with external pump, temperatures and volume flow

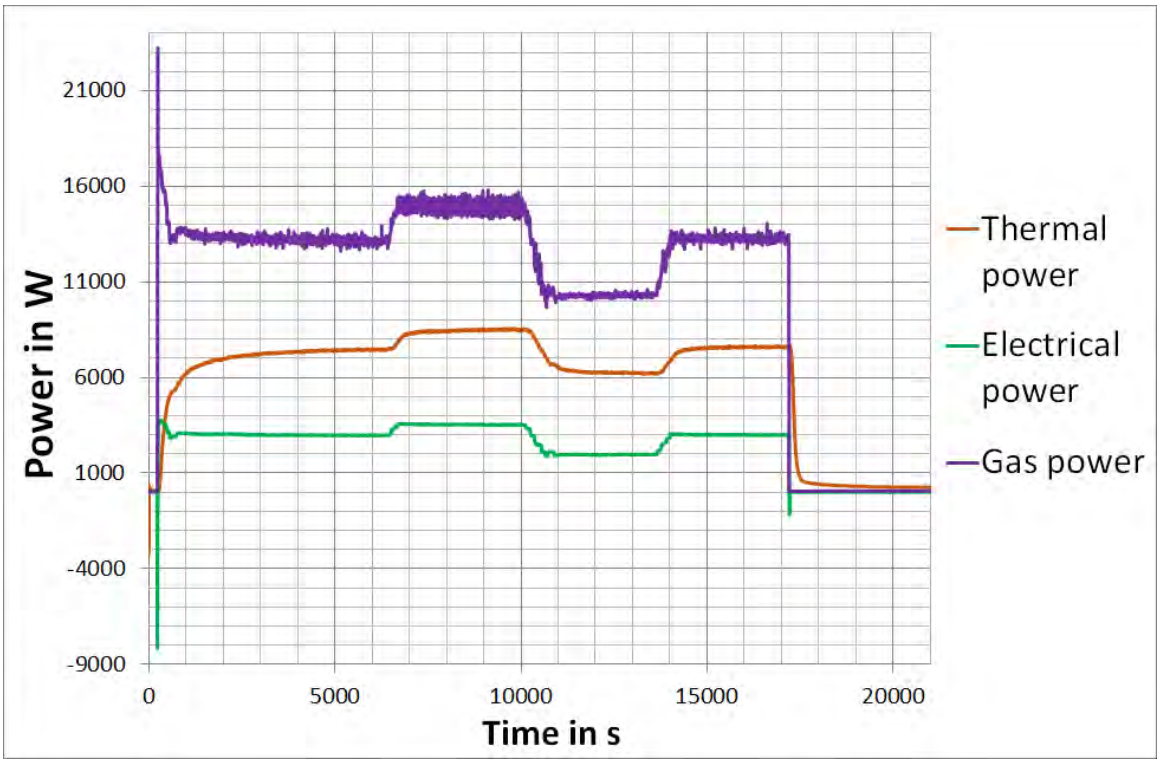

Fig.4.4.6 - Transient with external pump, powers' trends

Regarding the starting phase transient, the flow temperature reaches the steady state condition without oscillations. In this case the system is linear. The raise time is about $t_r \cong 380\ s$.

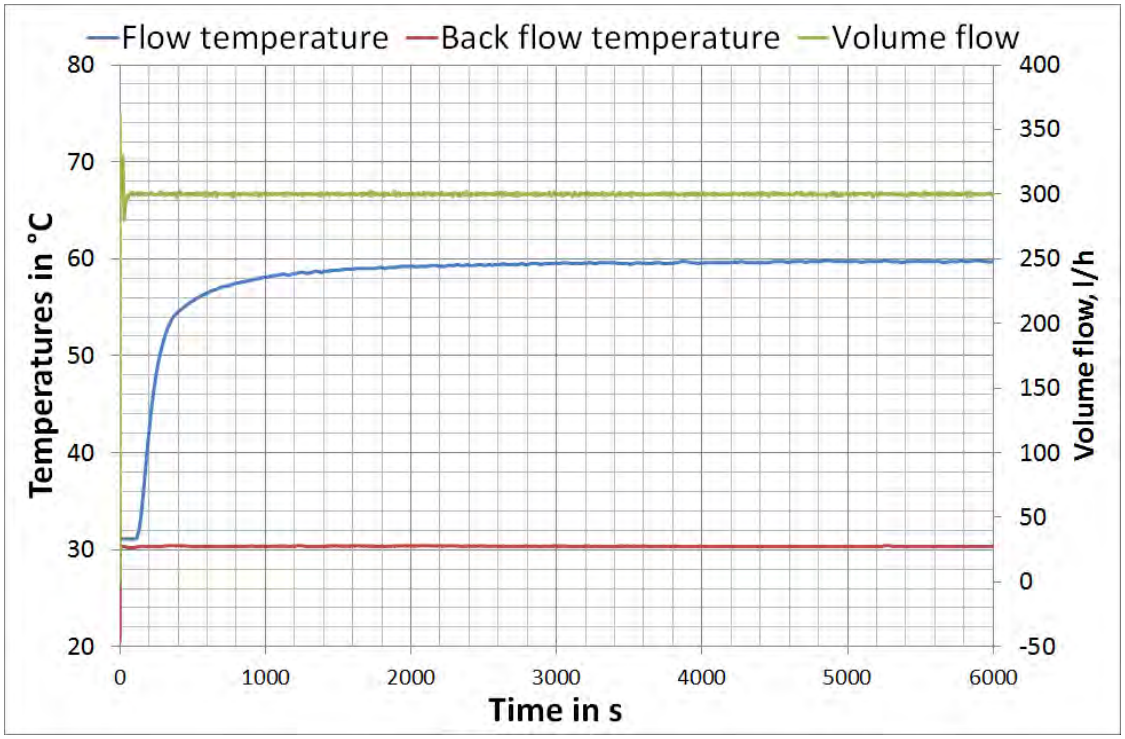

Fig.4.4.7 - Start transient with external pump, temperatures and volume flow

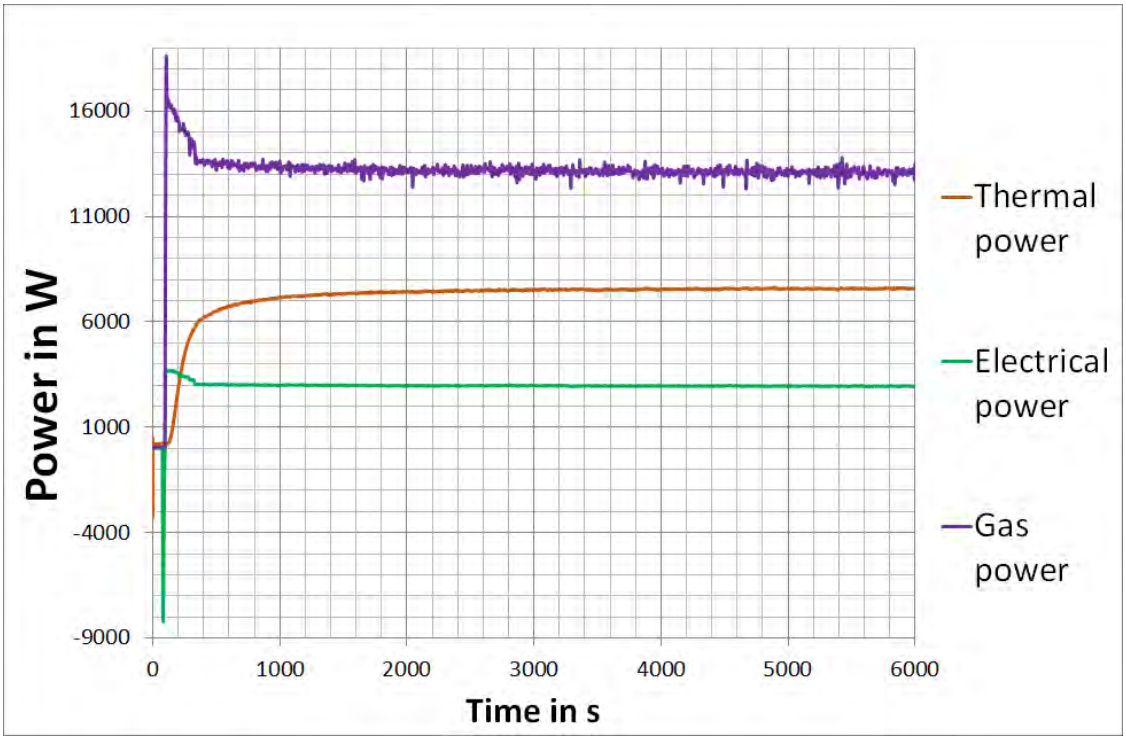

Fig.4.4.8 - Start transient with external pump, powers' trends

In Fig.4.4.6 and Fig.4.4.8 is possible to see a negative electrical power's pick. It occurs at the beginning of the measure when the engine needs to be started and the generator receives electrical power from the net.

4.4.3 Standard efficiency calculation

To obtain the standard efficiency of the micro CHP system, a 24 hours dynamic measure has been made. To emulate a boiler of a conventional house, a storage tank has been installed. The tank has no coil inside, it only contains water. It has two input and two output valves. Furthermore it has three thermal sensors connected to the CHP generator in order to detect the temperature along the whole tank.

The storage tank is connected to the CHP generator on one side, and to the thermal exchange module to the other side. As is shown in Fig.4.4.5, it has been installed a three-ways valve (5) facing the flow and the back flow temperature on the thermal exchange module's side.

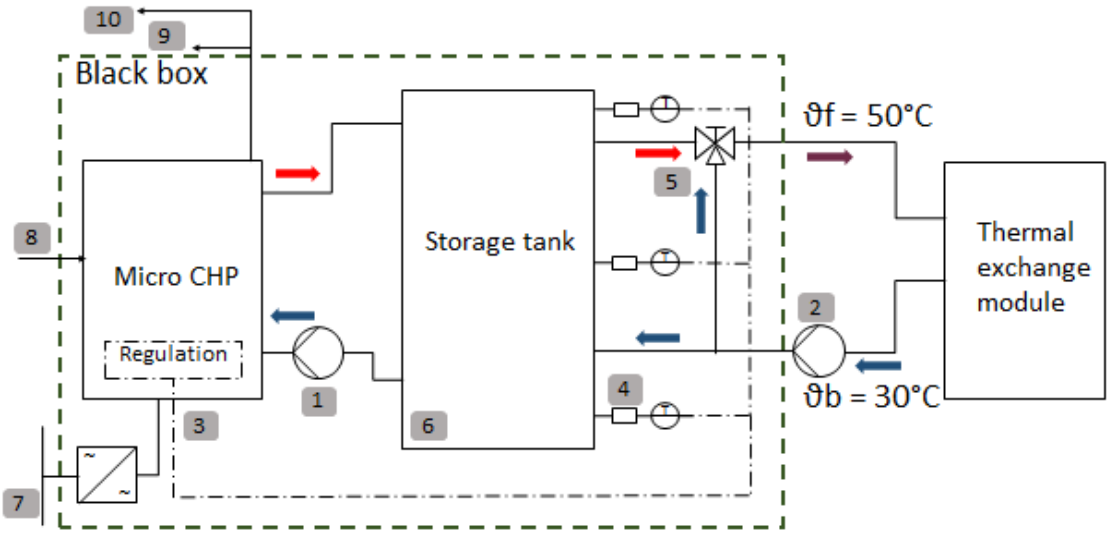

1 Internal pump
2 External pump
3 Temperatures' monitoring
4 Temperature sensors
5 Three-ways valve for the flow temperature
6 Storage tank
7 Electrical power
8 Fuel
9 Condensing water
10 Exhaust

In order to calculate the standard efficiency according to the regulations, the flow and the back flow temperature must be fixed. This is possible thanks to the three-ways valves installed, respectively, on the flow temperature of the storage tank, and on the back flow temperature in the thermal exchange module (Fig.3.1.1 number 9).

In this way, the micro CHP generator and the tank together should be thought as a “black box”. From this “black box” flows out a certain volume flow at a fixed temperature and flows in the same volume flow at another fixed temperature; a certain amount of fuel goes in, and a certain amount of electrical power is produced.

The hydraulic circuits between the micro CHP generator and the tank, and the one between the tank and the thermal exchange module are separated by a hydraulic point of view. In fact they are regulated by two different pumps; respectively, the internal and the external ones. The connection element between the two circuits is the tank. Anyway, the circuits are thermally connected because both the circuits can influence the temperature trend in the storage.

In order to follow the regulations, the flow and back flow temperatures must have these values:

$\vartheta_f = 50°C$
$\vartheta_b = 30°C$

Thus, to tune the thermal power absorbed by the load, is only possible to vary the volume flow. In fact, have being fixed the temperatures, the only unknown remained is the volume flow. The electrical power is set to $P_{el,net} = 3\ kW$ for the whole measurement.
According to DIN 4709 [27], the storage tank must supply the thermal load with a definite thermal power trend during the 24 hours measurement. DIN 4709 allows the calculation of the standard efficiency for the micro-CHP systems with a fuel power up to $\dot{Q}_f = 70\ kW$. The thermal trend is shown in Fig.4.4.6.

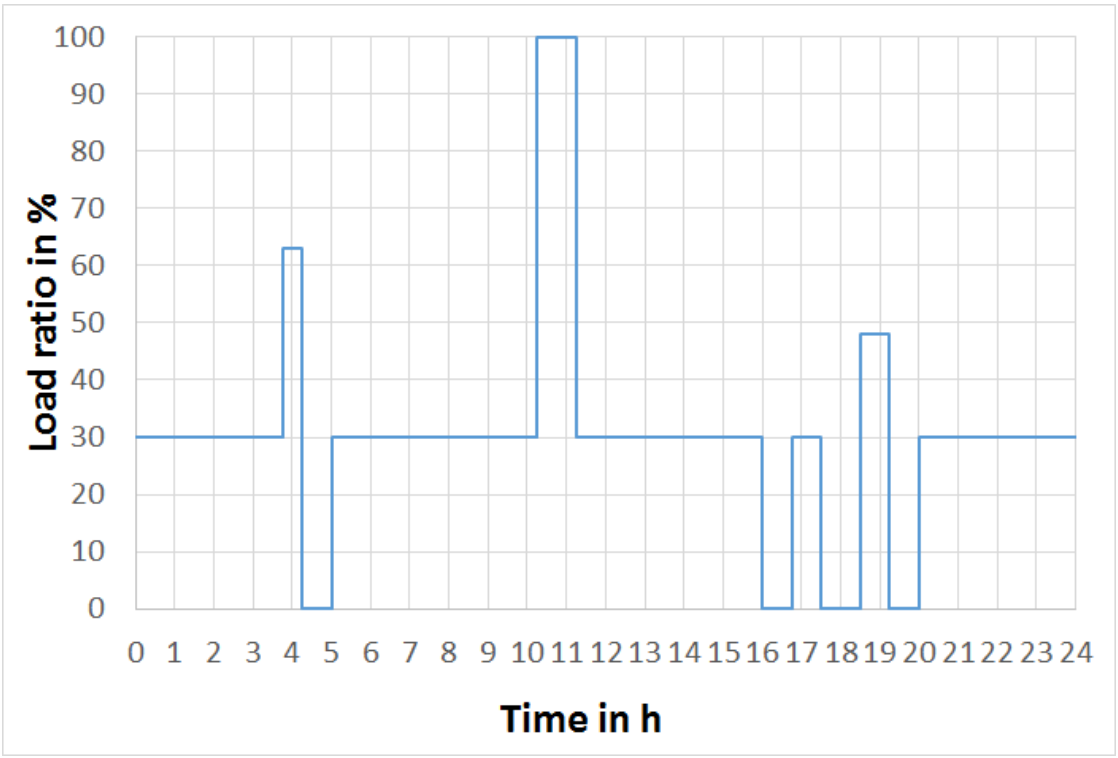

Fig.4.4.6 - Load ratio for the standard efficiency calculation

The y-axis refers to $\dot{Q}_{average,3kW}$. This value represents the average of all the thermal powers $\dot{Q}_{th,net}$ produced in steady state conditions with $P_{el,net} = 3\ kW$ with different volume flows.

$$\dot{Q}_{average,3kW} = 10200 \qquad [kW]$$

So, for each thermal power of Fig.4.4.6 has been calculated the respectively volume flow value. These values have been imposed to the hydraulic circuit between the tank and the heat exchange module, by setting the external pump throughout a time table from the software.
Thus, during the 24 hours the load absorbed different thermal powers from the tank. The tank is fed by the CHP generator throughout the internal pump. The CHP generator is set to work till the thermal sensor on the bottom of the tank reaches a temperature of $\vartheta_{bottom} = 50°C$. Thereafter the machine switches off automatically. After the thermal sensor on the top of the tank has been cooled down under $\vartheta_{top} = 68°C$, the machine switches on again.

The measure can begin just when the tank reaches the maximum storage load, and so when $\vartheta_{bottom} = 50°C$ and the CHP generator has been just switched off.

The final results of this measurement are shown in the table below.

Tab.4.4 - results of the standard efficiency measurement

Supplied fuel energy	119,34	kWh
Supplied electrical power	0,25	kWh
Electrical power produced	27,01	kWh
Thermal power produced	79,03	kWh
Electrical efficiency	22,42	%
Thermal efficiency	66,22	%
Overall efficiency	88,64	%
Thermal efficiency with DIN 4709	119,21	%

5 Convenience evaluation

5.1 Economic comparison

In order to evaluate the economic impact of the KIRSCH CHP generator usage, the domestic energy requirements in a well insulated building have been considered. The total annual costs have been analyzed for both the case of the KIRSCH CHP generator and for a standard boiler with an efficiency of $\eta_{boiler} = 0{,}797$.
The standard trend of electrical energy, thermal heating energy, and drinkable water energy requirements is given hourly for the whole year. The annual energy requirements are shown in Tab. 5.1.1.

Tab. 5.1.1 - Energy requirements

Electrical energy	3400	kWh/year
Heating	3181	kWh/year
Drinkable water	2674	kWh/year
Total heating demand	5855	kWh/year

For the sake of simplicity, the electrical output of the CHP generator has been maintained constant and equal to $P_{el,net} = 3\ kW$. The maintenance costs are included into the investment costs, equal to $cost_{inv\ CHP} = 16000€$. The residual value of the equipment is neglected.
The operation strategy chosen is the heat-lead operation. Thus, for each hourly heating demand amount, comprehending the drinkable water, is calculated the input gas energy amount needed. Then, using the electrical efficiency value, the hourly electrical output is given. For these calculations have been use the efficiency values shown in Tab. 4.4, related to the 24 hours measurement.
For each hour the electrical output can be higher or lower than the electrical energy demand. If it is lower, the whole electrical energy produced by the generator is self-consumed by the domestic utilities. If it is higher, a part equal to the demand is self-consumed and the remaining amount is sold to the electrical grid according to the selling price. The calculation process is shown in Fig. 5.1.1.

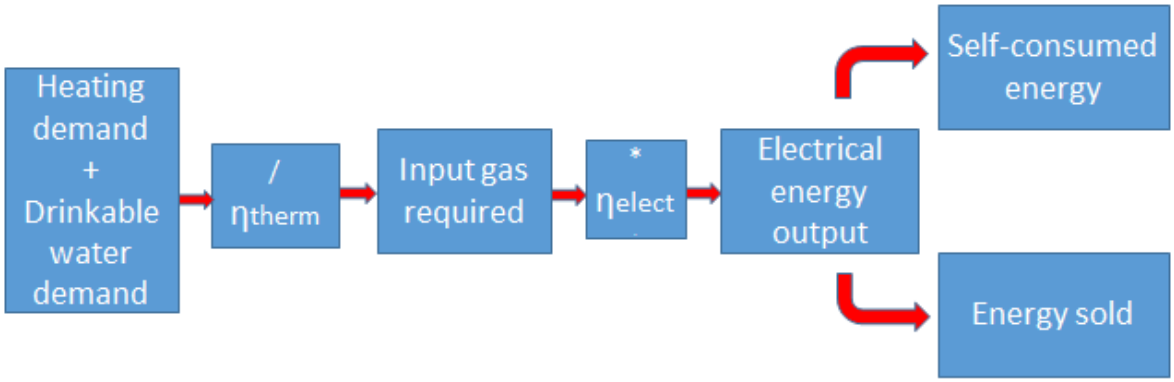

Fig. 5.1.1 - Logic flow for the calculation

5.1 Economic comparison

According to the italian tariff called “scambio sul posto” the purchase and sell prices are the following:

$p_{purchase} = 0.25€/kWh$

$p_{sell} = 0.1€/kWh$

Dealing with the natural gas the price considered is:

$p_{gas} = 0.3€/Smc$

and so, with a calorific power of $H_i = 10{,}01\ MJ/m^3_N$:

$p_{gas} = 0.11€/kWh$

The investment cost of the boiler here considered is:

$cost_{inv\ boiler} = 800€$

with a nominal power $P = 24kW$ and a operating life of 20 years.

The yearly energy amounts resulting from the calculation are the following:

Tab. 5.1.2 - Energy values of the CHP generator, operating with P=3kW

Gas input required	8841 kWh/year	1007 €/year
Electrical energy output	1982 kWh/year	/
Electrical energy self-consumed	1117 kWh/year	279 €/year
Electrical energy purchased	2282 kWh/year	570 €/year
Electrical energy sold	864 kWh/year	86 €/year

It is possible to notice that the difference between the electrical energy requirements and the electrical energy output is not equal to the electrical energy purchased, because the calculation has been made for every hour of the year and not on the yearly gross values.

From table 5.1.2 it can be seen that the energy self-consumed is only 56% of the total electrical output. The revenues rising up from this technology increase with the increasing of the self-consumed ratio.

The annual costs using the CHP generator hail from the amortization cost of the machine, the purchasing of the gas fuel, and the purchasing of the electrical energy. Revenues derive from the selling of the energy surplus and from the self-consumed energy.

$costs_{CHP} = amortization_{CHP} + E_{purchased} + Gas_{purchased} = 2378$ €/year

$revenues_{CHP} = E_{sold} + E_{self\ consumed} = 366$ €/year

Hence, the consumer has to bear a $cost_{total\ CHP} = 2012\ €/year$.

Dealing with the boiler, no revenues come out. The cost are related again to the investment and to the purchasing of electricity and gas.

$$costs_{boiler} = amortization_{boiler} + E_{purchased} + Gas_{purchased} = 1727\ €/\text{year}$$

Obviously the amount of gas used by the boiler is lower because of its higher thermal efficiency. The amount of electricity purchased is necessarily higher because the whole electrical demand must be covered thanks to the public net.

From an economic point of view, the usage of Kirsch generator in this case (well insulated residential building) is not convenient because of its high investment cost and the low heating demand, especially during the summer.

Micro CHP is yet a young technology and, hence, it can not be economically convenient without subsidies. The too high investment cost, in fact, comprehend also the cost of the research. The main problem of the residential buildings is that the heating demand is not constant during the year. In summer, in fact, the heat is not required and so the electricity is not produced.

5.2 Annual energy balance

In order to analyze the efficiency of the two solutions, has been calculated the usage of primary energy. Lower is the primary energy absorbed by the system to face a fixed demand and higher is the efficiency.
For this calculation have been used the overall annual values and not the hourly one.

Important for this evaluation is the concept of primary energy. From the consumption of *1kWh* of gas derives a different value of primary energy respect to *1kWh* of electricity. This is due to the different efficiencies that arise from the generation, transmission and distribution of both gas and electricity. In this way results:

$$1\ kWh_{gas} = 1\ primary\ energy\ unit$$
$$1\ kWh_{electricity} \cong 2{,}17\ primary\ energy\ unit$$

The electricity absorbed from the grid has a different impact compared to the gas.
The electricity absorbed in the CHP configuration $E_{absorbed}$ is the difference between the overall electricity demand and the electricity output. In the case here analyzed results:

$$E_{el\ absorbed,CHP} = E_{el\ demand,CHP} - E_{el\ output,CHP} = 1417\ kWh/year$$

Thus, the overall primary energy amount for the CHP configuration is:

5.2 Annual energy balance

$$\boldsymbol{Primary\ Energy_{CHP}} = E_{gas\ absorbed,CHP} + E_{el\ absorbed,CHP} * 2{,}17 = 11917\ kWh/year$$

Dealing with the boiler, follows:

$$\boldsymbol{Primary\ Energy_{boiler}} = E_{gas\ absorbed} + E_{el\ absorbed} * 2{,}17 = 14723\ kWh/year$$

The primary energy saved in one year with this specific energy demand and in these operating conditions is 20%. Even thou the CHP generation applied in a domestic background can be not convenient by an economic point of view, it performs better consuming overall less primary energy.

6 Comparison with other models

6.1 Prototype and pre-serie 1.0

In this chapter the performance of KIRSCH L 4.12, analyzed in the previous chapters, will be compared with the values related to the prototype and the pre-serie 1.0 of the same machine. The data of the prototype have been gained by Mathias Kopf during the summer semester of 2010. The data of the pre-serie 1.0 have been analyzed by Dr.-Ing. habil. Joachim Seifert in 2012.

In the prototype version of KIRSCH L 4.12 was not possible to regulate the output electrical power from $P_{el,net} = 2\ kW$ to $P_{el,net} = 4\ kW$ directly through the machine's software. For this reason the electrical power amount depends on the opening value of the input gas valve. Similar electrical power levels are reached with three different valve's opening values. They are respectively:

- X = 15%
- X = 25%
- X = 50%

In order to evaluate the differences between the performance of the three models, have been analyzed the trends of the overall and of the electrical efficiencies, shown in tab.5.1. and tab.6.2.

Tab.6.1 - Prototype/pre-serie1.0/serie2.0 overall efficiency, 2kW

ϑr	**Volume flow, l/h**						
	150	**200**	**250**	**300**	**350**	**400**	**450**
25°C	-	99,5	103	106,6	107,6	107,9	-
	-	97,18	98,87	100,22	100,41	100,4	101,48
	95,02	97,04	98,45	99,4	100,6	100,5	101,9
30°C	-	99,5	103	103,6	105	105	-
	-	97,18	98,87	97,67	98,73	99,15	99,87
	94,02	97,04	98,45	98,1	98,7	99,4	101
35°C	-	-	96,5	98	102,6	103,5	-
		-	95,11	96,79	96,64	97,2	98,13
		94,58	96,27	97,4	97,7	98,4	99,4
40°C	-	-	-	93,1	97,5	99	-
	-	-	92,52	93,67	95,11	95,42	95,42
	-	93	94,46	96,1	96	96,5	98,1
45°C	-	-	-	-	91,7	94,1	-
	-	-	-	91,9	92,3	93,21	93,67
	-	90,94	92,02	93,7	94	94,5	95,9
50°C	-	-	-	-	-	86,9	-
	-	-	-	-	-	-	-
	-	-	-	-	-	-	-

Tab.6.2 - Prototype/pre-serie1.0/serie2.0 electrical efficiency, 2kW

ϑr	Volume flow, l/h						
	150	**200**	**250**	**300**	**350**	**400**	**450**
25°C	-	21,2	21,8	22,7	23,2	23,2	-
	-	18,57	18,49	18,47	18,44	18,32	18,39
	18,7	19	18,8	18,5	18,6	18,7	18,6
30°C	-	21,2	22	22,4	22,7	22,6	-
	-	18,49	18,52	18,57	18,52	18,5	18,53
	18,7	19,1	19	18,8	18,5	18,7	18,9
35°C	-	-	20,4	20,7	21,8	21,1	-
	-	-	18,58	18,53	18,45	18,47	18,53
	-	18,8	19,1	19,3	18,9	19,2	18,8
40°C	-	-	-	20	20,7	20,8	-
	-	-	18,79	18,61	18,58	18,53	18,48
	-	18,8	19	19,2	19	19,2	18,4
45°C	-	-	-	-	19	19,6	-
	-	-	-	18,64	18,59	18,56	18,68
	-	18,9	19	19,1	19,2	19,2	18,4
50°C	-	-	-	-	-	16,9	-
	-	-	-	-	-	-	-
	-	-	-	-	-	-	-

From the two tables is clearly possible to see that the values of the prototype are substantially higher than the other. This is due to the not precise regulation of the input gas valve. In fact, analyzing the diagrams of the prototype's electrical power, here not shown, it is possible to see that a constant electrical power level is not maintained. For a back flow temperature $\vartheta_r = 25\ °C$ it is reached a power level of about $P_{el,net} \cong 2500\ W$, and so the efficiencies are higher. The electrical power produced by the prototype decreases with the increasing of the back flow temperature.
For $\vartheta_r = 45\ °C$, the electrical power is about $P_{el,net} \cong 2000\ W$. For this back flow temperature, in fact, the efficiencies reach values similar to the other two machines.

Furthermore, the error in prototype's measures is much more higher than the ones of the other two machines. The error is mainly caused by the thermal sensors. Their error increases substantially with the increasing of the temperature.

The engine and the generator of the three machine is the same. Thus, the electrical efficiencies, in same conditions, remain almost the same. The prototype, however, having a better insulation, has in some conditions a higher efficiency.
Doing a comparison with the same electrical power and considering a high back flow temperature, the prototype's overall efficiency is lower than the one of KIRSCH L 4.12 serie2.0.

The values of the overall and the electrical efficiency related to the $P_{el,net} = 3000\ W$ and $P_{el,net} = 4000\ W$ operating are shown below.

Tab.6.3 - Prototype/pre-serie1.0/serie2.0 overall efficiency, 3kW

ϑr	Volume flow, l/h						
	150	**200**	**250**	**300**	**350**	**400**	**450**
25°C	-	97,8	100	102,5	105,4	104,1	-
	-	-	99,85	101,3	101,18	102,35	102,8
	-	99	100,4	101,9	102,3	102,3	103
30°C	-	96,8	97,8	101,9	102,9	103,6	-
	-	-	97,91	99,22	99,7	100,53	100,75
	-	98,2	99,5	100,2	100,5	100,5	102,1
35°C	-	-	96,9	98,9	98,5	99,7	-
		-	-	96,1	98,17	98,45	99,08
		-	98	99,1	99,1	99,1	99,9
40°C	-	-	-	96,5	95,4	95,9	-
	-	-	-	94,1	95,94	96,69	96,77
	-	-	96	96,9	96,9	97,2	98,1
45°C	-	-	-	-	93,6	94,9	-
	-	-	-	-	93,03	94,09	95,02
	-	-	-	94,8	94,8	95,6	96
50°C	-	-	-	-	-	-	-
	-	-	-	-	-	-	-
	-	-	-	-	-	-	-

Tab.6.4 - Prototype/pre-serie1.0/serie2.0 electrical efficiency, 3kW

ϑr	Volume flow, l/h						
	150	**200**	**250**	**300**	**350**	**400**	**450**
25°C	-	21,9	22,8	22,8	23,5	23,3	-
	-	-	22,13	22,04	21,76	21,95	21,93
	-	22,1	22,2	22,2	22,3	22,3	22,3
30°C	-	21,9	22,1	22,3	22,7	22,8	-
	-	-	21,93	21,91	22,15	22,14	22,16
	-	22,3	22,3	22,2	22,4	22,3	22,3
35°C	-	-	20,3	22,4	21,9	22,1	-
	-	-	-	22,3	22,31	22,26	22,33
	-	-	22,4	22,3	22,3	22,3	22,5
40°C	-	-	-	21,5	21	21,7	-
	-	-	-	22,41	22,37	22,33	21,95
	-	-	22,5	22,4	22,4	22,3	22,5
45°C	-	-	-	-	21,2	21,3	-
	-	-	-	-	22,29	22,25	22,3
	-	-		22,4	22,5	22,3	22,4
50°C	-	-	-	-	-	-	-
	-	-	-	-	-	-	-
	-	-	-	-	-	-	-

Tab.6.5 - Prototype/pre-serie1.0/serie2.0 overall efficiency, 4kW

ϑr	Volume flow, l/h						
	150	**200**	**250**	**300**	**350**	**400**	**450**
25°C	-	-	-	91,5	93,1	93,6	-
	-	-	-	101,7	102,81	102,92	102,94
	-	-	101,8	101,5	101,8	103,5	104,2
30°C	-	-	-	90,7	91,8	93,5	-
	-	-	-	99,7	100,78	101,47	102,02
	-	-	101,8	101,4	101,8	102,3	102,5
35°C	-	-	-	92	92,1	93,2	-
	-	-	-	-	99,38	99,59	100,38
	-	-	-	99,9	100,4	101,2	101,5
40°C	-	-	-	-	89,6	91,7	-
	-	-	-	-	-	97,34	98,72
	-	-	-	98,5	98,4	100,2	100,1
45°C	-	-	-	-	-	-	-
	-	-	-	-	-	-	96,33
	-	-	-	96,1	97,3	98	98,6
50°C	-	-	-	-	-	-	-
	-	-	-	-	-	-	-
	-	-	-	-	-	-	-

Tab.6.6 - Prototype/pre-serie1.0/serie2.0 electrical efficiency, 4kW

ϑr	Volume flow, l/h						
	150	**200**	**250**	**300**	**350**	**400**	**450**
25°C	-	-	-	21,8	21,8	21,8	-
	-	-	-	23,19	23,11	23,16	23,09
	-	-	23,3	23,3	23,3	23,3	23,2
30°C	-	-	-	21,4	21,4	21,8	-
	-	-	-	23,24	23,2	23,2	23,17
	-	-	23,6	23,5	23,6	23,3	23,3
35°C	-	-	-	22,2	22,1	22,1	-
	-	-	-	-	23,42	23,42	23,43
	-	-	-	23,6	23,5	23,3	23,4
40°C	-	-	-	-	21,8	22,3	-
	-	-	-	-	-	23,43	23,43
	-	-	-	23,6	23,5	23,5	23,5
45°C	-	-	-	-	-	-	-
	-	-	-	-	-	-	23,66
	-	-		23,6	23,7	23,6	23,6
50°C	-	-	-	-	-	-	-
	-	-	-	-	-	-	-
	-	-	-	-	-	-	-

6.1 Prototype and pre-serie 1.0

In order to show the results in a more clear way, the diagrams of all the three electrical power output are plotted as function of the back flow temperature for a constant volume flow of $\dot{V} = 300\ l/h$. The diagrams are shown below.

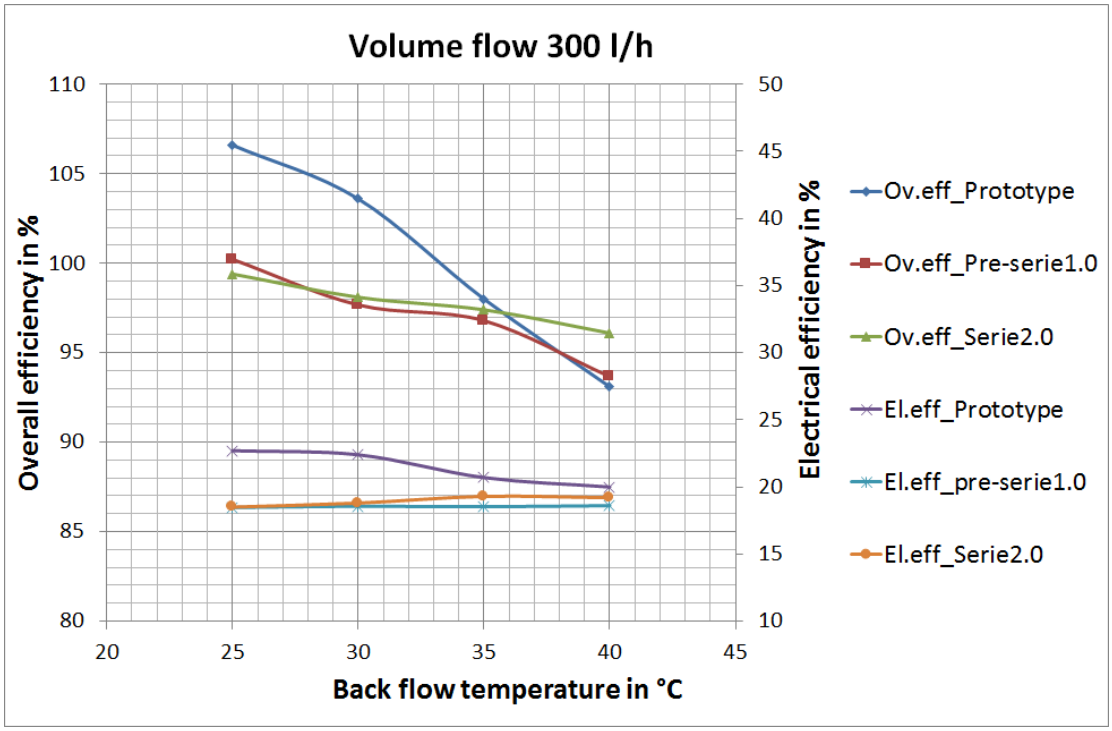

Fig.6.1.1 - Prototype/pre-serie1.0/serie2.0 overall and electrical efficiency, 2kW

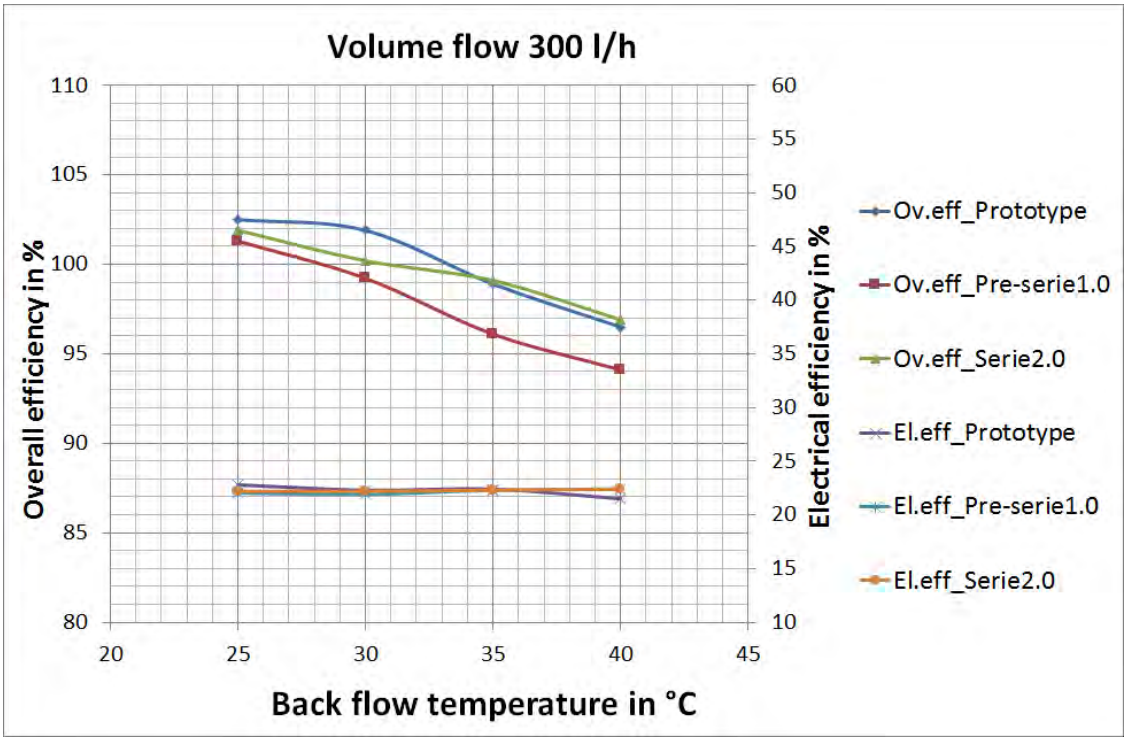

Fig.6.1.2 - Prototype/pre-serie1.0/serie2.0 overall and electrical efficiency, 3kW

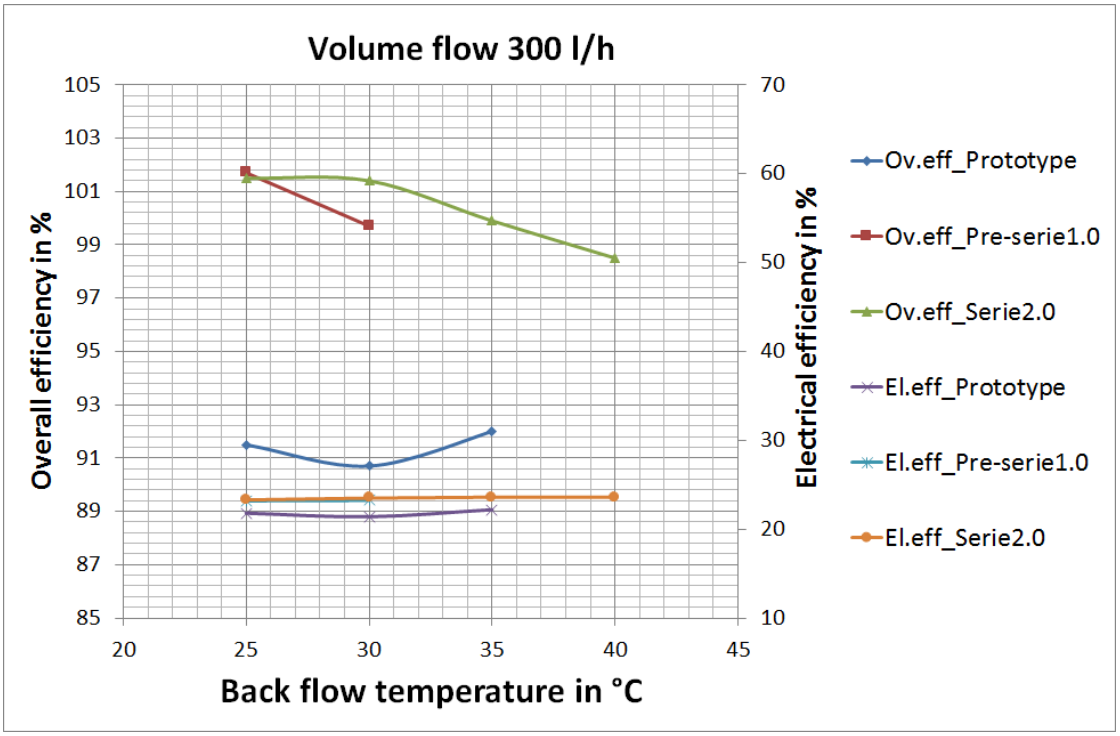

Fig.6.1.3 - Prototype/pre-serie1.0/serie2.0 overall and electrical efficiency, 4kW

From the diagrams it possible to figure out that most of the time the efficiency of KIRSCH L 4.12 serie 2.0 is higher than the one of the pre-serie 1.0. This is due to a more performing internal software.
Furthermore, KIRSCH L 4.12 serie 2.0 can work bearing higher temperatures. It can work with low volume flows and high back flow temperatures even producing $P_{el,net} = 4000\ W$.

The prototype can have the highest overall efficiency in particular conditions, thanks to its better insulation, but actually has strong floating trends for different valve's opening values. This counts against the reliability of the machine.
The problem came out because is not present a software that regulate the internal operation of the machine.

7 Conclusion

After a long row of precise measurements oriented towards a complete performance analysis, it is now possible to state that KIRSCH L 4.12 serie 2.0 is a reliable, environment-compatible and autonomous machine with high level of efficiency.

Considering the steady state operation, the values of the efficiencies and of the power's output have been reached.
The highest overall efficiency has been occurred in the $P_{el,net} = 4000\ W$ operation with the highest volume flow and the lowest back flow temperature, in correspondence to the highest thermal power output. Its maximum values is $\eta_{overall} = 104{,}2\%$ and the minimum one is $\eta_{overall} = 90{,}94\%$. The electrical efficiency is comprehend in a range between $18{,}5\% \leq \eta_{el,net} \leq 23{,}7\%$ and the thermal efficiency between $72\% \leq \eta_{th,net} \leq 83{,}3\%$. These values are related to different operating conditions, otherwise it could be possible to achieve an overall efficiency higher than the one actually reached.

Dealing with powers, the electrical power takes values between $1928\ W \leq P_{el,net} \leq 3612\ W$ and the thermal power between $7380\ W \leq P_{el,net} \leq 12418\ W$.
The fuel's amount, increasing with the power's demand, varies from a minimum of $\dot{m}_f \cong 16{,}6\ l/h$ up to a maximum of $\dot{m}_f \cong 25{,}5\ l/h$. The maximum amount of condensing water is about $\dot{m}_{cond} \cong 2\ l/h$.
Thanks to the results obtained with the dynamic measurements, it can be said that the machine requires a time of about $t_r \cong 350\ s$ to warm up and feed the utility with the nominal power level. This values has been obtained referring to $P_{el,net} = 3000\ W$, $\dot{V} = 300\ l/h$ and $\vartheta_r = 30°C$.

A rather good improvement has been achieved compared with the KIRSCH L 4.12 pre-serie 1.0 thanks to a new reliable software. The overall efficiency is higher in most cases and the working operation is extended to a wider range of volume flows and back flow temperatures.

A micro CHP system like KIRSCH L 4.12 can be a great solution to ensure high efficiency and so low emissions. Installed in a standard family well insulated house, it can satisfy the whole thermal energy demand, producing in addiction electrical energy useful for the utility.

In order to be economically competitive this young technology requires an appropriate incentives system to cover the high investments cost.

8 Bibliography

[1] COGENCO, Dalkia company, United Kingdom: “Cogeneration”.
http://www.cogenco.com/en/lowcarbonsolutions/chp_cogeneration/
Date of research: 06/2014

[2] COGEN Europe: “What is cogeneration?”
http://www.cogeneurope.eu/what-is-cogeneration_19.html
Date of research: 04/2014.

[3] Prof.-Ing. G.Lazzaretto:
Course of: “Impianti energetici”. Cogenerazione. Introduzione alla cogenerazione di piccola taglia.
University of Padova, 2011.

[4] C. Nellen and K. Boulouchos:
Natural gas engines for cogeneration.
SAE technical papers series.

[5] A. Ferreira, L. Martins, S.Teixeira, M.Nunes:
Techno-Economic Assessment of Micro-CHP Systems.
International Conference on Industrial Engineering and Operations Management, July 9-11 2012.

[6] K.T. Ahumada:
Understanding the Impact of Large-Scale Penetration of Micro Combined Heat & Power Technologies within Energy Systems.
Massachusetts institute of technology.

[7] A.D. Hawkes, M.A. Leach.
Cost-effective operating strategy for residential micro-combined heat and power.
http://www.sciencedirect.com/

[8] KIRSCH:
Kirsch home energy, micro.
Produkte Datenblatt.

[9] Internet research: http://elios.augustana.edu
Date of research: 04/2014.

[10] A. Cavallini, L. Mattarolo
Termodinamica applicata, CLEUP, 1990.
Chapter: “Combustibili e combustione”.

[11] VEM:
Three-phase asynchronous generators. On-line English catalog.
Tolerances and electrical parameters, page 8.

[12] Prof.-Ing. S. Bolognani:
Course of: “Azionementi elettrici”: Motore ad induzione.
University of Padova, 2008.

[13] Herman, Stephen L., E8, 2011.
Alternating Current Fundamentals, eighth edition.
Chapter: “Alternating-current generators”.

[14] Dr.-Ing. Habil. Joachim Seifert:
Mikro BHKW Systeme für den Gebäude Bereich, VDE, 2013.
Chapter: “Messtechnische Analysen”, pages 97,98;
Chapter: ” Hydraulik/ Regelung/ Informationsgewinnung”, page 57;

Chapter: "Messtechnik", page 91.

[15] KELLER:
Intelligenter Transmitter mit digitaler Anzeige.
Eigenschaften als pdf-Datei.

[16] SIEMENS:
Stetige Regelventile mit Magnetantrieb, PN16.
Haupt-Datenblatt.pdf.

[17] Dott.-Ing. G. Emmi:
Course of "Impianti termici e frigoriferi": Valvole e regolazione idronica.
University of Padova, 2013.

[18] REFLEX:
Membran-Druckausdehnungsgefäße.
Produktbeschreibung.

[19] VIESSMANN:
Vitocell B-100.
Datenblatt: Speicher-Wasserwarmer mit zwei Heiswendeln.

[20] Wikipedia:
Resistance thermometer.
http://en.wikipedia.org/wiki/Resistance_thermometer
Date of research: 05/2014.

[21] ABB:
ProcessMaster Electro-magnetic flowmeter FEP300.
Data sheet DS/FEP300-En Rev.1.

[22] WILO:
Datenblatt. Umwälzpumpe Wilo-Stratos 4071-12.

[23] Wikipedia:
Thermal mass flow meter.
http://en.wikipedia.org/wiki/Thermal_mass_flow_meter
Date of research: 05/2014.

[24] KERN:
Pcb precision balance.
Operating manual version 1.0 12/2006.

[25] ECOM:
J2KN pro flue gas analyzer.
Operations manual version 3.3.2

[26] Wikipedia:
Gas chromatography.
http://en.wikipedia.org/wiki/Gas_chromatography
Date of research: 05/2014.
http://web.ing.puc.cl/~power/

[27] Deutsches Institut für Normung e.V.: *DIN 4709: Normnutzungsgrad für Mikro-KWK-Geräte bis 70 kW Nennwärmedlastung. 2011.* – Beuth Verlag GmbH, Berlin.